DIFFUSION FROM AN INSTANTANEOUS POINT SOURCE INTO A TURBULENT BOUNDARY LAYER

by

Suresh Chandra

U.S. Army Research Grant
DA-AMC-28-043-65-G20

FLUID MECHANICS PROGRAM
ENGINEERING RESEARCH CENTER
COLLEGE OF ENGINEERING
COLORADO STATE UNIVERSITY
FORT COLLINS, COLORADO

Technical Report

DIFFUSION FROM AN INSTANTANEOUS POINT SOURCE INTO A TURBULENT BOUNDARY ~~LAYER~~

by

Suresh Chandra

U.S. Army Research Grant
DA-AMC-28-043-65-G20

Distribution of This Report Is Unlimited

Fluid Dynamics and Diffusion Laboratory
College of Engineering
Colorado State University
Fort Collins, Colorado

August 1967

CER67-68SC7

ABSTRACT

DIFFUSION FROM AN INSTANTANEOUS POINT SOURCE INTO A TURBULENT BOUNDARY LAYER

Diffusion of helium gas from an instantaneous point source within a neutral boundary layer has been studied. The investigation was made in a wind tunnel of the Fluid Dynamics and Diffusion Laboratory.

Concentrations from a simulated point source, located at a fixed height of eight inches above a smooth surface, were measured for several downstream cross-sections of the diffusing cloud. The free stream velocity for the entire study was 20 ft./sec. Statistical parameters have been used to describe the concentration data in terms of the time-average as well as the maximum instantaneous concentration at a point in the diffusion field.

The lateral and vertical diffusivities are determined from the diffusion data. Comparison of data from the instantaneous point source, in terms of the time-averaged concentration parameters, with the continuous point source data of other investigators shows good agreement. The concentration data are presented in terms of dimensionless parameters.

Separation of the total dispersion into two components, spreading and meandering, is obtained on the basis of Gifford's fluctuating plume model. The results of this analysis have been used to determine the Hay-Pasquill scale parameter which relates the Lagrangian and Eulerian scales of turbulence. The values of the scale factor, obtained on the basis of spreading variance alone, are in close agreement with those of other investigators. Meandering is shown to have a significant effect on these values.

Suresh Chandra
Department of Civil Engineering
Colorado State University
Fort Collins, Colorado
August 1967

ACKNOWLEDGMENTS

The author wishes to express his sincere gratitude to his Major Professor, Dr. Erich J. Plate, whose guidance and constant encouragement have contributed enormously to the accomplishment of this work. Dr. Plate's constructive advice and suggestions during the preparation of this dissertation have been of the greatest value to the author. Appreciation is due to other members of his research and dissertation committee, Dr. J. E. Cermak, Dr. L. V. Baldwin, Dr. M. M. Siddiqui, and Dr. H. W. Shen.

The author is also thankful to Dr. G. J. Binder, Dr. R. N. Meroney, and Mr. W. W. Sayre for many useful discussions and suggestions; to Mr. F. F. Yeh for helping in the collection of basic data; and to Miss Hanae Akari for the careful and accurately made diagrams.

Last but not the least, the author is grateful to his wife, Jane, whose eternal patience and sacrifice have been rewarded with the completion of this work.

Sponsorship for the present investigation was provided by U. S. Army Materiel Command under Grant No. DA-AMC-28-043-65-G20. Financial assistance received under this sponsorship is gratefully acknowledged.

TABLE OF CONTENTS

TABLE OF CONTENTS - Continued

TABLE OF CONTENTS - Continued

LIST OF FIGURES

LIST OF FIGURES - Continued

LIST OF FIGURES - Continued

LIST OF SYMBOLS

Symbol	Definition	Dimension*
A	Constant	- -
C	Concentration level of the diffusing gas, ppm	- -
C_p	Equivalent instantaneous concentration from a continuous point source at a point, ppm	- -
$(C_p)_{max}$	Peak concentration based on m readings, ppm	- -
C^*	Sutton's virtual coefficient of diffusion	$L^{1/8}$
$\overline{C}$	Average area under concentration profiles at a point (time-average of concentration of a continuous point source at a point), ppm	- -
$c(x_i)$	Concentration on a profile, corresponding to distance x_i along the sampler length, ppm	- -
$c(x_i)_{max}$	Maximum concentration on a profile, along the sampler length, ppm	- -
$\overline{D^2}$	Variance due to meandering of diffusion cloud	L^2
$F_E(n)$	Eulerian spectrum function at frequency n	T
H	Source height	L
K_x	Longitudinal mass diffusivity in x-direction	L^2/T
K_y	Lateral mass diffusivity in y-direction	L^2/T
K_z	Vertical mass diffusivity in z-direction	L^2/T
K_1	Constant	- -

* The symbols designating dimensions have the following meaning: M = mass , L = length , T = time.

LIST OF SYMBOLS - Continued

Symbol	Definition	Dimension
k	Wave number	L^{-1}
m	Number of consecutive profiles at a point	- -
n	Frequency	L^{-1}
Q	Flux of diffusing matter per unit time from the instantaneous point source	M/T
$R_E(t)$	Eulerian correlation coefficient	- -
$R_L(\xi)$	Lagrangian auto-correlation coefficient	- -
t	Time coordinate	T
T	Dispersion time, sec.	T
U_∞	Mean ambient velocity, ft./sec.	L/T
$\overline{u}, \overline{v}, \overline{w}$	Components of mean velocity in x-, y-, and z-directions, ft./sec.	L/T
u, v, w	Instantaneous turbulent velocity fluctuation in the x-, y-, and z-directions, ft./sec.	L/T
u', v', w'	Root mean square values of u, v, w	L/T
x, y, z	A right-hand coordinate system with origin at simulated point source	L
X	Distance measured from the center of the source parallel to direction of flow	L
X_i	Distance from the inlet of the wind tunnel test-section	L
x_i	Distance measured along the sampler length	L
$\overline{Y^2}$	Variance due to spreading of the diffusion cloud	L^2

Symbol	Definition	Dimension
y	Lateral coordinate axis	L
z	Vertical coordinate axis	L
β	Hay-Pasquill scale parameter	- -
δ	Momentum boundary layer thickness	L
η	Vertical characteristic length of the diffusion cloud $\frac{C(x, 0, \eta)}{C_{max}} = 0.5$	L
λ	Horizontal characteristic length of the diffusion cloud $\frac{C(x, \lambda, 0)}{C_{max}} = 0.5$	L
ν	Kinematic viscosity	L^2/T
ξ	Time coordinate	T
ρ	Mass density	M/L^3
$\sigma^2_{C_p}$	Variance of concentration C_p	L^2
σ^2_y	Variance of concentration $\overline{C}$ in the lateral direction	L^2
σ^2_z	Variance of concentration $\overline{C}$ in the vertical direction	L^2
$\mathcal{T}_L$	Characteristic time scale of eddy diffusion	T

Chapter I

INTRODUCTION

Atmospheric diffusion has been and continues to be a subject of considerable activity and research in the area of fluid dynamics and meteorology. The atmosphere possesses a varying capacity to transport and dilute gases, small particles or droplets, and plays an important role in operating the release or escape of such materials. A systematic research leading to sound comprehension of the basic processes of atmospheric diffusion is also necessary in the proper evaluation of the requirements of public health and safety, careful planning of urban developments, and foreseeing the potential hazards of radioactive contaminants. At the present time, our knowledge of the transport mechanisms is far from being complete and consequently, a great deal of faith cannot be placed in the quantitative predictions based on it. The great need for a comprehensive understanding of these transport mechanisms necessitates a vigorous and continuing research in the field of atmospheric diffusion.

One of the possible ways to obtain the information on atmospheric diffusion is to conduct actual experiments in the field. However, field studies serve the purpose only to a limited extent since there is

no control over atmospheric conditions. Field tests are expensive, and the significant variables of the phenomenon cannot be easily controlled.

In view of the complex nature of the problem, it is not feasible to obtain answers based on a purely mathematical analysis. Based on K-theory or molecular model of diffusion, several equations have been derived to describe the atmospheric diffusion but the various simplifying assumptions made by mathematicians have not proved to be fully justifiable. The other approach, based on the statistical theory of turbulent diffusion, has been highly successful in describing the idealized situation of isotropic and homogeneous turbulence but its application to boundary layer flows presents problems.

A more promising approach than the field study consists of investigating the possibility of modeling turbulent diffusion processes in a controlled atmosphere of a laboratory wind tunnel. Since a great deal of practical interest centers at the diffusion in lower atmosphere, it is of significance to note that lower atmospheric conditions can be simulated within the boundary layer generated near the wall. The aerodynamic characteristics of the air stream strongly influence the propagation of turbulence in a boundary layer. The diffusing entity, or the tracer gas, is transported under the influence of the mean velocity and simultaneously diffused in directions transverse to the mean flow by small, chaotic motions which characterize turbulence.

In the present investigation, helium gas was released in the form of a puff from an instantaneous point source located within the turbulent boundary layer over a smooth surface. The source location and height were kept fixed throughout the investigation and instantaneous puffs were sampled by taking concentration measurements at several points at each of the four stations. The samples were analyzed with a mass spectrometer.

In this dissertation, the following investigations relating to diffusion from an instantaneous point source into a turbulent boundary layer have been made:

1. Characteristics of the velocity and turbulence fields,
2. Diffusivities in the lateral and vertical directions,
3. Separation of the total dispersion into the components of spreading and meandering,
4. The Hay-Pasquill scale parameter and its role in predicting the particle spread, and
5. Comparison with existing data.

One of the main objectives of the present investigation was to study Gifford's fluctuating plume model for diffusion from a continuous point source and apply it to diffusion from an instantaneous point source. On the basis of this model, the total dispersion can be separated into two parts, spreading and meandering. The results of this analysis, based on Gifford's model, can be further used to

determine the Hay-Pasquill scale parameter relating Lagrangian and Eulerian scales of turbulence.

Chapter II

REVIEW OF LITERATURE

The review of literature in this chapter contains pertinent information about the present study and the general background of the problem. This review, therefore, has been limited to turbulent diffusion over a smooth boundary. It is developed in the following two sections:

1. Basic theoretical approaches, and deductions for continuous and instantaneous point sources.
2. Experimental investigations.

Basic Theoretical Approaches

Two distinct theories have been developed in analyzing diffusion processes: the K-theory and the statistical theory. Each theoretical approach is first reviewed briefly and then the related solutions for a continuous as well as an instantaneous point source are examined.

The K-theory or exchange coefficient gradient-type diffusion theory

Much of the early analytical work in atmospheric diffusion was based on an assumed analogy with the model of molecular diffusion. Many practically useful solutions have been obtained by

this method, although the recently introduced statistical methods are proving more powerful in describing the general problem of turbulent diffusion. The basic differential equation is

$$\frac{\partial C}{\partial t} + u\frac{\partial C}{\partial x} + v\frac{\partial C}{\partial y} + w\frac{\partial C}{\partial z} = \frac{\partial}{\partial x}\left(K_x \frac{\partial C}{\partial x}\right) + \frac{\partial}{\partial y}\left(K_y \frac{\partial C}{\partial y}\right) + \frac{\partial}{\partial z}\left(K_z \frac{\partial C}{\partial z}\right) \tag{2-1}$$

For the case of mean wind $v = w = 0$, and considering that $\frac{\partial}{\partial t_x}\left(K_x \frac{\partial C}{\partial x}\right)$ is small compared with other diffusion terms, the basic Eq.(2-1) reduces to the commonly used form for a continuous point source

$$\frac{\partial C}{\partial t} + u\frac{\partial C}{\partial x} = \frac{\partial}{\partial y}\left(K_y \frac{\partial C}{\partial y}\right) + \frac{\partial}{\partial z}\left(K_z \frac{\partial C}{\partial z}\right) \tag{2-2}$$

Historically, the developments of the K-theory serve to emphasize the principal factors which render difficult any simple approach to atmospheric diffusion or turbulent diffusion in shear flows with density stratification close to a boundary. The mechanism of turbulent diffusion is controlled by the following principal factors:

1. the diffusivities or exchange coefficients K_x, K_y, K_z, and
2. the velocity profile and shear stress as influenced by nature of the boundary surface.

Essentially, the success of the solutions arrived at by means of the K-theory depend on the accuracy of the simplifications introduced to facilitate the mathematical solutions of Eq.(2-2). The commonly used simplifications include:

a. K_x, K_y, K_z: assumed constant, isotropic or nonisotropic, and varying with height according to specific power laws (19),

b. velocity profiles which reflect the effects of surface roughness and density stratification or stability, but are of a form sufficiently simple to make possible the integration of Eq.(2-2). Such profiles have been suggested and used by Calder, Deacon and others (21).

Although the mathematical achievements of the K-theory are considerable, there are two serious objections. First, concerning the fundamental assumption of gradient-type exchange-coefficient diffusion, Sutton (19) cautions that this approach, although mathematically feasible, is artificial and unlikely to be fruitful unless the underlying physical processes are of the type envisaged in the kinetic theory. Second, concerning the exchange coefficients K_i, Richardson (21) has pointed out that values can range from 0.2 cm.^{2}/sec. for molecular diffusion to 10^{11} cm.^{2}/sec. in atmospheric storms. The K-coefficients are not universal parameters but are controlled by the scale of turbulence; different K-coefficients would apply to different diffusion regimes. Thus, this theory may not provide generalized comparisons between diffusion processes generated by widely different scales of turbulence unless relations are established between the K-coefficients for different regimes. Extensive applications have been made of the K-theory under different assumptions for the K-coefficients and velocity profiles. Several useful results derived

from this theory have been reviewed and discussed in the book by Sutton (19) and in AEC's monograph (21).

The statistical theory of turbulent diffusion

Statistical models and methods have proven to be very powerful techniques in analysis of turbulent diffusion. The most comprehensive approach originates from theories formulated on the basis of statistical mechanics. The statistical model of diffusion, as described by Monin (13), assumes that each individual diffusing particle moves randomly and its coordinates alter in time according to a Markov random process. The primary concept is the dispersion of the coordinate of a diffusing particle, in contrast to the exchange coefficient gradient-type model which is constructed essentially on the physical concept of coefficients of turbulent diffusion. Monin (13) indicates that the application of the Fokker-Planck diffusion equation to this random process reduces to

$$\frac{\partial C}{\partial t} \quad u\frac{\partial C}{\partial x} = \frac{\partial}{\partial x}\left(K_x \frac{\partial C}{\partial x}\right) + \frac{\partial}{\partial y}\left(K_y \frac{\partial C}{\partial y}\right) + \frac{\partial}{\partial z}\left(K_z \frac{\partial C}{\partial z}\right) \tag{2-3}$$

where

$$K_x = \frac{1}{2}\frac{d\,\overline{Y_x^2}(t)}{dt}\,, \quad \overline{Y_x^2}(t) = \overline{\left[x(t) - x(o)\right]^2} \tag{2-4}$$

analogous expressions hold for K_y and K_z.

It is to be noted that Eq. (2-3) is identical to the equation of diffusion (2-2) arrived at on the basis of the K-theory model of

gradient-type diffusion. As stated, this equation makes no distinction between turbulent and molecular diffusion, the K_i being free to vary in space, as in a non-homogeneous turbulent field. But as turbulent diffusion is accomplished by eddies, it is appropriate that eddy size should enter the differential equation of diffusion. The initial and very significant contribution connecting the statistical characteristics of the turbulent field with the mechanism of diffusion is due to classical work of G. I. Taylor (20).

Taylor's formulation provided the unique advantage of extending the analysis for a one-dimensional random walk to diffusion by continuous movements. By considering the path of a marked fluid particle during its traverse through a homogeneous turbulent flow field, Taylor arrived at the well-known result, sometimes called Taylor's theorem,

$$\overline{Y_i^2} = 2\,\overline{u_i'^2} \int_o^T \int_o^t R_L(\xi)\, d\xi\, dt \qquad (2\text{-}5)$$

where $\overline{Y_i^2}$ = variance or one-dimensional spread, $\overline{u_i'^2}$ = mean square value of instantaneous velocity fluctuation, $R_L(\xi)$ = Lagrangian correlation coefficient, and T, t, ξ represent time.

The motions of the fluid particle are continuous and no restriction is implied on a continuous exchange of a transferable property between particles. Taylor's theorem, for the first time, established a relation between turbulent diffusion and the statistical characteristics of the turbulent flow field. For a group of particles

in such a field, it demonstrated that the dispersion experienced by the group is dependent on (1) the intensity of the turbulent velocity fluctuations u_i' , and (2) the form of the correlation function $R_L(\xi)$ which influences a particle at various times.

Two limiting conditions for Taylor's theorem offer useful information for obtaining turbulence characteristics from diffusion measurements. These are (1) T very small, and (2) T very large; both compared to ξ^* , the time when $R_L(\xi)$ remains zero.

(1) For very small T : $(T << \xi^*)$

$$R_L(\xi) \simeq 1.0$$

$$\overline{Y_i^2} \simeq 2\,\overline{u_i'^2} \int_o^T t'\,dt' \simeq \overline{u_i'^2}\; T^2$$

which gives $\overline{Y_i^2}^{\,1/2} \sim T$

The diffusion proceeds linearly with time.

(2) For large T : $(T > \xi^*)$

$$\overline{Y_i^2} \simeq 2\,\overline{u_i'^2} \int_o^T dt \left[\int_o^t R_L(\xi)\, d\xi \right]$$

$$\simeq 2\,\overline{u_i'^2} \int_o^T dt \;\; \mathcal{J}_L = 2\,\overline{u_i'^2}\;\mathcal{J}_L\, T \qquad (2\text{-}6)$$

which gives $\overline{Y_i^2}^{\,1/2} \sim T^{1/2}$.

Thus diffusion proceeds proportional to $T^{1/2}$ for large T . Here $\mathcal{J}_L$ may be defined as a characteristic time scale of eddy diffusion.

Frenkiel (6) considered an instantaneous point source in a field of homogeneous and isotropic turbulence in a fluid at rest, and studied the solution based on the Fickian law of diffusion, Eq. (2-3), with $K_x = K_y = K_z = K =$ constant,

$$\frac{\partial C(x, y, z, t)}{\partial t} = K \nabla^2 C \qquad (2\text{-}7)$$

where C = mean concentration at a point (x, y, z) at instant t,

K = coefficient of eddy diffusion independent of dispersion time.

The solution for this differential equation is

$$C(x, y, z, t) = \frac{Q_o}{(4\pi kt)^{3/2}} \exp\left[-\frac{x^2 + y^2 + z^2}{4kt}\right]. \qquad (2\text{-}8)$$

A similar solution was obtained using the statistical theory of turbulent diffusion for the case when the dispersion time T is very large as compared to the Lagrangian scale of turbulence; this solution can be written as

$$C(x, y, z, t) = \frac{Q_o}{(2\pi \overline{Y_i^2})^{3/2}} \exp\left[-\frac{x^2 + y^2 + z^2}{2\overline{Y_i^2}}\right] \qquad (2\text{-}9)$$

where $$\overline{Y_i^2} = 2\overline{u_i'^2} \int_o^T dt \int_o^t R_L(\xi)\, d\xi \quad . \qquad (2\text{-}5)$$

Comparing Eqs. (2-8) and (2-9), it is noted that these equations are identical if molecular diffusion is negligible, and

$$\overline{Y_i^2} = 2(\overline{u_i'^2}\, \mathcal{J}_L)t = 2Kt \quad . \qquad (2\text{-}10)$$

In this manner Frenkiel demonstrated an important relation, that for a homogeneous and isotropic turbulent field, for very large diffusion times ($T >> \mathcal{J}_L$), the exchange coefficient gradient-type model of diffusion expressed by the Fickian law of diffusion , Eq. (2-3), and the statistical theory model based on Taylor's theorem, lead to identical results. Frenkiel cautions that the use of the Fickian law in experimental investigation will thus lead to inconsistent K-values unless it is first established that $T >> \mathcal{J}_L$. Similar extensions appear probable for the more complex case of non-homogeneous and non-isotropic turbulence as indicated by Frenkiel (6).

Sutton (19) adopted the fundamental idea of Taylor's statistical theory of diffusion by continuous movements, that the rate at which diffusion takes place depends on the variance $\overline{Y_i^2}$ of the wind velocity fluctuations u_i' , or

$$\overline{Y_i^2} = 2\overline{u_i'^2} \int_o^T dt \int_o^t R_L(\xi)\, d\xi \qquad (2\text{-}5)$$

From dimensional considerations, Sutton obtained an equivalent expression for the Lagrangian auto-correlation coefficient so that

$$R_L(\xi) = \frac{u_i'(t)\, u_i'(t+\xi)}{\overline{u_i'^2}} = \left[\frac{\nu}{\nu + \overline{u_i'^2}\,\xi}\right]^n \qquad (2\text{-}11)$$

where ν is the kinematic viscosity of air and n is a number ranging between 0 and 1 which reflects the wind structure near the boundary.

The exponent n is defined for an aerodynamically smooth surface by reference to the velocity profile law

$$\frac{\bar{u}}{U_\infty} = \left(\frac{z}{\delta}\right)^{1/s} = \left(\frac{z}{\delta}\right)^{\frac{n}{2-n}} \quad . \tag{2-12}$$

Integrating Eq. (2-5) after inserting $R_L(\xi)$ as defined in Eq. (2-11), gives

$$\overline{Y_i^2} = 2\,\overline{u_i'^2} \int_0^T dt \int_0^t \frac{\nu}{\nu + \overline{u_i'^2}\,\xi}\, d\xi$$

$$= \frac{2\,\nu^n}{(1-n)(2-n)\,\overline{u_i'^2}} \left[\nu + \overline{u_i'^2}\;T\right]^{2-n} - \frac{2\nu^2}{(1-n)(2-n)\,\overline{u_i'^2}} - \frac{2\nu T}{1-n} \tag{2-13}$$

Neglecting terms of order ν in comparison with $\overline{u_i'^2}\;T$, one obtains for large T,

$$\overline{Y_i^2} = \frac{2\,\nu^n}{(1-n)(2-n)\,\overline{u_i'^2}} \left[\overline{u_i'^2}\;T\right]^{2-n} \tag{2-14}$$

$$= 1/2\; C_i^{*2}\,(\bar{u}\;T)^{2-n} \tag{2-15}$$

where the virtual coefficient of diffusion C_i^* is given by

$$C_i^{*2} = \frac{4\,\nu^n}{(1-n)(2-n)(\bar{u})^n} \left\{\frac{\overline{u_i'^2}}{(\bar{u})^2}\right\}^{1-n} \tag{2-16}$$

For the non-isotropic case, Sutton's equation for an instantaneous point source is

$$C(x, y, z, t) = \frac{Q}{\pi^{3/2}\, C_x^* C_y^* C_z^* (\bar{u}\,T)^{3/2[2-n]}} \exp\left[(\bar{u}\,T)^{n-2}\left\{\frac{x^2}{C_x^{*2}} + \frac{y^2}{C_y^{*2}} + \frac{z^2}{C_z^{*2}}\right\}\right] \tag{2-17}$$

and for a continuous point source at the boundary, assuming that the boundary acts as a perfect reflector and can thus be treated by the method of images, the equation is

$$C(x, y, z) = \frac{2Q}{C_y^* C_z^* \bar{u} x^{2-n}} \exp\left[-x^{n-2} \left\{ \frac{y^2}{C_y^{*2}} + \frac{z^2}{C_z^{*2}} \right\} \right] \qquad (2\text{-}18)$$

This expression is valid for constant C_y^* and C_z^* in a uniform velocity field. Sutton introduces a macroviscosity to include the effect of fully rough surfaces; the effect of thermal stability is presumably included in the exponent n for the velocity profile. However, for conditions of the experimental work, the boundary was an aerodynamically smooth surface and stability conditions were approximately neutral. Sutton's Eq. (2-18) is therefore applicable for a point source located at the boundary, for the assumed conditions of constant C_y^* and C_z^* in a uniform velocity field. Except in the region close to the wall, the value of n obtained from actual velocity profiles measured within the boundary layer can be taken as reliable. The generalized diffusion coefficients depend on the intensity of turbulence $\frac{\overline{u_i'^2}}{\bar{u}^2}$, the mean velocity $\bar{u}$, and the parameter n. In deriving Eq. (2-17) and its consequence (2-18), it was assumed that $\bar{u}$, C_y^* and C_z^* remain constant which is not true but it is claimed that the formulation is not sensitive to these discrepancies. For nearly neutral conditions, Sutton's formulas have provided satisfactory working solutions.

Sutton has also offered an expression for an elevated continuous point source. In this expression, he has suggested the use of a mean diffusion coefficient appropriate to the layer defined by the height of the source. This procedure is justified on the basis of a relatively slow variation of C_i^* with height. When there are no buoyancy effects, or loss of particles at the boundary, the relation is given by

$$C(x, y, z) = \frac{Q \exp\left\{\frac{-y^2}{C_y^{*2} x^{2-n}}\right\}\left[\exp\left\{-\frac{(z-h)^2}{C_z^{*2} x^{2-n}}\right\} + \exp\left\{-\frac{(z+h)^2}{C_z^{*2} x^{2-n}}\right\}\right]}{\pi C_y^* C_z^* \bar{u} x^{2-n}} \qquad (2\text{-}19)$$

Experimental Investigations

Because of the non-existence of a model for the turbulent motion in shear flow from which a detailed theory of turbulent diffusion may be formulated, many early investigators carried out field experiments with sources of an idealized nature under selected conditions of terrain and weather. Some important surveys in the atmospheric surface layer were devoted mainly to the determination of the maximum or average level of concentration and the magnitude of the lateral spread under various stability conditions. All of these data and a wide variety of field data, gathered under uncontrolled conditions, did not permit satisfactory correlations with the theoretical results. A brief summary of the main conclusions drawn from the early investigations, namely at the Salisbury Plains, Porton, in 1923, and Cardington, England, in 1931 and reported by Pasquill (14) and at

the Round Hill Field Station of the Massachusetts Institute of Technology and at O'Neill, Nebraska, and reported by Cramer, et al. (4), has been given by Bhaduri (2) in his review of literature.

In the Fluid Dynamics and Diffusion Laboratory of Colorado State University diffusion studies in the turbulent boundary layer have been done by Davar (5), Malhotra (11), Poreh (16), Bhaduri (2), and Quraishi (17) using anhydrous ammonia as a tracer gas.

Davar (5) used a continuous point source over a smooth neutral boundary at an ambient air velocity of 6.0 ft./sec. He varied the source height over a range of 0 to 5 in. He found that for a ground level source the attenuation of ground level concentration with longitudinal distance from the source can be given by the empirical relation

$$C \quad \alpha \quad X^{-1.47} \quad . \tag{2-20}$$

Malhotra (11) used a continuous point source and took data for both neutral and unstable conditions over smooth boundary for velocities 6.5 and 9.0 ft./sec. With his and Davar's (5) data he showed that for both neutral and unstable conditions, the concentration distribution is given by

$$\frac{C(x, y, z)}{C\,max} = \exp\left[-\left\{\left(\frac{y}{\lambda}\right)^{1.95} + \left(\frac{z}{\eta}\right)^{1.40}\right\}\right] \tag{2-21}$$

where the length parameters λ and η are defined by

$$\frac{C(x, \lambda, o)}{C\,max} = 0.5 \tag{2-22}$$

and

$$\frac{C(x, o, \eta)}{C\,max} = 0.5 \quad . \tag{2-23}$$

Malhotra (11) also observed that within the range of Davar's (5) and his experimental data, the dimensionless concentration distribution function was independent of the ambient velocities (range 6.0 - 25.0 ft./sec.).

For the same range of ambient velocities, Malhotra (11) finds that the vertical growth of the plume is also independent of the ambient velocity and is approximated by the relation

$$\eta \propto X^{0.71} \quad . \tag{2-24}$$

From the diffusion data of Malhotra (11) and Davar (5) on the lateral growth of plume spread, Malhotra (11) observes that the rate of growth is not quite independent of the variation of ambient velocities and that it has a tendency to decrease with the increase in ambient velocity but he considers this trend to be erratic and derives an empirical relation between λ and X as follows:

$$\lambda \propto X^{0.6} \quad . \tag{2-25}$$

Bhaduri (2) used a continuous point source with a turbulent boundary layer over a fixed geometric roughness, neutral stability and ambient air velocity of 12.5 ft./sec. His variation of source height was from 0 to 1 in. He found the attenuation law of the form

$$\frac{C(x, y, z)}{C\,max} = \exp\left[- 0.692 \left\{ \left(\frac{y}{\lambda}\right)^{\alpha} + \left(\frac{z}{\eta}\right)^{\beta'} \right\} \right] \quad . \qquad (2\text{-}26)$$

The values of α and β' were slightly different from those of Malhotra (11) and also varied for different source heights. He also found that the dimensionless concentration distribution function was independent of the ambient velocities. The vertical growth of the plume was also found to be independent of the ambient velocity and was approximated by Bhaduri (2) by the relation

$$\eta \propto X^{\beta'}$$

where β' had values of 0.7, 0.6, and 0.56 for source heights of 1/16, 1/2, and 1 in., respectively.

Diffusion in Relation to Spectrum and Scale of Turbulence

Gifford (7) has suggested a mathematical model of continuous source which is unique in the sense that it makes provision for fluctuations of the plume to occur, by separating the total plume dispersion into two components, spreading and meandering. Based on this model, he was able to deduce the various properties of the resulting material concentration distribution. The development of Gifford's ideas is presented next.

A steady state plume dispersion model can be visualized as a superposition of an infinite number of overlapping puffs, each emanating from a fixed origin and being translated by the mean wind. This is

shown in Fig. 1(a). For methematical convenience, dispersion in the direction of mean wind (x-direction) is neglected in practice, leading to the "spreading disk" dispersion model for plumes, shown in Fig. 1(b). Real smoke plumes present a far more complicated appearance. If they are regarded as being formed through the superposition of individual elementary puffs, they might be pictured as in Fig. 1(c). The motion of a plume element seems to consist of an irregular spreading, superimposed on an overall wandering, or meandering, of its center. The fluctuating plume model can also be conceived as being built up of spreading, Gaussian disk elements, like the spreading disk model of Fig. 1(b), except that the position of the disk centers, relative to the x-axis, fluctuates in a random way. Fig. 1(d) illustrates this model schematically. Considering a two-dimension dispersion problem, then, one can write the following expression for the material concentration, C , at any point in a particular cloud of material that is undergoing dispersion:

$$\frac{C}{R} = \left[2 \, \overline{Y^2} \, \bar{u}\right]^{-1} \exp\left[-\frac{(y - D_y)^2 + (z - D_z)^2}{2\,\overline{Y^2}}\right] \qquad (2\text{-}28)$$

where R = rate of emission of meterial at the source,

$\overline{Y^2}$ = variance of the material distribution in individual disk elements,

$\bar{u}$ = mean wind speed, and

D_y, D_z = distances from the x-axis in the y- and z-directions.

The variance $\overline{Y^2}$ is a function of the dispersion time and the disk shape of the plume elements amounts to ignoring dispersion in the x-direction. The instantaneous material concentration in the plume, $\frac{C}{R}$, is a random function, fluctuating at any point as a result of variability of D_y and D_z.

Under the assumption of Gaussian distribution for the mean plume concentration, the average over many trials, M, of the relative concentration distribution is given by

$$M\left\{\frac{C}{R}\right\} = \left[2\,(\overline{Y^2} + \overline{D^2})\,\bar{u}\right]^{-1} \exp\left[-\frac{r^2}{2(\overline{Y^2} + \overline{D^2})}\right] \qquad (2\text{-}29)$$

where $r = (y^2 + z^2)^{1/2}$,

$\overline{D^2}$ = variance of the function $g(r)$, and

g = frequency function associated with the variability of D_y over all trials. The y- and z-dispersion are assumed independent and equal.

In the above analysis, the symbols $\overline{Y^2}$ and $\overline{D^2}$ are used to denote the relative dispersion of a plume element (i.e., a puff) and the dispersion with respect to the x-axis of the center of gravity of a plume element, respectively. Forming the ratio of Eq. (2-28) to Eq. (2-29), it is clear that, for isotropic dispersion, the ratio of peak to average values of concentration should be, essentially,

$$\frac{\text{Peak Concentration}}{\text{Average Concentration}} = \frac{\overline{Y^2} + \overline{D^2}}{\overline{Y^2}} \qquad (2\text{-}30)$$

According to the results of the similarity theory of turbulent dispersion, $\overline{Y^2}$ is expected to vary as $(t - t_o)^3$ for clouds being dispersed by turbulence fluctuations lying entirely in the inertial subrange. On the other hand, $(\overline{Y^2} + \overline{D^2})$ should vary as the square of dispersion time, for small $(t - t_o)$. Both $\overline{Y^2}$ and $(\overline{Y^2} + \overline{D^2})$ must, for large values of dispersion time, vary as $(t - t_o)$. As a result, the expected behavior of the peak-to-average ratio is

$$\frac{\text{Peak Concentration}}{\text{Average Concentration}} \propto \begin{cases} (t - t_o)^{-1}, & (t - t_o) \text{ small} \\ \text{constant}, & (t - t_o) \text{ large.} \end{cases}$$

Hay and Pasquill (9) treated the problem of relating the spread of particles released serially from a fixed point to features of the turbulent flow which can be measured or estimated. They started with Taylor's well-known relation for steady, homogeneous turbulence, which can be written as follows:

$$\overline{Y^2} = 2\,\overline{v'^2} \int_o^T \int_o^t R_L(\xi)\, d\xi\, dt \qquad (2\text{-}5)$$

where Y is the displacement of a particle along the y-axis under the action of the corresponding component of eddy velocity, v', affecting the particle and $R_L(\xi)$ is the correlation coefficient (Lagrangian in type) between this velocity at one instant and the velocity of the same particle at a time ξ later. For horizontal diffusion over level uniform ground, or for diffusion in any plane at positions well away from the ground, it is reasonable to assume quasi-homogeneity and applicability of Eq. (2-5).

Hay and Pasquill attacked the problem of interpreting $R_L(\xi)$ in terms of Eulerian properties by starting with the assumption that Lagrangian and Eulerian correlations are similar in shape and that the ratio of the Lagrangian to the Eulerian scale is a parameter to be estimated from experiments. It can be shown that a change in shape of the correlogram is much less important than a several-fold change in scale. Thus, as long as the requirement of similarity in shape is satisfied roughly, the assumption of precise simliarity is unlikely to introduce large error. Thus, the Lagrangian correlation coefficient $R_L(\xi)$ for a particle might decay with time in a similar manner to the Eulerian correlation coefficient $R_E(t)$ measured at a fixed point, but with a different time scale, i.e.,

$$R_L(\xi) = R_E(t) \quad \text{when} \quad \xi = \beta t \tag{2-31}$$

where β is the ratio of the Lagrangian to the Eulerian time scales. The relation between the corresponding spectral functions $F(n)$, where n is the frequency (cycles/sec.), may then be obtained as follows:

$$\begin{aligned} F_L(n) &= 4 \int_0^\infty R_L(\xi)\, \mathrm{Cos}(2\pi n\xi)\, d\xi \\ &= 4 \int_0^\infty R_L(\beta t)\, \mathrm{Cos}(2\pi n\beta t)\, d(\beta t) \\ &= 4\beta \int_0^\infty R_E(t)\, \mathrm{Cos}(2\pi n\beta t)\, dt \\ &= \beta\, F_E(\beta n) \end{aligned} \tag{2-32}$$

By definition, $F(n)dn$ represents the fraction of the turbulent energy contained in fluctuations of wind speed with frequencies in the range n to $n + dn$ and hence,

$$\int_o^\infty F_L(n)dn = \int_o^\infty F_E(n)dn = 1$$

For a lateral spread of particles $\overline{Y^2}$ after a time of travel T from a continuous point source, Eq. (2-5) can be written as

$$\overline{Y^2} = \overline{v'^2}\ T^2 \int_o^\infty F_L(n) \left\{ \frac{\mathrm{Sin}(\pi n T)}{\pi n T} \right\}^2 dn \qquad (2\text{-}33)$$

where $\overline{v'^2}$ is the variance of the lateral component of particle velocity, v'. Then, from Eqs. (2-32) and (2-33),

$$\overline{Y^2} = \overline{v'^2}\ T^2 \int_o^\infty \beta\ F_E(\beta n) \left\{ \frac{\mathrm{Sin}(\pi n T)}{\pi n T} \right\}^2 dn$$

or

$$\overline{Y^2} = \overline{v'^2}\ T^2 \int_o^\infty F_E(n) \left\{ \frac{\mathrm{Sin}(\pi n T/\beta)}{(\pi n T/\beta)} \right\}^2 dn \qquad (2\text{-}34)$$

This form of Taylor's equation displays a basic property of diffusion from a continuous point source, namely, as travel time from the source point increases and the plume grows in size, the smaller turbulent eddies become increasingly less effective in further diffusion of the plume. The filter function $\frac{\mathrm{Sin}^2(\pi n T)}{(\pi n T)^2}$ is equivalent to smoothing the velocity record by an averaging period T.

As a further simplification, if the time of travel T is not much greater than the period of emission of the particles, it is assumed that

$\overline{v'^2}$ may be equated to the variance of the lateral component of eddy velocity measured at the source over the period of emission. Thus, the dispersion of particles after a time of travel T from a continuous point source is determined completely by β , $\overline{v'^2}$, and the form of $F_E(n)$, and the observations of dispersion and turbulence may be used to evaluate β . Hay and Pasquill tested their analysis scheme on a series of eight diffusion experiments, where σ_t^2 , the variance of the arc wise tracer distribution, was maesured at a travel distance of 100 m., by computing the appropriate value of β for each experiment. They obtained β ranging, for the most part, from 1 to 10 with an average value of 4 and then went on to show that using this average value was of significant practical value in predicting values of σ_t^2 .

Baldwin and Mickelson (1) assumed approximate equality of Eulerian and Lagrangian time correlations and made Eulerian space-time correlation measurements as well as measurements of dispersion from a continuous point source, both in the center line region of a fully turbulent pipe flow. They used their dispersion data to estimate β and obtained values of β in the range of 4 to 18 . This provided a fairly remarkable comparison of laboratory data with the atmospheric data of Hay and Pasquill, considering the various difficulties faced in running controlled parameter experiments in the atmosphere.

Haugen (8) analyzed selected Prairie Grass experiments to determine the Hay-Pasquill scale factor β and found that an average

value of β equal to four, as suggested by Hay and Pasquill, is obtained only under conditions closely approximating stationary processes. Only 13 of his 35 experiments produced results comparable to those of Hay and Pasquill. For these 13 experiments, the values of β lay between 1 and 10 and the average value was 4.64, not appreciably different from the suggested value of 4 . In addition, no significant or systematic variation of β was noticed with travel distance for these experiments. This observation supports the assumption of a fairly constant scale factor. The remarkably frequent occurrence of β less than unity for other experiments, however, is contrary to expectation and is particularly noteworthy for occurring most consistently in the cases of strong thermal instability and stability. From his investigation of the degree of stationarity in the Eulerian records, he concluded that non-stationary conditions inherently produce non-systematic variations of β with distance as well as the unexpected result of $\beta < 1$. He further asserted that the possibility remained that practical and useful results can be obtained because of the relative insensitivity of $\overline{Y^2}$ to the actual form of $R_L(\xi)$. Thus, even though one might obtain results with large variation in the values of β and values of $\beta < 1$, useful predictions of the particle spread versus travel distance may still be possible by using an average value of β . Finally, Haugen obtained a roughly inverse relationship between β and v' for experiments which produced β-value of greater than one.

In this dissertation, Gifford's ideas regarding the fluctuating plume model for a continuous point source will be applied to the diffusion data of the present study by considering a puff from a short duration point source as being squeezed into a disk element of Gifford's model. Thus, the total dispersion for diffusion from a short duration point source will be separated into the components of spreading and meandering. The Hay-Pasquill scale parameter, β , will then be calculated for the diffusion data of this study by first disregarding the meandering effect and then including it. The effect of meandering on the values of the scale parameter will thus be studied. The β-values for the present case will be compared with those obtained by other investigators for various field and laboratory studies.

Chapter III

THE EXPERIMENTAL SYSTEM AND PROCEDURE

The primary objective of this chapter is to describe the experimental equipment and procedure pertinent to this investigation.

The Equipment

Micrometeorological wind tunnel

The diffusion data were taken in the U.S. Army meteorological wind tunnel of the Fluid Dynamics and Diffusion Laboratory at Colorado State University. A schematic diagram of this wind tunnel is shown in Fig. 2.

The wind tunnel is constructed from plywood on lumber studs supported by a framework of steel. Between the studs there is a layer of 4 in. insulating fibre glass mats which keep hear losses from or heat gains to the inside of the wind tunnel at a low level. The wind tunnel is of recirculating type, that is, the same air is recirculated in the duct. The air enters the test section from a stilling chamber of 18 ft. x 18 ft. cross section through a set of four stainless steel screens and a contraction section in which the area is reduced from 18 ft. x 18 ft. to 6 ft. x 6 ft. The turbulence which is present in the air stream due to action of the fan is reduced by the screens and the

contracted section which also serves to maintain the initial boundary layer at the test section entrance at a minimum thickness. Thus, it is assured that the air enters the test section with uniform velocity and at a low initial level of turbulence.

The air velocity is maintained at a constant value by controlling the revolutions per minute of the propeller with a stabilized DC motor. The speed is set by either adjusting the rpm of the DC motor or by adjusting the pitch of the propeller blades. Since no load changes develop during operation, a constant fan speed assures constant test-section velocities. The test section ceiling was adjusted so that experiments were performed at zero pressure gradient.

The controls for the drive are located in the control room between the test section and the return duct. The control room also houses the mass spectrometer which measures the concentration of helium in helium-air samples.

The performance characteristics of the wind tunnel are described by Plate and Cermak (15). The present study was done at a constant ambient velocity of 20 ft./sec. for the case of neutral stability.

Instantaneous source

The source consists of an injection probe through which a continuous stream of air is emitted into the boundary layer at a mean velocity which is 9.5 ft./sec. in the undisturbed boundary layer at a

point where the source is located. An injection rate of 14.0 ft.^{3}/hr. (corresponding to an exit velocity of 9.5 ft./sec.) was maintained by a Matheson flowmeter (Tube No. 605, flow range 0-120 ft.^{3}/hr.). To this air stream, a volume of helium is added at a predetermined time by means of a helium supply arrangement which is located outside the wind tunnel.

The injection probe was made in the form of a nozzle, with its projecting end being of 3/8 in. O. D. and the narrow end of 1/8 in. O. D. as shown in Fig. 3. It was made of acrylic plastic and was mounted on an aluminum stand so that the height of the center of the injection funnel was 8 in. above the test section floor. Polyethylene or "mayon" tubing of 1/8 in. I. D. was used to connect the injection probe to the helium supply arrangement through a hole in one of the wind tunnel windows.

The helium supply arrangement is shown diagrammatically in Fig. 4. It consists of two three-way brass valves V_2 and V_3 between which a piece of 1/4 in. I. D. copper tubing, 1 ft. long, is held. The length of the copper tubing was predetermined by a calculation based on the mass spectrometer sensitivity, as shown in Appendix B. V_4 and V_5 are solenoid valves which can be energized with the help of a switch in the control box to be described later. Helium gas of 99.9% purity is filled between the valves V_2 and V_3 at atmospheric pressure and these valves are then placed in position

2 in order to hold the gas between them. When the solenoid valves are not energized, air from a displacement type vacuum pump takes path 1 through V_4 and V_5 and the flowmeter to the wind tunnel. The flowmeter is adjusted at the desired flow rate with the air passing through it. When the solenoid valves are in energized state, the air takes path 2 through valves V_4, V_2, V_3, and V_5 to the wind tunnel, thus carrying with it helium gas which enters the atmosphere of the wind tunnel as a helium puff. At the above-mentioned flow rate of 14.0 ft.^{3}/hr., the helium gas which is contained in the 1/4 in. I. D. tubing of one foot length of the supply arrangement comes out of the source nozzle in approximately 0.1 sec.

In order to investigate whether the helium supply arrangement released helium puffs of a constant strength each time, a part of the copper tubing (provided to store helium between valves V_2 and V_3) was cut out and replaced by a 1/4 in. I. D. polyethylene tubing. The modified tubing was then filled with 0.5% standard helium mixture (containing 99.5% nitrogen) at atmospheric pressure. The concentration of the helium mixture in the tubing was determined by inserting a hypodermic needle from the standard leak end of the mass spectrometer into the plastic part of the tubing between V_2 and V_3. The experiment was repeated several times and a new plastic tubing was used each time. It was noticed that the concentration readings were identical within 5% in each case. Therefore, a helium puff of constant strength was released during each experiment.

The sampling system

The sampler system consists of the sampling probe, through which the helium-air sample is withdrawn from the wind tunnel, and the sampler with sampling traps. The detailed drawing of the sampling system is given in Fig. 5.

The sampling probe was made of copper tubing (1/8 in. O.D.) and was held parallel to the streamline at the sampling point on a manually adjustable stand. One-eighth in. I.E. polyethylene tubing was used to connect the sampling probe to the sampler which was also placed inside the wind tunnel. Care was taken to make the plastic tubing as short as possible. As will be shown later, the tubing length did not appreciably affect the concentration pattern.

The sampling apparatus consists of an aluminum base (22 in. x 3 in. x 3/8 in.) which is fastened to a wooden base structure with hinges. L-shaped brackets are screwed onto the base plate in such a way that between each pair of brackets there is just enough space for an aluminum lever (3 in. x 1/2 in. x 1/16 in.) to move in the vertical plane. The free ends of the 21 levers are connected to solenoids with piano wire loops which are fastened to the solenoids. The solenoids are also fastened to the wooden base structure. One-eighth in. I.D. polyethylene tubing fits into the slot provided along the length of the base plate under the sluminum levers. When the solenoids are actuated, the tubing is divided by this arrangement

into twenty 0.9 in. long compartments. The current for all the solenoids is supplied through a switch in the control box which controls the operation of taking the diffusion data. After the plastic tubing containing the samples is clamped shut, the levers are held in their position by a steel rod which is inserted through the holes in the brackets. The base plate with the clamped samples can be removed from the wooden structure so that the samples can be moved without carrying the heavy wooden part with the solenoids.

The size of the solenoids was determined from preliminary experiments with a single bar and a piece of 1/8 in. I.D. plastic tubing. By using a mechanical advantage of 3, the minimum weight required to close the tubing completely was determined experimentally and was used to specify the pulling force and the stroke of the solenoids.

The control system

The release of the helium puff and the energization of the solenoids are synchronized through a control box whose performance is giverned by a timer. The sampling apparatus, timer, and the helium supply arrangement are connected to the control box. A switch on the panel of the control box is pressed to actuate the solenoid valves of the supply arrangement which can be de-actuated by operating the switch again. The control box also serves as the relay station which provides the time delay between actuating of the helium supply system and the solenoids. If a time, t sec., is set on the timer,

then t sec. will elapse between the actuation of the supply system (thereby letting a helium puff out in the wind tunnel) and the operation of the solenoids (thereby collecting a sample of helium-air cloud in the sampler).

A reliable timer is necessary to obtain identical conditions for all experiments. Approximate calculations of time needed for the helium in the supply system to reach the sampler indicated that a timer with an upper limit of 15 sec. was required. The timer selected for this purpose (Lectra Laboratories, New York; range 0-100 sec. in intervals of 0.1 sec.) was calibrated with an electronic counter and showed excellent reproducibility .

The rate at which the samples were withdrawn from the wind tunnel in actual diffusion data was adjusted with a Matheson flowmeter (Tube No. 602, range 0-800 $cm.^3/min.$) at 190 $cm.^3/min.$ This suction rate corresponded to an average velocity of 1.31 ft./sec. through the plastic tubing between the sampling probe and the sampler.

The mass spectrometer

For measuring the concentrations of the helium-air samples, a leak detector type mass spectrometer (Model MS-9A, Vacuum Electronics Corp.) was employed. A hypodermic needle was directly connected to the standard leak which formed the inlet of the mass spectrometer vacuum chamber. In order to measure the helium concentration in a sample contained in polyethylene tubing, the needle

was inserted into the tubing. The concentration reading can be taken directly from the meter or, alternatively, can be plotted as a function of time on a sensitive recorder.

Calibration of mass spectrometer readings

After each concentration profile, the mass spectrometer is calibrated by noting the readings obtained with three different helium-nitrogen standard mixtures (containing 0.5%, 0.2% , and 0.05% helium). These standard mixtures were chromatographically tested for their helium contents and were found to conform to their guaranteed specifications within ± 10%. A calibration plot between the mass spectrometer scale reading and the ppm helium is then constructed by joining the three points obtained with the standard mixtures. This calibration plot yields a straight line on a log-log paper and subsequent calibrations also are straight lines parallel to others. The change in calibration lines is due to changes in sensitivity of the mass spectrometer. This change in sensitivity is especially significant in the first few hours after the electronics of the machine has been turned on. With the passage of time, the sensitivity of the machine becomes more and more stable and the calibration remains fairly constant. When the sensitivity of the machine is very low, as indicated by very low calibration readings, the mass spectrometer needs a "tune-up" which requires replacing the standard leak by the sensitivity calibrator, SC-4 , and following the recommended procedure to bring the indicator

reading to its maximum possible value. The sensitivity calibration is more frequently necessitated in the first few hours after starting the mass spectrometer.

A calibration curve depends on the standard leak rate and thus different standard leaks will yield different calibration curves. The calibration plot for a particular standard leak can be extended beyond the end points so that helium concentration in ppm can be extimated corresponding to mass spectrometer readings over a large range.

The calibration plot can be represented by the relation

$$y = A\, x^{n} \qquad (3\text{-}1)$$

which gives a straight line plot between $\log y$ and $\log x$. In Eq. (3-1), x is the concentration of helium in ppm and y is the mass spectrometer indicator reading.

Sources of errors

It was considered significant to estimate the correspondence between the mass spectrometer readings and the concentration at the sampling point in the wind tunnel. For this purpose, the various sources of error were investigated with the help of some special experiments outside the wind tunnel and the results of these investigations are presented next.

(1) Sample storing time: The length of time for which the sample is stored after the sampling process may somewhat change

the concentration reading as a result of diffusion through the tubing. The samples were stored for various lengths of time after having been made and were then analyzed for their helium content by recording the output of the mass spectrometer as a function of time on a recorder. No appreciable change in the maximum concentration reading or the concentration-time pattern was detected.

(2) Tubing length: The length of the plastic tubing in which the helium-air sample is collected may or may not have significant effect on concentration measurements with a mass spectrometer. For the investigation of this effect, several tubing lengths ranging from 1.0 in. to 8.0 in. were taken for making the samples. The results with three different tubing lengths, namely 2.0 in., 5.0 in., and 8.0 in., are shown in Fig. 6. These results show that the tubing length has negligible bearing on concentrations.

(3) Sample withdrawal time: It was feared that the mass spectrometer reading would change rapidly with time due to change of pressure across the standard leak which results from the withdrawal of the sample from the plastic tubing. A theoretical calculation (as reproduced in Appendix A) was performed with pressure data supplied from a special experiment which showed that even the largest leak rate would give a well-defined reading for a sample tubing of 1/8 in. I.D. and 5.0 in. length. Experiments were performed to check the calculations. A typical experimental result with a standard gas containing 0.05% helium and 99.95% nitrogen is shown in Fig. 7.

These experiments were conducted using all three available standard leaks with flow rates of 86.0, 15.0, and 3.0 μ CFH. The results show that even for the largest leak rate, the reading has dropped by only 10% over a recording period of 500 sec. and so it is concluded that the withdrawal rate would not appreciably affect the concentration reading over reasonably long time intervals.

In the above described investigations, helium-air samples were made by a special procedure which is shown diagrammatically in Fig. 8. In this procedure, the 1/8 in. I.D. plastic tubing was connected to the helium tank containing a standard helium-nitrogen mixture. The pressure gas valve was opened only slightly, thereby ensuring flow of the gas through the plastic tubing at a low pressure. After making sure that the gas was coming out of the free end of the tubing, the tubing was clamped first at position 1 and then at 2; the distance between points 1 and 2 had been decided in advance. Finally, the tubing was cut at 3 and analyzed. The probe thus consisted of a known volume of helium-air sample, contained between points 2 and 1, of known concentration , at atmospheric pressure.

(4) Variation in standard gas specifications: In order to verify the manufacturers' specifications on the standard helium-nitrogen mixtures, the latter were chromatographically tested and were found to conform to the specified helium concentrations within ± 10%. Thus, the standard mixture guaranteeing 0.5% helium (5,000

ppm) was actually found to contain (0.5 ± 0.05)% helium. This, however, is a systematic error which should not affect the observed results.

(5) Stability of mass spectrometer: The sensitivity of the mass spectrometer plays a major role in concentration measurements. It can change rapidly, and these changes are not always easy to be accounted for. As a precaution, the machine is calibrated after the analysis at each point or about every 30 min. but this does not take care of the sensitivity changes undergone during this period. Changes in temperature and other external conditions of the laboratory can affect the sensitivity to some extent.

(6) Indicator reading: The concentration reading on the mass spectrometer indicator scale was recorded by reading the average location of the needle. Sometimes, when the indicator shows fluctuations around a mean value, the mean value could be somewhat different from the actual reading.

(7) Sampling time: The length of time for which the helium-air mixture sample is drawn into MS-9 from the tubing compartment in the sampler can be an important factor in measuring concentrations. In order to investigate the effect of this sampling time, several samples at a point in the wind tunnel were analyzed for various time intervals and the concentrations of helium in ppm were obtained from the calibration plots for the same time intervals. During this time, the mass

spectrometer reading rises from 0 to a final steady value. It was found that a sampling time of 1.0 min. would be required for the mass spectrometer reading to become steady. Reduction of sampling time changed the concentration appreciably although no quantitative estimate of the error due to this reduction was made. Based on the finding of this investigation, it was decided to analyze each sample for 1.0 min., thus minimizing the possibility of error as a result of insufficient sampling time.

(8) Background contamination: Since the tunnel used for the present investigation was of recirculating type, it was feared that the concentration level of the ambient air might keep building up. To get a quantitative idea of the helium concentration in the free stream, the sampling probe was raised to about 2.5 ft. above the floor, and samples of ambient air were collected in the sampler several times during a typical experimental day. The ambient concentration was found to be negligibly small in each case and it was thus concluded that no appreciable background contamination existed for the present study.

(9) Distortion of diffusion cloud through the tubing:

(a) Suction side tubing - In order to investigate any possible distortion of the diffusion cloud during its passage through 3 ft. long plastic tubing (when the cloud is sucked from the sampling probe to the sampler), a special experiment was conducted outside the wind

tunnel. In this experiment, the helium supply arrangement was directly connected to the sampling apparatus through 3 ft. of polyethylene tubing of the same size as used to connect the sampling probe to the sampler in taking the diffusion data in the wind tunnel. The other end of the tubing in the sampler was connected to a suction pump so that the average velocity in the tubing was 1.31 ft./sec., which was the value of the suction velocity maintained throughout the measurements of the present study. The 1/4 in. I. D. copper tubing in the helium supply arrangement was then filled with a standard gas mixture containing 0.2% helium by weight. Using the control box and timer, helium was released from the source and was trapped in the sampler by solenoids. Because of difference in diameters of the copper tubing of the supply system and the plastic tubing connecting the supply system to the suction pump through the sampler, the helium originally contained in 1 ft. long copper tubing would extent to 4 ft. in the 1/8 in. I. D. plastic tubing. By usind a proper timer setting, a response pattern was obtained in which the concentration reading increased from approximately zero to a steady value of 6.5 through about five compartments along the length of the sampler. This showed that the instantaneous pulse actually becomes a continuous pulse of short duration. Several experiments at the same timer setting produced identical patterns. A typical result is shown in Fig. 9. The steady concentration value on the mass spectrometer scale corresponded

to approximately 2,000 ppm (0.2%) helium, from calibration charts at the specified sensitivity.

The plot shown in Fig. 9 indicates resemblance with the response of a continuous source except that, in the case of a continuous source, the concentration reading continues to maintain the steady value and does not drop to zero again. The response in Fig. 9 is then an accumulative or integrated form of a time instantaneous pulse and can be interpreted as the response to a continuous pulse of short duration. In order to determine the variance of this curve, slopes $f(x_i)$ at various values of x_i (along the sampler length) were determined and a new curve for $f(x_i)$ vs. x_i was plotted. The variance of this curve was then graphically calculated from the general formula:

$$\sigma^2 = \frac{\int_0^\infty x_i^2 \, f(x_i) \, dx_i}{\int_0^\infty f(x_i) \, dx_i} - \left[\frac{\int_0^\infty x_i \, f(x_i) \, dx_i}{\int_0^\infty f(x_i) \, dx_i} \right]^2 \qquad (3\text{-}2)$$

The value of the variance was calculated to be 0.005 ft.^{2} (or standard deviation = 0.07 ft.) which is a measure of the distortion of the diffusion cloud through the tubing.

This distortion can alter the shape of the concentration profiles which are obtained in the diffusion experiments. The spread of the profile, as given by variance, would then change and the corrected value of the variance for the data would be given by

$$\sigma^2 = \sigma_1^2 - \sigma_2^2 \qquad (3\text{-}3)$$

where σ_1^2 = variance of longitudinal dispersion,

and σ_2^2 = 'source directly connected' variance.

Considering that a time of approximately 0.1 sec. is needed for the whole helium puff to come out of the injection source, one finds that a length of 4 ft. in the directly-connected experiment corresponds to 1.31 x 0.1 = 0.131 ft. of the wind tunnel experiment in which the distance between the source and the sampler was exposed to diffusion in the atmosphere of the wind tunnel. Therefore, the corresponding value of σ_2^2 in terms of the wind tunnel experiment will be 0.000005 ft.^{2}. This value of σ_2^2, which represents the distortion of the diffusion cloud through the suction tubing, is about 0.5% of the minimum value obtained for σ_1^2 (0.0010 ft.^{2}) under the assumption that the longitudinal dispersion variance σ_1^2 is approximately equal to the lateral variance for spreading, $\overline{Y_y^2}$. It will, therefore, be justifiable to assume that the distortion that the diffusion cloud undergoes by its passage through the suction tubing does not significantly alter the shape of the concentration profiles.

(b) Source side tubing - In order to investigate the effect of the source tubing on the diffusion characteristics of the present study, several experiments were performed by placing the sampling probe within the nozzle of the source. In these experiments, the distance between the base of the source nozzle and the sampling

probe was kept at 1.0 in. or less. When the concentration samples were analyzed with the mass spectrometer, concentration profiles similar to the diffusion profiles were obtained. This observation appears to indicate that the source has a definite effect on the helium puff emanating from the nozzle.

The data of the direct-connection experiments were also used to obtain an estimate of error due to experimental set-up without source. For this purpose, the concentration readings at some arbitrary point along the sampler length were chosen for different experiments with constant reference concentration and the mean and variance of the readings were computed. The coefficient of variance (ratio of standard deviation to mean) was found to be 0.04. This analysis did not include the error due to the source since the source was not used for direct-connection experiments.

(10) Manual control:

(a) Since the injection and suction flowmeters are adjusted manually, there is a probability of error due to minor shifts in adjustments.

(b) The timer was calibrated with an electronic counter and was found to have a precision error of less than ± 1%.

(c) The Trans-Sonics Manometer, which is used to adjust the ambient velocity in the wind tunnel, has an error of less than 1% (pressure) when compared with an alcohol tilting pressure tube.

In order to estimate the total possible error due to all the above described sources, the diffusion data of the wind tunnel experiments in the present study were examined at several arbitrary points in the diffusion field. For 8 to 10 samples at a point, the coefficient of variation was found to be 0.3 or less for these cases. However, this estimate includes the effects of diffusion and meandering as well.

Consecutive profiles at a point

The concentration data of the present study were used to estimate the number of consecutive concentration samples to be taken at a point in the wind tunnel such that the mean of these samples would not differ from the true mean (mean of infinite observations) by more than 15%. For this purpose, the following statistical procedure was adopted:

If μ is the true mean (mean of an infinite number of samples) at a point in the wind tunnel and $\bar{x}_m$ is the mean of m samples at that point, then, in order that $\bar{x}_m$ may not differ from μ by more than 15%, one finds

$$\left| \bar{x}_m - \mu \right| \leq 0.15\,\mu \tag{3-4}$$

Now, if we are interested in finding m such that condition (3-4) may be stated with 85% confidence, then

$$P\left[\left| \bar{x}_m - \mu \right| \leq 1.45\,\sigma_{\bar{x}_m} \right] = 0.85 \tag{3-5}$$

But, since $\sigma_{\bar{x}_m} = \frac{\sigma_x}{\sqrt{m}}$ where σ_x is the standard deviation based on individual observations, one obtains

$$1.45 \frac{\sigma_x}{\sqrt{m}} = 0.15\mu \tag{3-6}$$

which can be written as

$$m = 9.6 \left(\frac{\sigma_x^2}{\mu^2} \right) \tag{3-7}$$

σ_x^2 and μ are replaced by s^2 and $\bar{x}$, which are the sample estimates of variance and mean, to calculate m. Strictly speaking, one will have to use the "t-distribution" with m degrees of freedom to determine the factor in front of $\frac{\sigma_x}{\sqrt{m}}$ in Eq. (3-6), but since m is unknown, the above approximate solution has been adopted. Thus, m can be estimated from the relation

$$m = 9.6 \left(\frac{s^2}{\bar{x}^2} \right) \tag{3-8}$$

Calculations based on s and $\bar{x}$ from the concentration data of the wind tunnel showed that 8 to 12 consecutive concentration samples would be required to limit the deviation of the mean of these samples from the true mean to 15%.

Plan of Data

Concentration data

The height and location of the source were maintained constant throughout this investigation. The source was located at a distance

of 24 ft. from the leading edge of the aluminum plate where the boundary layer thickness is approximately 16 in. Starting with the point directly downstream from the source center, diffusion data were taken around this point in both lateral and vertical directions. Eight or more consecutive profiles were taken at each point. The operating procedure for concentration data is given in Appendix D.

Velocity data

The statistical analysis of the concentration data, outlined in the next chapter, requires the use of local mean velocity at each point in the wind tunnel where the concentration profiles are obtained. Measurements of sampling point velocities were made by using a micromanometer (Trans-Sonics, Inc.) to measure the pressure difference between the dynamic pressure, as indicated by a pitot tube mounted 2.5 ft. above the floor of the test section, and the wall pressure in the wind tunnel. The manometer error is less than 1% (pressure) when compared with an alcohol tilting pressure tube. The wind velocity was obtained from the manometer reading by using the following relation based on Bernoulli's equation:

$$u = K_1 \sqrt{\Delta h} \qquad (3\text{-}9)$$

where u = wind velocity

Δh = pressure difference as indicated by the manometer, and

K_1 = a constant dependent upon air temperature and atmospheric pressure.

Since the closest point from the floor of the test section was at 6 in., the pitot tube could be relied upon to give satisfactory results. The same pitot tube arrangement was also employed to adjust the free stream velocity at 20 ft./sec.

Chapter IV

EXPERIMENTAL RESULTS

When the helium puff leaves the source, its diffusion in the atmosphere of the wind tunnel is coused by two major factors: (a) the mean wind motion which carries the puff downstream and (b) the turbulent velocity fluctuations which disperse helium particles in three dimensional space. After an interval of time, the center of the puff will be at a distance from the source depending on the mean wind velocity, and the puff will have grown to a size and shape dependent on the turbulent diffusion. Consequently, an analysis of the concentration data for diffusion from an instantaneous point source must account for the motion of the puff in the mean wind direction as well as the diffusion process in the puff.

Statistical Analysis of Data

Consider the motion of a spherical puff in the mean wind direction as shown in Fig. 11. The three-dimensional concentration distribution in the puff is also shown. As the expanding puff arrives at the sampling probe, located at a point (x, y, z) of the diffusion field, a part of the cloud enters the sampling probe and is moved over the length of the sampler, also shown in Fig. 11. Then, for a

symmetrical distribution of concentration over the sampler, the following parameters can be defined:

1. $c(x_i)_{max} = c(x_i)_{max}(x, y, z, t)$ = the maximum instantaneous concentration at the point (x, y, z). Here x_i is the distance from the front end of the sampler where the cloud first enters, and $c(x_i)$ is the concentration on the distribution profile over the sampler corresponding to distance x_i.

2. $C_p = C_p(x, y, z, t)$ = the equivalent concentration from a continuous point source, at point (x, y, z), and is given by the area of the concentration profile over the sampler length. Because of the diffusion characteristics of the source, the diffusion cloud behaves more like a continuous source of short duration than an instantaneous source. Therefore, C_p is the basic quantity on which all analyses are based.

3. $$\overline{C} = \frac{1}{T}\int_o^T C_p\, dt = \frac{1}{m}\sum_{i=1}^{m} C_{p_i} \qquad (4\text{-}1)$$

In Eq. (4-1), $\overline{C}(x, y, z)$ is the average of C_p - values obtained from m consecutive profiles over the sampler, with the sampling probe at the same point in the diffusion field. Statistically, $\overline{C}$ is the time average of the continuous source concentration at a point (x, y, z) according to the ergodic hypothesis.

4. $$\sigma^2_{C_p} = \frac{\sum_{i=1}^{m}\left(C_{p_i} - \overline{C}\right)^2}{m-1} \qquad (4\text{-}2)$$

where $\sigma^2_{C_p}$ is the variance of C_p and is a measure of the spread of C_p . It provides an estimate of the accuracy of the time-averaged concentration $\overline{C}$ at a point.

Concentration Data

The concentration data at different y and z for stations X = 1, 2, 3, 4 ft. are presented in dimensionless form in Fig. 12 and Fig. 13. Fig. 12 gives the dimensionless concentration $\frac{\overline{C}}{\overline{C}_{max}}$ as a function of $\frac{y}{\sigma_y}$ where σ^2_y is the variance of $\overline{C}$ in the lateral direction and is obtained from the distribution of $\overline{C}$ along the y-axis for z = 8 in. with the help of the following relation:

$$\sigma^2_y = \frac{\sum y^2 \overline{C}}{\sum \overline{C}} - (\overline{y})^2 \qquad (4\text{-}3)$$

where $\overline{y} = \frac{\sum y \overline{C}}{\sum \overline{C}}$

Fig. 13 shows the dimensionless concentration $\frac{\overline{C}}{\overline{C}_{max}}$ as a function of $\frac{z}{\sigma_z}$ where σ^2_z is the variance of $\overline{C}$ in the vertical direction and is computed from the $\overline{C}$ - distribution along the z-axis for y = 0 with the help of the following relation:

$$\sigma^2_z = \frac{\sum z^2 \overline{C}}{\sum \overline{C}} - (\overline{z})^2 \qquad (4\text{-}4)$$

where $\overline{z} = \frac{\sum z \overline{C}}{\sum \overline{C}}$

The profiles in Fig. 12 and Fig. 13 are similar. The calculated values of σ_y^2 and σ_z^2 are given below:

Station	$10^4 \times \sigma_y^2$, ft.^{2}	$10^4 \times \sigma_z^2$, ft.^{2}
X = 1 ft.	27.0	25.7
X = 2 ft.	63.4	71.6
X = 3 ft.	65.2	84.7
X = 4 ft.	114.0	110.0

The variances σ_y^2 and σ_z^2 are plotted as functions of dispersion distance X in Fig. 14 which shows a linear relationship between σ_y^2 and X and also between σ_z^2 and X . Thus, one obtains

$$\sigma_y^2 \alpha X = \bar{u} T \tag{4-5a}$$

which gives

$$\sigma_y^2 \alpha T \tag{4-5b}$$

where T is the dispersion time.

Similarly,

$$\sigma_z^2 \alpha X = \bar{u} T \tag{4-6a}$$

from which

$$\sigma_z^2 \alpha T \tag{4-6b}$$

The results given by Eqs. (4-5b) and (4-6b) have also been obtained by Gifford (7) for large dispersion times, under the assumption of isotropic turbulence.

The consideration that $\overline{C}$ is the time average of the continuous source concentration at a point provides a useful method of comparing the concentration data of an instantaneous point source with those of a continuous point source. The experimental law for attenuation of source level ($H = z = 8$ in., $\frac{H}{\delta} \simeq 0.5$) concentration for the present work is given by

$$\overline{C}_{max} \sim X^{-1.45} \tag{4-7}$$

This relationship between $\overline{C}_{max}$ and X for $y = 0$ is presented in Fig. 14.

The relationship in Eq. (4-7) compares closely with Davar's (5) experimental law for concentration at $H = z = 2$ in., $\frac{H}{\delta} \simeq 0.66$, given by

$$C \sim X^{-1.43} \tag{4-8}$$

It should be noted that the above comparison is made at $\frac{H}{\delta} \geq 0.5$ for which the mean velocity $\overline{u}$ is essentially constant, so that $\overline{u}\,C$ is determined by the distribution of C.

In Fig. 14 are also plotted the $\overline{C}_{max} \cdot \sigma_y \cdot \sigma_z$ values against the travel distance X. If the concentration distribution were governed by similarity, then one should obtain the following relationship:

$$\overline{C}_{max} \cdot \sigma_y \cdot \sigma_z \simeq \text{constant} \tag{4-9}$$

From Eq. (4-9) and Eqs. (4-5a) and (4-6a), one obtains the following form for $\overline{C}_{max}$:

$$\overline{C}_{max} \sim X^{-1} \tag{4-10}$$

However, the data of the present study show that $\overline{C}_{max}$ varies as $X^{-1.45}$, as shown in Eq. (4-7) . Davar's data, expressed in Eq. (4-8), also give a similar relationship. This discrepancy can find its explanation only in the fact that perhaps the similarity assumption is not valid. This conclusion, however, is not borne out by the experimental data.

In order to obtain a realistic estimate of the shape of the diffusion cloud at different stations, isoconcentration contours were drawn by using the average concentration $\overline{C}$ at different y and z for each station. These contours are presented in Fig. 15 to Fig. 18. It appears that the helium puff has a circular cross section in the mean wind direction.

Velocity Field

Although no velocity profiles were actually taken by the author, the mean velocities at all the sampling points in the wind tunnel were measured. Fig. 19 gives the typical velocity profiles in the wind tunnel employed for the diffusion data of the present study. The velocity profiles in Fig. 19 are based on data by Sandborn and Marshall (18) at X_i = 0, 10, 20, 30, 69 ft. for U_∞ = 30 ft./sec. These velocity

data show similarity, as evidenced from the plot of $\frac{\bar{u}}{U_\infty}$ vs. $\frac{z}{\delta}$ in Fig. 19. The following relationship is obtained for the velocity data:

$$\frac{\bar{u}}{U_\infty} = \left(\frac{z}{\delta}\right)^{\frac{1}{7.5}} \qquad (4\text{-}11)$$

Turbulence Field

The turbulence structure of the flow ever a smooth boundary can be arbitrarily divided into three zones: (a) a shallow region close to the wall where the flow is predominantly viscous and thus the molecular forces are significant, (b) a buffer zone where turbulence is present but the viscous effects are also important, and (c) a turbulent region where turbulence characteristics predominate and the effects of viscosity can be neglected when compared with the turbulent effects. In the case of a two-dimensional boundary layer, experimental investigations have been mostly used to formulate the mechanisms of turbulence and that of related transport processes and, therefore, the existing theories which can be used for interpreting these mechanisms are only of semi-empirical character.

A turbulent region is characterized by chaotic agitations or "eddies" which are responsible for the mechanism of turbulent diffusion. In a boundary layer over a smooth wall, the generated turbulence is non-isotropic and non-homogeneous. It tends to assume isotropy and homogeneity in the uppermost part of the boundary layer near the free stream. The eddies are very small close to the boundary

and gradually increase in size with distance from the wall. The mechanism of momentum and mass transfer is intimately connected with the eddy structure of the flow but a comprehensive theory giving a complete explanation of the phenomenon is lacking.

The degree of turbulence in a flow field is commonly expressed by the relative intensities $\frac{u'}{U_\infty}$, $\frac{v'}{U_\infty}$, and $\frac{w'}{U_\infty}$ in the longitudinal, lateral, and the vertical directions, respectively. Figure 20 gives the dimensionless relationships of $\frac{u'}{U_\infty}$ vs. $\frac{z}{\delta}$ from data by Sandborn and Marshall (18) for $U_\infty = 30$ ft./sec. at $X_i = 69$ ft., $\frac{w'}{U_\infty}$ vs. $\frac{z}{\delta}$ from data by Cermak and Chaung (3) for $U_\infty = 10$ ft./sec. at $X_i = 78$ ft., and $\frac{v'}{w'}$ vs. $\frac{z}{\delta}$ from data by Klebanoff (10) for smooth wall with zero pressure gradient. No measurements of $\frac{v'}{U_\infty}$ were made for the wind tunnel in which the diffusion data of the present study were taken. From Klebanoff's data in Fig. 20 , it is clear that for the greater part of the height, $\frac{v'}{w'} = 1.2$ is a fairly close approximation. This relationship between v' and w' has been used in later sections of this study.

One-dimensional energy spectrum density function was determined from the recorded values of horizontal longitudinal $\overline{u^2}$ between frequencies n and $(n + dn)$ by Sandborn and Marshall (18). Fig. 21 gives the data of Sandborn and Marshall at $X_i = 69$ ft. in the form of plots of F vs. wave number k for $\frac{z}{\delta} = 0.167$, 0.500 , and 0.750 at $U_\infty = 30$ ft./sec. The spectra here are plotted in wave number coordinates which are related to frequency by relations:

$$k = \frac{2\pi n}{u} \quad \text{and} \quad F_1(k) = \frac{u}{2\pi} F_2(n) \tag{4-12}$$

The analysis of the experimental data, presented in this chapter, is given in the next chapter.

Chapter V

ANALYSIS OF EXPERIMENTAL DATA

The two main objectives of the present study were: (a) to study diffusion from an instantaneous point source in relation to spectrum and scale of turbulence, and (b) to obtain diffusivity characteristics of the turbulent flow.

Spreading and Meandering of the Diffusion Cloud

Gifford's mathematical model of a continuous point source, described in Chapter II, can be conceived as being built up of spreading Gaussian disk elements and differs from other models in that it provides for the fluctuations of the plume to occur by separating the total plume dispersion into two components, spreading and meandering. The mean concentration distribution derived from the fluctuating plume model is identical with the material concentration in steady plume models. Other important properties such as the variance of point concentration, and the frequency distribution of point concentrations which do not follow from steady plume models, can be obtained with the fluctuating plume model. Thus, the fluctuating plume model provides a rational approach to practical air pollution

problems which depend on concentration properties other than the mean level of concentration.

By considering a helium puff from the point source of this study as being squeezed into a disk, Gifford's ideas can be usefully applied to diffusion for this disk and hence, the components of spreading and meandering can be separated. The results obtained on the basis of Gifford's model can also be arrived at from similarity considerations, as presented next.

Consider the distribution of concentrations $C_p(x, y, z, t)$ and $\overline{C}(x, y, z)$ in the y- and z-directions at station X. C_p is the equivalent concentration from a continuous point source, and its distribution at different points of the same station is shown in Fig. 22. The C_p-distribution thus represents an instantaneous picture of the cloud and this distribution does not change with respect to the center of the cloud. The center, however, can be shifted in location due to fluctuations in the turbulence field. Thus, one always obtains the same peak value of C_p in spite of the shift in the center of the C_p-distribution.

Considering a fixed X and essentially constant velocity, the concentration C, at any point (y, z) for this station, can be written on the basis of similarity considerations as follows:

$$\frac{C}{\overline{C}_{max}} = f\left[\frac{y}{\sigma_y} ; \frac{z}{\sigma_z}\right] \qquad (5-1)$$

and

$$\frac{C}{(C_p)_{max}} = f\left[\frac{y}{(\overline{Y_y^2})^{1/2}} \; ; \; \frac{z}{(\overline{Y_z^2})^{1/2}}\right] \tag{5-2}$$

where σ^2 and $\overline{Y^2}$ are the variances for the $\overline{C}$- and C_p-distribution, respectively, and functions f on the right-hand side of Eqs. (5-1) and (5-2) are the same.

Integration over an area dA gives

$$\int_{-\infty}^{\infty} C\,dA = (C_p)_{max}\left\{\int_{-\infty}^{\infty} f\left[\frac{y}{\sigma_y} \; ; \; \frac{z}{\sigma_z}\right] d\left(\frac{y}{\sigma_y}\right) d\left(\frac{z}{\sigma_z}\right)\right\} (\sigma_y \sigma_z) \tag{5-3}$$

and

$$\int_{-\infty}^{\infty} C\,dA = (C_p)_{max}\left\{\int_{-\infty}^{\infty} f\left[\frac{y}{(\overline{Y_y^2})^{1/2}} \; ; \; \frac{z}{(\overline{Y_z^2})^{1/2}}\right] d\left[\frac{y}{(\overline{Y_y^2})^{1/2}}\right] d\left[\frac{z}{(\overline{Y_z^2})^{1/2}}\right]\right\}$$

$$\left[(\overline{Y_y^2})^{1/2} (\overline{Y_z^2})^{1/2}\right] \tag{5-4}$$

Equating Eqs. (5-3) amd (5-4) , one obtains

$$\overline{C}_{max} \cdot \sigma_y, \sigma_z = (C_p)_{max} (\overline{Y_y^2})^{1/2} (\overline{Y_z^2})^{1/2}$$

which gives

$$\frac{(C_p)_{max}}{\overline{C}_{max}} = \frac{\sigma_y \sigma_z}{(\overline{Y_y^2})^{1/2} (\overline{Y_z^2})^{1/2}} \tag{5-5}$$

Since the variance of the total plume dispersion, σ^2 , is the sum of variances due to spreading and meandering, one can write

$$\sigma_y^2 = \overline{Y_y^2} + \overline{D_y^2} \tag{5-6}$$

$$\sigma_z^2 = \overline{Y_z^2} + \overline{D_z^2} \tag{5-7}$$

where $\overline{D^2}$ = the variance due to plume meandering.

Combining Eqs. (5-5), (5-6), and (5-7), one has

$$\frac{(C_p)_{max}}{\overline{C}_{max}} = \frac{\sqrt{\overline{Y_y^2} + \overline{D_y^2}} \quad \sqrt{\overline{Y_z^2} + \overline{D_z^2}}}{(\overline{Y_y^2})^{1/2} \quad (\overline{Y_z^2})^{1/2}} \tag{5-8}$$

Gifford (7) considered a special case of isotropic turbulence and assumed that

$$\overline{Y_y^2} = \overline{Y_z^2}$$

and

$$\overline{D_y^2} = \overline{D_z^2}$$

On the basis of the above assumption, Gifford's result, from Eq. (5-8), is

$$\frac{\text{Peak Concentration}}{\text{Average Concentration}} = \frac{\overline{Y_y^2} + \overline{D_y^2}}{\overline{Y_y^2}} \tag{5-9}$$

Since the total dispersion variances in y- and z-direction are nearly equal at all four travel distances for data of the present study, one can assume that $\overline{Y_y^2} = \overline{Y_z^2}$ as an approximation. Then, Eq. (5-8) becomes

$$\frac{(C_p)_{max}}{\overline{C}_{max}} = \frac{\sqrt{\overline{Y_y^2} + \overline{D_y^2}}\ \sqrt{\overline{Y_z^2} + \overline{D_z^2}}}{\overline{Y_y^2}} \qquad (5\text{-}10)$$

With the knowledge of the total dispersion variances in the lateral and vertical directions, namely $(\overline{Y_y^2} + \overline{D_y^2})$ and $(\overline{Y_z^2} + \overline{D_z^2})$ from Eqs. (4-3) and (4-4), the peak concentration $(C_p)_{max}$, and the time average concentration $\overline{C}_{max}$, one can obtain $\overline{Y_y^2}$, the variance due to dispersion by spreading in the lateral direction. Realistically, the peak concentration $(C_p)_{max}$ must be replaced by an estimate of $(C_p)_{max}$ on the basis of a large number of samples. Also, by considering the range of accuracy for $\overline{C}$, on the basis of m samples, one can get an estimate of the accuracy for $\overline{Y_y^2}$. The resulting expression, then, becomes

$$\frac{E\left[(C_p)_{max}\right]}{\overline{C} \pm \sigma_{C_p}} = \frac{\sqrt{\overline{Y_y^2} + \overline{D_y^2}}\ \sqrt{\overline{Y_z^2} + \overline{D_z^2}}}{\overline{Y_y^2}} \qquad (5\text{-}11)$$

In the determination of $\overline{Y_y^2}$ from Eq. (5-11), the value of the peak concentration should be an estimate of $(C_p)_{max}$ over a large number of samples. Considering the entire puff one finds that the probability of this spherical puff striking the sampling probe is highest at the small area around the center of the puff. Also, the probability of the outer parts of the cloud coming in contact with the sampling probe is relatively much smaller but these parts involve a large area

of the total cloud. It follows, therefore, that the probability distribution of C_p in the spatial region will be much flatter than the C_p-distribution. It is, as a first approximation, assumed that C_p is uniformly distributed over m samples and thus one can obtain an estimate of $(C_p)_{max}$ from the following expression which is derived in Appendix E:

$$E\left[(C_p)_{max}\right] = \frac{m}{m-1}\left[(C_p)_{max} - (C_p)_{min}\right] + (C_p)_{min} \qquad (5\text{-}12)$$

In Eq. (5-12), $(C_p)_{max}$ and $(C_p)_{min}$ are the maximum and minimum C_p-values on the basis of m samples.

The variance $\overline{Y_y^2}$ was calculated from Eq. (5-11) for diffusion data of the present study at X = 1, 2, 3, 4 ft., with values of y and z fixed at y = 0, and z = 8 in. The values of $\overline{D_y^2}$ were obtained by subtracting $\overline{Y_y^2}$ from the total dispersion σ_y^2 in the lateral direction. The resulting values of the variance due to spreading, $\overline{Y_y^2}$, and those of the variance due to meandering, $\overline{D_y^2}$, are given below:

Station	$10^4 \times \overline{Y_y^2}$, ft.^{2}	$10^4 \times \overline{D_y^2}$, ft.^{2}
(1', 0, 8")	13.8 ± 5.6	12.6 ± 5.6
(2', 0, 8")	48.1 ± 16.9	19.6 ± 17.2
(3', 0, 8")	50.5 ± 10.9	23.7 ± 10.8
(4', 0, 8")	64.7 ± 23.5	47.3 ± 23.5

The values of $E\,(C_p)_{max}$, $\overline{C}_{max}$, and σ_{C_p}, used to compute $\overline{Y_y^2}$ and $\overline{D_y^2}$, are presented in Appendix F.

The mean values of $\overline{Y_y^2}$ and $\overline{D_y^2}$ are plotted as a function of the travel distance X in Fig. 23 and linear relationships are obtained. Thus,

$$\overline{Y_y^2} \alpha X = \bar{u} T$$

which gives

$$\overline{Y_y^2} \alpha T$$

and

$$\overline{D_y^2} \alpha X = \bar{u} T \tag{5-13}$$

from which

$$\overline{D_y^2} \alpha T \tag{5-14}$$

where T is the dispersion time.

The above results have also been obtained by Gifford (7) for large dispersion times under the assumption of isotropic turbulence.

The ratio of the peak concentration, $E\left[(C_p)_{max}\right]$, to the average concentration, $\overline{C}_{max}$, at $X = 1, 2, 3, 4$ ft. for $y = 0$, $z = 8$ in. is plotted as a function of the travel distance in Fig. 24 which indicates the following approximate result:

$$\frac{\text{Peak Concentration}}{\text{Average Concentration}} \simeq \text{constant} \tag{5-15}$$

This relationship was also arrived at by Gifford (7) for large dispersion times in the case of isotrapic turbulence. Gifford tested the above relationship for field data of Wanta and Gartrell (22) in

whose case the source height was 250 ft. and the dispersion distances from about two to six miles. Their data, extending to large dispersion times, are plotted in Fig. 25 and approximately confirm the constant relation between peak-to-average concentration ratios and the dispersion distances.

It is noteworthy that the results of the present study as represented in Eqs. (4-5), (4-6), (5-13), (5-14) and (5-15) confirm the trends obtained by other investigators for large dispersion times, indicating thereby that large dispersion times are presumably obtained for travel distances of 4 ft. or less in the wind tunnel used in this study.

The Hay-Pasquill Scale Parameter

Hay and Pasquill (9) analyzed diffusion data from a continuous ground level source by assuming that the Lagrangian and Eulerian correlograms have similar shapes but different scales (ratio β:1). With the help of this scale parameter β , they showed that the turbulent spread of particles can be derived from wind fluctuation records directly. Their method, based on this scale parameter β , has been applied to various wind tunnel and field data of different investigators and predictions of particle spread have been obtained as a function of the travel distance on the basis of an average value of β . It was, therefore, considered worthwhile to investigate the diffusion data of the present study in the light of the Hay-Pasquill scale parameter β .

With a previous knowledge of $\overline{Y_y^2}$, the variance due to dispersion by spreading in the lateral direction, the diffusion data of the present study can be used to estimate the scale parameter β at the four stations, X = 1, 2, 3, 4 ft. For steady, homogeneous turbulence, the following equation is obtained (Chapter II):

$$\overline{Y_y^2} = \overline{v'^2}\, T^2 \int_o^\infty F_E(n) \left\{ \frac{\mathrm{Sin}\,(\pi n T/\beta)}{(\pi n T/\beta)} \right\}^2 dn \qquad (2\text{-}34)$$

It seems reasonable to assume that the statistical properties of turbulence do not vary rapidly with changing position in the atmosphere and, therefore, the horizontal diffusion, over level uniform ground can be specified in terms of the turbulent properties of the flow by means of Eq. (2-34). This expression can also be applied for the diffusion data of the present study and the scale parameter β can be evaluated by using known values of $\overline{Y_y^2}$, $\overline{v'^2}$, dispersion time T, and the form of the spectrum function $F_E(n)$.

It must be noted that the increase in plume width on one hand and the general plume meandering on the other usually is due to two widely separated eddy sizes. Thus, the contribution to dispersion by plume spreading, $\overline{Y^2}$, is statistically independent of that due to meandering, $\overline{D^2}$, and Gifford's technique of obtaining the separation of the spreading and meandering effects does not depend either on the presence of a spectrum gap or on limitation to any special meteorological conditions. It follows that the independence of spreading and

meandering is a general property of dispersion and is not especially related to the particular assumptions of the fluctuating plume model of Gifford.

The values of $\overline{Y_y^2}$, the variance due to dispersion by spreading, from the diffusion data of the present study were used to estimate β from Eq. (2-34). The spectrum function was obtained from the data of Sandborn and Marshall (18) on the spectra of the horizontal longitudinal component in u' (Fig. 20). From these data, the spectra of the lateral component v' can be obtained by assuming that the spectrum shape for the lateral and horizontal components is the same and adjusting the values in Fig. 20 by using the relationship $\frac{\overline{u'^2}}{\overline{v'^2}} \simeq 1.5$ which has been shown to be a reasonable value of $\frac{\overline{u'^2}}{\overline{v'^2}}$ by Klebanoff (10) and others. A value of $\overline{v'^2} = 0.36$ ft.^{2}/sec.^{2} was chosen for use in Eq. (2-34). This value was based on $\frac{w'}{U_\infty} = 0.026$ at $\frac{z}{\delta} = 0.5$, from Fig. 20, and the relation $\frac{v'}{w'} = 1.2$, from the data of Klebanoff, also shown in Fig. 20. In the absence of turbulent intensity data at different distances from the source, a constant value of $\overline{v'^2} = 0.36$ ft.^{2}/sec.^{2} was taken for all calculations from Eq. (2-34) at all four stations (X = 1, 2, 3, 4 ft.). The dispersion time was obtained by dividing the distance between the source and the sampling point by the mean velocity which was close to 15 ft./sec. at $y = 0$ and $z = 8$ in. for each of the four stations.

The procedure of estimating the scale parameter β from Eq. (2-34), for given values of dispersion time T, and $\overline{v'^2}$ at a

station and for a given relation between the spectrum function $F_E(n)$ and the frequency n, consisted of considering different values of β and computing the corresponding value of $\overline{Y_y^2}$ at each station. This involved a graphical integration to evaluate $\int_0^\infty F_E(n)\left\{\frac{\sin(\pi nT/\beta)}{(\pi nT/\beta)}\right\}^2 dn$. For this graphical integration, the computed value of $F_E(n)\left\{\frac{\sin(\pi nT/\beta)}{(\pi nT/\beta)}\right\}^2$ was plotted as a function of frequency n for each assumed value of β and the area under the resulting curve was determined. A universal plot of $\frac{\overline{Y_y^2}}{\overline{v'^2}\ T^2}$ (which was equal to the area from the above graphical procedure) as a function of T/β was prepared. This is shown in Fig. 26. Appendix G gives a typical set of different values used in the graphical integration.

For the evaluation of the scale parameter β from the diffusion data of the present study, the $\overline{Y_y^2}$ -values were used and the β-values were obtained from Fig. 26 by using the appropriate values of the dispersion time T and $\overline{v'^2}$. The following results were obtained:

Station	Scale parameter β
(1', 0, 8'')	18.3 ± 12.7
(2', 0, 8'')	21.1 ± 13.8
(3', 0, 8'')	5.5 ± 2.6
(4', 0, 8'')	3.7 ± 1.7

The above results for the Hay-Pasquill scale parameter were obtained by considering $\overline{Y_y^2}$, the variance due to dispersion by spreading, only. If, however, one considers the meandering effect as well, the β could be calculated on the basis of the combined

variance for spreading and meandering, namely, $(\overline{Y_y^2} + \overline{D_y^2})$. The results for the β-analysis in the latter case are given below:

Station	Scale parameter β
(1', 0, 8")	44
(2', 0, 8")	39
(3', 0, 8")	12.4
(4', 0, 8")	11.5

The above results indicate that the meandering of the diffusion cloud produces a significant increase in the values of the Hay-Pasquill scale parameter. It must be noted, however, that the assumption of similarity in shape of Eulerian and Lagrangian correlograms is a good assumption only in the case of fine scale motion which disregards any large scale meandering. Since the derivation of Eq. (2-34) is based on the above assumption, it would be more realistic to determine the scale parameter β by using $\overline{Y_y^2}$ in Eq. (2-34) rather than the combined variance $(\overline{Y_y^2} + \overline{D_y^2})$ for spreading and meandering.

Thus, for results at the four stations (travel distances of 1, 2, 3, 4 ft.), the mean values of the scale parameter β were found to be between 3.7 and 21.1 on the basis of the variance for spreading only. By including the meandering effect, the β-values were between 11.5 and 44. Although there is variation in the β-values with travel distance, conclusions regarding any systematic pattern of this variation cannot be firmly established on the basis of the above results.

Hay and Pasquill (9) measured the variance of the particle spread at a distance of 100 meters downwind from a continuous point

source, by carrying out experiments over downland with grass of length 1 to 2 in., in a variety of stability conditions. Simultaneous measurements were made of the fluctuations in wind speed and direction at the source. They tested their analysis scheme, represented by Eq. (2-34), on a series of eight diffusion experiments by computing the appropriate value of β for each experiment. They obtained β ranging from 1 to 10 with an average of 4, and concluded that this average value was independent of wind speed and stability and therefore was of great significance in predicting the variance of particle spread at different stations.

Baldwin and Mickelsen (1) considered their data on diffusion of helium from a continuous point source in the center line region of a fully turbulent pipe flow and obtained rough values of β from 4 to 18, depending on the mean flow rate. Their diffusion results were obtained within a 2 in. radius core of ambient air flowing through a commercial 8 in. diameter pipe.

Some data on a small scale of turbulence are reported by Mickelsen (12) who measured the spread of helium injected continuously at a fixed point in the air stream. The turbulent field was generated in an 8 in diameter duct having an inlet length-to-diameter ratio of 36. The scale of turbulence was approximately 0.02 m. Using Mickelsen's spectrum data and the assumed values of β, Hay and Pasquill (9) calculated $(\overline{Y^2})^{1/2}$ from Eq. (2-34) and plotted the

calculated values of $(\overline{Y^2})^{1/2}$ as a function of travel distance X . This relationship for stream velocity of 50 ft./sec. and 100 ft./sec. is shown in Fig.27 in which $(Y^2)^{1/2}$-values from Mickelsen's data are also presented. It is seen that no single value of β gives a fit over the whole range of travel up to 2.5 ft.; but for distances up to 1 ft., i.e., up to 15 times the scale of turbulence, a value of 6 provides a close approximation at 100 ft./sec. and a value of 4 is more suitable at 50 ft./sec. The β-values lie roughly between 4 and 9 for the travel distances up to 2.5 ft.

Haugen (8) analyzed selected Prairie Grass diffusion data to determine the scale parameter β . Thirty-five experiments were analyzed. Of these, only thirteen experiments were found to give β-values between 1 and 10. In nine cases, β-values were greater than 10; the maximum value of β being 160. In the remaining cases, the scale parameter was found to have values of less than 1. Haugen concluded that non-stationary conditions inherently produce non-systematic variations of β with travel distance as well as the unexpected result of $\beta < 1$.

The results of the various field and laboratory studies of diffusion described above yield a fairly wide scatter for the values of the Hay-Pasquill scale parameter. The results for β-values, based on the present study, are no exception. The β obtained on the basis of the spreading variance $\overline{Y_y^2}$ has values which are more

in agreement with the β-values of Mickelsen, Baldwin and Mickelsen, Hay and Pasquill, and Haugen. When β is calculated by taking the total plume dispersion into consideration, the β-values of the present study are higher than those of others, with the exception of Haugen whose results include β-values of 160, 32, 28, 26, 24, 21, 20 on the high side. It shows that meandering affects the β-results significantly Both Baldwin and Mickelsen (1), and Mickelsen (12) conducted their experiments in a narrow duct or a circular pipe in which only a restricted degree of meandering could be produced at small distances downstream from the source. On the other hand, Haugen's high β-values might be attributed to the significant meandering effect in the atmosphere. This apparently explains why the β-values are higher when the meandering is not disregarded. The results for β from the diffusion data of the above investigators also show that β is essentially insensitive to the scale of turbulence.

In spite of the scatter in the β-values, the possibility remains that practical and useful results can be obtained since the analysis of Hay and Pasquill, based on the scale parameter β, leads to a simple method of deriving the turbulent spread of particles directly from wind fluctuation records.

Investigation Concerning Diffusivities

The method for determining the lateral and vertical diffusivities K_y and K_z is based on the statistical model described in Eq. (2-10).

In the upper half of the boundary layer, turbulence conditions are nearly isotropic and homogeneous, and the effect of shear deformation is a minimum. The basic relations for obtaining K_y and K_z are:

$$\sigma_y^2 = 2K_y\left(\frac{X}{u}\right) \tag{5-16}$$

and

$$\sigma_z^2 = 2K_z\left(\frac{X}{u}\right) \tag{5-17}$$

Strictly speaking, the relations in Eq. (5-16) and Eq. (5-17) are valid for large dispersion times and for $\frac{z}{\delta} > 0.5$. For the determination of K_y and K_z at the source height (8 in.), the requirement for $\frac{z}{\delta}$ is approximately satisfied since the boundary layer thickness for the range of travel distances (1 to 4 ft.) is about 16 in. The results of the above analysis are presented below:

Station	$10^4 \times K_y$, ft.^{2}/sec.	$10^4 \times K_z$, ft.^{2}/sec.
X = 1 ft.	202	192
X = 2 ft.	237	267
X = 3 ft.	164	212
X = 4 ft.	212	205

Davar (5), in his study of diffusion from a continuous point source, has estimated the magnitude of the lateral diffusivity by graphically solving the diffusion equation. The comparison of his K_y values at X = 2 ft. and X = 4 ft. for y = 0, z = 0.5 in. with those of the present work is given in Fig. 28 .

With the conditions of the present experimental set-up, it is not possible to draw any conclusions regarding the values of the longitudinal diffusivity K_x .

Characteristic Time Scale of Eddy Diffusion

An estimate of the order or magnitude of $\mathcal{T}_L$, the characteristic time scale of eddy diffusion, may be obtained from Eq. (2-10) under the assumption that nearly homogeneous and isotropic conditions exist. Eq. (2-10) gives

$$\sigma_y^2 = 2\,\overline{v'^2}\,\mathcal{T}_L\left(\frac{X}{u}\right) \tag{5-18}$$

from which

$$\mathcal{T}_L = 1/2\,\frac{\sigma_y^2}{\overline{v'^2}\left(\frac{X}{u}\right)} \tag{5-19}$$

Taking $v' = 1.2\,w'$, as before, the following results are obtained for $y = 0$, $z = 8$ in.:

X, ft.	$\mathcal{T}_L$, sec.
1	0.049
2	0.063
3	0.046
4	0.052

The computed $\mathcal{T}_L$ - values are considered to represent the time scale during which a particle motion is essentially in one direction.

Suggestions for Further Research

The experimental results obtained in the present study are based on a limited range of variables and hence, it is necessary that further efforts be made before conclusions can be established. From this point of view, the following investigations would be desirable:

1. Use various types of surfaces over a wide range of ambient velocities.

2. Study the effect of source height on concentration pattern.

3. Increase the range of the diffusion field studied in the present investigation. This would help in obtaining a better estimate of the form and magnitude of the diffusivities K_y and K_z and would also enable a determination of K_x .

4. Extend the scope to the heated boundary as well as a line source. It would be significant to investigate the trend of meandering and of the Hay-Pasquill scale parameter over a larger range of diffusion field and also the effect of thermal stratification on the value of the scale parameter.

It is hoped that further research on the above suggested lines will enhance the chances of a positive contribution towards the laboratory modeling of mass diffusion in the atmosphere and, also, towards a more sound comprehension of the diffusion phenomena in turbulent shear flow.

Chapter VI

CONCLUSIONS

As a result of this study of turbulent diffusion from an 8-in. high short duration point source within a neutral boundary layer, several conclusions may be drawn. The main conclusions are:

1. The comparison of the experimental point source data in terms of the time-averaged concentration parameters with those of other wind tunnel and field studies revealed close agreement. For instance, the experimental law for attenuation of source-level concentration was obtained as $\overline{C}_{max} \sim X^{-1.45}$. This agrees well with Davar's form $C \sim X^{-1.43}$ at the same $\frac{H}{\delta}$.

2. The total displacements in y- and z-directions, σ_y^2 and σ_z^2, are proportional to the dispersion time.

3. Estimates of lateral diffusivity K_y and vertical diffusivity K_z provided values whose order of magnitude agrees with the results of other investigators.

4. On the basis of Gifford's fluctuating plume model for diffusion from a continuous point source, the total dispersion was separated into the components due to spreading and meandering, $\overline{Y^2}$ and $\overline{D^2}$. Both $\overline{Y^2}$ and $\overline{D^2}$ in the lateral directions are proportional to dispersion

time. The ratio of the peak concentration to the average concentration, for the data of this study, was found to be approximately constant. This was in agreement with a similar conclusion for other field studies.

5. The Hay-Pasquill scale parameter was found to be between 3.7 and 21 on the basis of spreading variance only. These values increased significantly when meandering was also taken into consideration. No single value of the scale parameter gave a fit over the entire range of travel up to 4 ft. No systematic pattern of the variation of β with travel distance could be predicted on the basis of these results. The scale parameter appears to be insensitive to scale of turbulence.

BIBLIOGRAPHY

BIBLIOGRAPHY

1. Baldwin, L. V. and Mickelsen, W. R., Turbulent diffusion and anemometer measurements: Journal of Engineering Mechanics, 88:37-69, 1962.

2. Bhaduri, S., Mass diffusion from a point source in a turbulent boundary layer over a rough surface: Ph. D. Dissertation, Colorado State University, Fort Collins, Colorado, 167 p., July 1963.

3. Cermak, J. E. and Chuang, H., Vertical-velocity fluctuations in thermally stratified shear flows: Technical Report No. DA-AMC-28-043-65-G20, Fluid Dynamics and Diffusion Laboratory, Colorado State University, Fort Collins, Colorado, September 1965.

4. Cramer, H. E., Records, F. A., and Vaughan, H. C., The study of the diffusion of gases or aerosols in the lower atmosphere: Massachusetts Institute of Technology, Department of Meteorology , Final Report under Conctract No. AF 19(604)-1058, 70 p., 1958.

5. Davar, K. S., Diffusion from a point source within a turbulent boundary layer: Ph. D. Dissertation, Colorado State University, Fort Collins, Colorado, 161 p., July 1961.

6. Frenkiel, F. N., Turbulent diffusion: mean concentration distribution in a flow field of homogeneous turbulence: Advances in Applied Mechanics, 3:61-107, Academic Press, New York, 1953.

7. Gifford, F., Statistical properties of a fluctuating plume dispersion model: Advances in Geophysics, 6:117-137, Academic Press, 1959.

8. Haugen, D. A., Some Lagrangian properties of turbulence deduced from atmospheric diffusion experiments: Journal of Applied Meteorology, 5:646-652, 1966.

9. Hay, J.S. and Pasquill, F., Diffusion from a continuous source in relation to the spectrum and scale of turbulence: Advances in Geophysics, 6:345-365, Academic Press, 1959.

10. Klebanoff, P.S., Characteristics of turbulence in a boundary layer with zero pressure gradient: National Advisory Committee for Aeronautics, Report 1247, Washington, 19p., 1955.

11. Malhotra, R.C., Diffusion from a point source in a turbulent layer with unstable density stratification: Ph.D. Dissertation, Colorado State University, Fort Collins, Colorado, 171 p., 1962.

12. Mickelsen, W.R., An experimental comparison of the Lagrangian and Eulerian correlation coefficients in homogeneous isotropic turbulence: National Advisory Committee for Aeronautics, TN 3570, Washington, 1955.

13. Monin, A.S., General survey of atmospheric diffusion: Advances in Geophysics 6:29-40, 1959, Academic Press, New York.

14. Pasquill, F., Atmospheric diffusion: the dispersion of windborne material from industrial and other sources: D. Van Nostrand Co., Ltd., London, 297 p., 1962.

15. Plate, E.J. and Cermak, J.E., Investigations to develop wind tunnel techniques for measuring atmospheric gaseous diffusion in model vegetative surfaces: Final Report on Contract No. 12-14-100-4546(41), Fluid Dynamics and Diffusion Laboratory, Colorado State University, Fort Collins, Colorado, July 1963.

16. Poreh, M., Diffusion from a line source in a turbulent boundary layer: Ph.D. Dissertation, Colorado State University, Fort Collins, Colorado, 110 p., 1961.

17. Quraishi, A.A., Effects of flexible roughness elements of diffusion in a turbulent boundary layer: Ph.D. Dissertation, Colorado State University, Fort Collins, Colorado, 190 p., December 1963.

18. Sandborn, V.A. and Marshall, R.D., Local Isotropy in wind tunnel turbulence: Technical Report on Contract No. DA-AMC-28-043-64-G-9, Fluid Dynamics and Diffusion Laboratory, Colorado State University, Fort Collins, Colorado, October 1965.

19. Sutton, O.G., Micrometeorology: McGraw-Hill, New York, 333 p., 1953.

20. Taylor, G.E., Diffusion by continuous movements: Proceedings, London Mathematical Society, 20:196-212, 1920.

21. U.S. Atomic Energy Commission, Meteorology and atomic energy: AECU 3066, Chapter 4, Washington, D.C., 169 p., 1955.

22. Wanta, R.C. and Gartrell, F.E., Private Communication with Gifford (7).

APPENDIX A

DETERMINATION OF THE MASS SPECTROMETER READING AS A FUNCTION OF TIME FOR A CONSTANT CONCENTRATION IN SMALL SAMPLE VOLUME

APPENDIX A

DETERMINATION OF THE MASS SPECTROMETER READING AS A FUNCTION OF TIME FOR A CONSTANT CONCENTRATION IN SMALL SAMPLE VOLUME

The mass spectrometer is a device which counts the total number of helium ions in the gas molecules per unit time passing between its deflection plates by producing a current which is proportional to the number of helium ions per unit time. Therefore, the current reading is proportional, for a constant concentration, to the flow rate through the orifice at the inlet to the mass spectrometer. This flow rate in turn depends on the pressure gradient across the orifice.

Now the suction pressure inside the mass spectrometer is maintained very closely to 0.0003 mm. Hg so that the decisive pressure for determining the flow rate is the pressure at the inlet end of the orifice, that is, the pressure in the sample. When the gas is withdrawn from the sample, the pressure changes in the sample. This change, however, is very small because of the small amount of gas which is withdrawn and due to deformation of the plastic tubing which adjusts to maintain the pressure difference between the inside and outside of the tubing small. Under the worst conditions, the plastic tubing acts like a rigid vessel whose interior pressure changes rapidly

if the rate of gas flow out of it is large. Under these circumstances, the concentration reading obtained from the mass spectrometer is meaningless unless the pressure inside the sample is known. In order to check the effect of the withdrawal rate on the reading, the discharge from the sample was calculated by the following procedure:

First, a differential equation relating mass M in the sample (which is assumed to be contained in a rigid vessel) and flow rate q was set up:

$$\frac{1}{\rho_m} \frac{dM}{dt} = q \qquad (A-1)$$

where ρ_m is the mean density of the sample and q is a function of the pressure p as given below:

$$q = C_1 p^n \qquad (A-2)$$

where C_1 is the discharge coefficient of the orifice used, and n is an exponent which has to be determined experimentally, while p is the pressure difference across the orifice which is close to the absolute pressure. Now, neither n nor p are known when an experiment is performed with the polyethylene tubing samples so that one has to construct the curve equation from other data.

Known are the reading r of the mass spectrometer scale which can serve as a measure of q and the original concentration in the sample. Thus, by performing an experiment, during which the hypodermic needle of the mass spectrometer leak is connected directly

into a piece of tubing in which the pressure is kept constant and adjustable and in which the concentration is constant, a curve can be obtained showing r as a function of p for C_1 = constant by measuring p with a manometer. This curve was obtained by blowing gas from a cylinder of pressurized helium-air mixtures through a tubing which is connected through T-sections to both the mass spectrometer and a water manometer, and whose opening to the air was throttled with a clamp to control the pressure. The result is shown in Fig. A-1 yielding

$$r = f_1(p, C_1 q) \quad \text{for } C_1 = \text{constant} \tag{A-3}$$

The relation was generalized by means of a plot of q versus r obtained with different leak rates and different concentrations, as shown in Fig. A-2 . From this, one obtains:

$$r = f_2(C_1 q) \quad \text{for } p = \text{constant} \tag{A-4}$$

By combining Eqs. (A-3) and (A-4) , one obtains a result

$$q = f_3(p) \tag{A-5}$$

which is dependent on the standard leak used but which is valid for all concentrations. The function has been plotted in Fig. A-3 . It can be approximated by the equation

$$q = 0.026\ p^{1.33} \tag{A-6}$$

which is valid for standard leak SCL-1730 (3.0 μ CFH). Combining Eq. (A-1), Eq. (A-6), and the ideal gas law yields:

$$-\frac{\pi}{4} d^2 l \rho_m RT \frac{1}{p^2} \frac{dp}{dt} = q \qquad \text{(A-7)}$$

Taking the plastic tubing length $l = 5$ in., $d = 1/8$ in., $T = 25^0$C and inserting other values, we obtain the $q - t$ relationship as

$$q = \left[\frac{1}{0.14 + 1.45\,t} \right]^{\frac{1}{1.77}} \qquad \text{(A-8)}$$

Fig. A-4 giving r as a function of q for different helium concentrations was derived from Fig. A-2 and can thus be used to obtain r corresponding to q from Eq. (A-8). We can, in this way, obtain the mass spectrometer reading r as a function of time.

Comparison of Theoretical Predictions with Experimental Data

Fig. A-5, Fig. A-6, and Fig. A-7 are concentration-time plots with standard leak SCL-1730 for 0.5%, 0.2%, and 0.05% helium mixtures, respectively. After a lapse of 500 sec., the readings on the mass spectrometer scale were 0.6, 0.21, and 0.055, respectively. However, if we put $t = 500$ sec. $= 5/36$ hr. in Eq. (A-8), we obtain $q = 1.86$. This value of q corresponds to 0.64, 0.23, and 0.05 respectively with 0.5%, 0.2%, and 0.05% helium as shown from Fig. A-4. Thus, we find that predictions based on theory and the experimental readings are reasonably close.

At higher time intervals, the results with 0.5% helium are tabulated below:

t, hr.	q	Theoretical	Experimental
0.14	1.86	0.64	0.60
0.50	1.08	0.52	0.55
1.0	0.77	0.44	0.40
1.5	0.624	0.40	- -
2.0	0.534	0.37	0.325

The theoretical and experimental values of r have been plotted as a function of time t in Fig. A-8 .

APPENDIX B

DETERMINATION OF SOURCE STRENGTH

APPENDIX B

DETERMINATION OF SOURCE STRENGTH

For determination of the strength of the source, the criterion has to be used that the mass spectrometer gives accurate readings at the highest sensitivity (leak rate at 86.0 μCFH) which correspond to helium concentration of about 2.5 ppm. Therefore, the helium puff must be of such an intensity that a concentration of 2.5 ppm occurs at the outermost edge of interest of the diffused puff.

Assume a three-dimensional Gaussian distribution for the diffusion cloud with $\sigma^*_x = \sigma^*_y = \sigma^*_z$ where σ^* = characteristic scale length of the diffusing plume in the direction denoted by subscript x or y or z , where $\frac{C(x, y, z)}{C_{max}} = 0.5$. Defining C_{sens} as the lowest concentration that the mass spectrometer can accurately detect at its highest sensitivity, one can write, then

$$C_{sens} = C_{max}\ e^{-A\left(\frac{x^2}{\sigma^{*2}_x}\right)} \qquad \text{(B-1)}$$

Using the definition of σ^* above, one obtains

$A = \ln 2$ and thus,

$$C_{sens} = C_{max}\ e^{-\ln 2\left(\frac{x^2}{\sigma^{*2}_x}\right)} \qquad \text{(B-2)}$$

Taking into consideration the y and z-directions as well, one gets:

$$C_{sens} = C_{max} \; e^{-\ln 2 \left[\frac{x^2}{\sigma^{*2}_x} + \frac{y^2}{\sigma^{*2}_y} + \frac{z^2}{\sigma^{*2}_z} \right]} \qquad (B\text{-}3)$$

Assuming that C_{sens} is located at some reasonable distance from the center where, for instance,

$$x = 2\sigma^*_x$$

$$y = 2\sigma^*_y$$

$$z = 2\sigma^*_z$$

In that case, on has

$$C_{sens} = C_{max} \; e^{-12 \ln 2} \qquad (B\text{-}4)$$

The discharge of helium from the injection nozzle is given by $Q = u\, A(y, z)$ and thus one can define mass sensitivity G as follows:

$$G = \int_{-\infty}^{\infty} u\, A(y, z)\, C \, dt \qquad (B\text{-}5)$$

Since the exit velocity u is approximately equal to U_∞, one can write that

$$u = U_\infty = \text{constant} \qquad (B\text{-}6)$$

and hence,

$$G = A\, u \int_{-\infty}^{\infty} C \, dt$$

$$= A\, C_{max} \int_{-\infty}^{\infty} e^{-(\ln 2) \frac{x^2}{\sigma^{*2}_x}} \, dx$$

which gives

$$G = A\, C_{max}\, \frac{\sigma_x^*}{\sqrt{\ln 2}}\, \sqrt{\pi} \qquad \text{(B-7)}$$

In the three-dimensional case, one obtains

$$G = C_{sens}\; e^{12 \ln 2}\; \frac{\sigma_x^*\, \sigma_y^*\, \sigma_z^*}{(\ln 2)^{3/2}}\; (\pi)^{3/2} \qquad \text{(B-8)}$$

Taking $\sigma_x^* = \sigma_y^* = \sigma_z^* = 0.00625$ ft. (Ref. 11)

and $C_{sens} = 2.5$ ppm , one obtains

$$G = \frac{2.5}{10^6}\; e^{12 \ln 2}\; \frac{(0.0625)^3 \times (3.14)^{3/2}}{(\ln 2)^{3/2}}$$

from which

$$G = 0.233 \times 10^{-4} \text{ ft.}^3$$

Tubing Length Required to Store Helium In the Instantaneous Source

Let L = length in ft. of 1/4 in. I. D. copper tubing required to store the amount of helium given by G , then

$$0.233 \times 10^{-4} = \frac{\pi}{4} \left(\frac{1}{4 \times 12}\right)^2 L$$

which gives

$$L \simeq 1 \text{ ft.}$$

APPENDIX C

DETERMINATION OF SAMPLE SIZE

APPENDIX C

DETERMINATION OF SAMPLE SIZE

The mass spectrometer has a response time of about 20 to 30 sec., and it takes about two min. for the indicator to reach a steady final reading. Calculations must, therefore, be made for a recording time of three min. in order to ensure sufficiently large sample size for a reliable determination of concentrations.

Now, the total volume needed for a three min. recording at a rate of 100 μ CFH is given by

$$V = \frac{180 \times 100 \times 10^{-6}}{3600} \times (12)^3 \text{ in.}^3$$

This volume of the helium-air sample will be contained in a 1/8 in. I. D. polyethylene tubing. If L' in. is the length of this tubing, then one obtains:

$$\frac{180 \times 100 \times 10^{-6}}{3600} \times (12)^3 = \frac{\pi}{4} \left(\frac{1}{8}\right)^2 L'$$

from which $L' \simeq 0.9$ in.

Thus, each compartment of the sampling apparatus would consist of 0.9 in. long polyethylene tubing (1/8 in. I. D.) in order to conform to the mass spectrometer specifications.

APPENDIX D

PROCEDURE FOR OPERATION

APPENDIX D

PROCEDURE FOR OPERATION

Set-Up Procedure of Helium Supply Arrangement

The valve V_1 (see Fig. 4) is kept closed at all times during the set-up procedure. The solenoid valves V_4 and V_5 are in the de-energized position and the flowmeter reading is recorded. The valves V_2 and V_3 are then placed in position 2 and the solenoid valves V_4 and V_5 are energized through the control box. The flowmeter is read again. If the two flowmeter readings are not the same, the procedure is repeated after adjusting the needle valve placed along the polyethylene tubing between valves V_4 and V_5 until the flowmeter gives the same readings for either valve position.

Operating Procedure for Instantaneous Source

After completing the set-up procedure, the solenoid valves are left in the de-energized position and the valves V_2 and V_3 are placed in position 1 as indicated in Fig. 4 . The valve V_1 is opened for a short period of time which is sufficient to fill the tubing between V_2 and V_3 with 99.9% pure helium gas. The valve V_3 is closed first after which the valve V_1 on the gas cylinder is closed. The

tubing between valves V_1 and V_2 consists of a metal connection at an intermediate point J at which the connection between V_1 and V_2 can be broken, and its end kept closed in such a way that the helium gas between J and V_3 is not exposed to the atmosphere. The tubing end at J is then exposed to the atmosphere for a fraction of a second, thus ensuring atmospheric pressure between point J and valve V_3. Long exposure to atmosphere might cause some helium to be displaced by air inside the tubing. The valve V_2 is then closed, still firmly closing the end of the tubing at J. Thus, a known amount of helium gas is enclosed in the copper tubing between the valves V_2 and V_3. By placing the valves V_2 and V_3 in position 2 after the solenoid valves V_4 and V_5 have been energized, this known amount of helium at atmospheric pressure is released at a determined flow rate into the flow of the wind tunnel.

Experimental Procedure for Taking Data

The flow rate on the suction flowmeter is adjusted at 190 $cm.^3/min.$ after starting the suction pump. This gives the rate at which the sample is withdrawn from the wind tunnel. The 1/8 in. I.D. polyethylene tubing is placed in the slot provided for it in the sampling apparatus and the two ends of the tubing are connected to the sampling probe and the suction flowmeter respectively. The solenoids are checked by pressing the aluminum bars hard in order to make sure that all solenoids will go down completely when energized. After the

connections between various components of the apparatus have been checked, the polyethylene tubing between the valves V_2 and V_3 of the instantaneous source is filled with helium gas at atmospheric pressure. The timer is set on a certain time (t sec.) and the operating switch on the control box panel is pressed. This releases an instantaneous puff of helium through the injection probe into the atmosphere of the wind tunnel and the sampling probe is subsequently exposed to a cloud which consists of helium and air as a result of diffusion of helium into air. A part of this cloud is sucked through the sampling probe into the sampling apparatus. A period of t sec. elapses between the release of the puff and the energization of solenoids of the sampling apparatus. As soon as the solenoids are energized, a metallic rod is inserted through the holes in the aluminum bars and the iron brackets and the switch on the control box panel is pressed again to de-energize the solenoids. Twenty samples consisting of helium-air mixtures are thus obtained and the aluminum base of the sampling apparatus can now be slid out for the subsequent analysis of these samples with the mass spectrometer. If the samples contain no helium, it implies that either the timer setting was too short (in which case the cloud did not even reach the sampler) or the setting was too long (in which case the cloud went past the sampler). This problem, then, calls for trying different timer settings until part of the cloud and eventually the whole cloud is symmetrically brought over the entire length

of the sampler. Often this requires several trials before most of the cloud can be centered at the sampler. The schematic lay-out of the method of taking data is shown in Fig. 10 .

In the analysis of the samples with the mass spectrometer, the sample is extracted from the polyethylene tubing by means of a hypodermic needle, as was described in Chapter II. The hypodermic needle is inserted in all the twenty compartments of the sampler and the mass spectrometer readings recorded. These concentrations, when plotted as a function of distance along the length of the sampler, give a concentration profile. Eight to ten such concentration profiles are taken consecutively at a point in the wind tunnel. Since the sensitivity of the mass spectrometer fluctuates, it is more worthwhile to convert the indicator scale readings into ppm of helium in the samples. This is done with the help of calibration procedure which was outlined in Chapter II.

APPENDIX E

DETERMINATION OF THE EXPECTED VALUE OF THE PEAK CONCENTRATION ON THE BASIS OF m READINGS

APPENDIX E

DETERMINATION OF THE EXPECTED VALUE OF THE PEAK CONCENTRATION ON THE BASIS OF m READINGS

Consider the m values of the concentration C_p . Then, the probability distribution of C_p is given by

$$P\left[C_p \leq x\right] = F(x) \quad . \tag{E-1}$$

If C_p^* is the maximum of the m values of C_p , then

$$F^*(x) = P\left[C_p^* \leq x\right] = P\left[C_{p_1} \leq x,\ C_{p_2} \leq x, \ldots, C_{p_m} \leq x\right]$$

$$= P\left[C_{p_1} \leq x\right]\ P\left[C_{p_2} \leq x\right] \ldots P\left[C_{p_m} \geq x\right]$$

or $$F^*(x) = F^m(x) \quad . \tag{E-2}$$

Assuming that C_p is uniformly distributed, one has

$$F(x) = \frac{x-a}{b-a} \qquad a \leq x \leq b \quad . \tag{E-3}$$

Thus, from Eq. (E-2) ,

$$F^*(x) = \frac{(x-a)^m}{(b-a)^m} \quad . \tag{E-4}$$

The corresponding density function is given by

$$f^*(x) = \frac{m\,(x-a)^{m-1}}{(b-a)^m} \tag{E-5}$$

Thus,

$$E\left[C_p^*\right] = \frac{m}{(b-a)^m} \int_a^b x(x-a)^{m-1}\,dx$$

$$= \frac{m}{m+1}(b-a) + a \qquad \text{(E-6)}$$

from which $\hat{b}$, the expected value of the upper limit b , is given by

$$\hat{b} = \frac{m+1}{m}\left[(C_p)_{max} - \hat{a}\right] + \hat{a} \qquad \text{(E-7)}$$

where $\hat{a}$ is an estimate of the lower limit a , based on m values.

Let C_{p_*} be the minimum of m values of C_p . Then, one can show that

$$E\left[C_{p_*}\right] = \frac{1}{m+1}(b-a) + a \quad . \qquad \text{(E-8)}$$

Combining Eq. (E-6) and Eq. (E-8) , one obtains

$$E\left[(C_p)_{max} - (C_p)_{min}\right] = \frac{m}{m+1}(b-a) + a - \frac{1}{m+1}(b-a) - a$$

$$= \frac{m-1}{m+1}(b-a)$$

or

$$\widehat{(b-a)} = \frac{m+1}{m-1}\left[(C_p)_{max} - (C_p)_{min}\right] \quad . \qquad \text{(E-9)}$$

Combining Eq. (E-8) and Eq. (E-9) , one has

$$\frac{1}{m+1} \cdot \frac{m+1}{m-1}\left[(C_p)_{max} - (C_p)_{min}\right] + \hat{a} = (C_p)_{min}$$

or

$$\hat{a} = (C_p)_{min} - \frac{1}{m-1}\left[(C_p)_{max} - (C_p)_{min}\right] \quad . \qquad \text{(E-10)}$$

Substituting $\hat{a}$ from Eq. (E-10) into Eq. (E-7),

$$\hat{b} = \frac{m+1}{m}\left[\left\{(C_p)_{max} - (C_p)_{min}\right\} + \frac{1}{m-1}\left\{(C_p)_{max} - (C_p)_{min}\right\}\right]$$

$$+ (C_p)_{min} - \frac{1}{m-1}\left[(C_p)_{max} - (C_p)_{min}\right]$$

from which one obtains, on simplification,

$$\hat{b} = E\left[(C_p)_{max}\right] = \frac{m}{m-1}\left[(C_p)_{max} - (C_p)_{min}\right] + (C_p)_{min} \qquad \text{(E-11)}$$

where $(C_p)_{max}$ and $(C_p)_{min}$ on the right-hand side are, respectively, the maximum and minimum values of C_p, based on m readings.

APPENDIX F

CONCENTRATION PARAMETERS BASED ON EXPERIMENTAL DATA USED TO CALCULATE THE VARIANCES DUE TO SPREADING AND MEANDERING

APPENDIX F

CONCENTRATION PARAMETERS BASED ON EXPERIMENTAL DATA USED TO CALCULATE THE VARIANCES DUE TO SPREADING AND MEANDERING

Station	$E\left[(C_p)_{max}\right]$, ppm	$\overline{C}_{max}$, ppm	σ_{C_p}, ppm
(1', 0, 8")	18, 663	9700	3890
(2', 0, 8")	5, 595	4000	1413
(3', 0, 8")	4, 040	2750	595
(4', 0, 8")	2, 340	1350	489

APPENDIX G

A TYPICAL SET OF VALUES FOR PARAMETERS USED IN THE GRAPHICAL DETERMINATION OF THE SCALE PARAMETER, β, FROM DIFFUSION DATA

APPENDIX G

A TYPICAL SET OF VALUES FOR PARAMETERS USED IN THE GRAPHICAL DETERMINATION OF THE SCALE PARAMETER, β, FROM DIFFUSION DATA

Station: (1', 0, 8")

Assumed value of β = 14

T = 0.067 sec.

$\overline{v'^2}$ = 0.36 ft.^{2}/sec.^{2}

n	$F_E(n)$	$\frac{\pi nT}{\beta}$	$\mathrm{Sin}\left(\frac{\pi nT}{\beta}\right)$	$F_E(n)\left\{\frac{\mathrm{Sin}(\pi nT/\beta)}{(\pi nT/\beta)}\right\}^2$
1	0.0404	0.015	0.0150	0.0404
4	0.0366	0.060	0.0599	0.0365
8	0.0296	0.120	0.119	0.0296
12	0.0189	0.180	0.179	0.0187
16	0.0125	0.240	0.236	0.0122
25	0.0049	0.376	0.367	0.0047
32	0.0031	0.480	0.462	0.0028
50	0.0018	0.752	0.682	0.0010
64	0.0010	0.960	0.819	0.0004

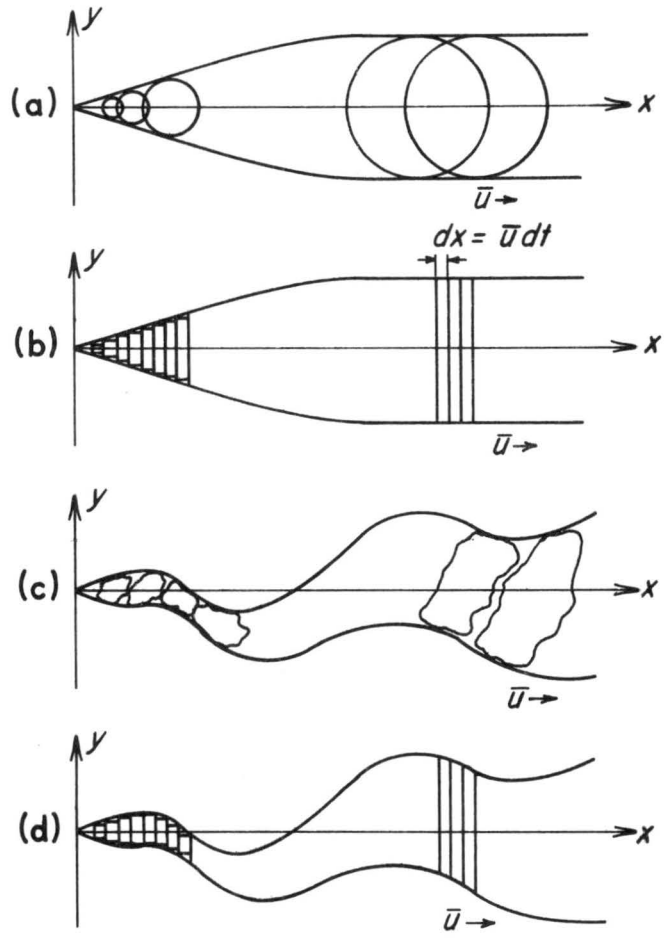

Fig. 1 SCHEMATIC PLAN VIEW OF PLUME MODELS

(a) Superimposed, spherical puff model

(b) Spreading disk models

(c) Real plume, considered as superposition of elementary puffs

(d) Fluctuating plume model with spreading disk elements

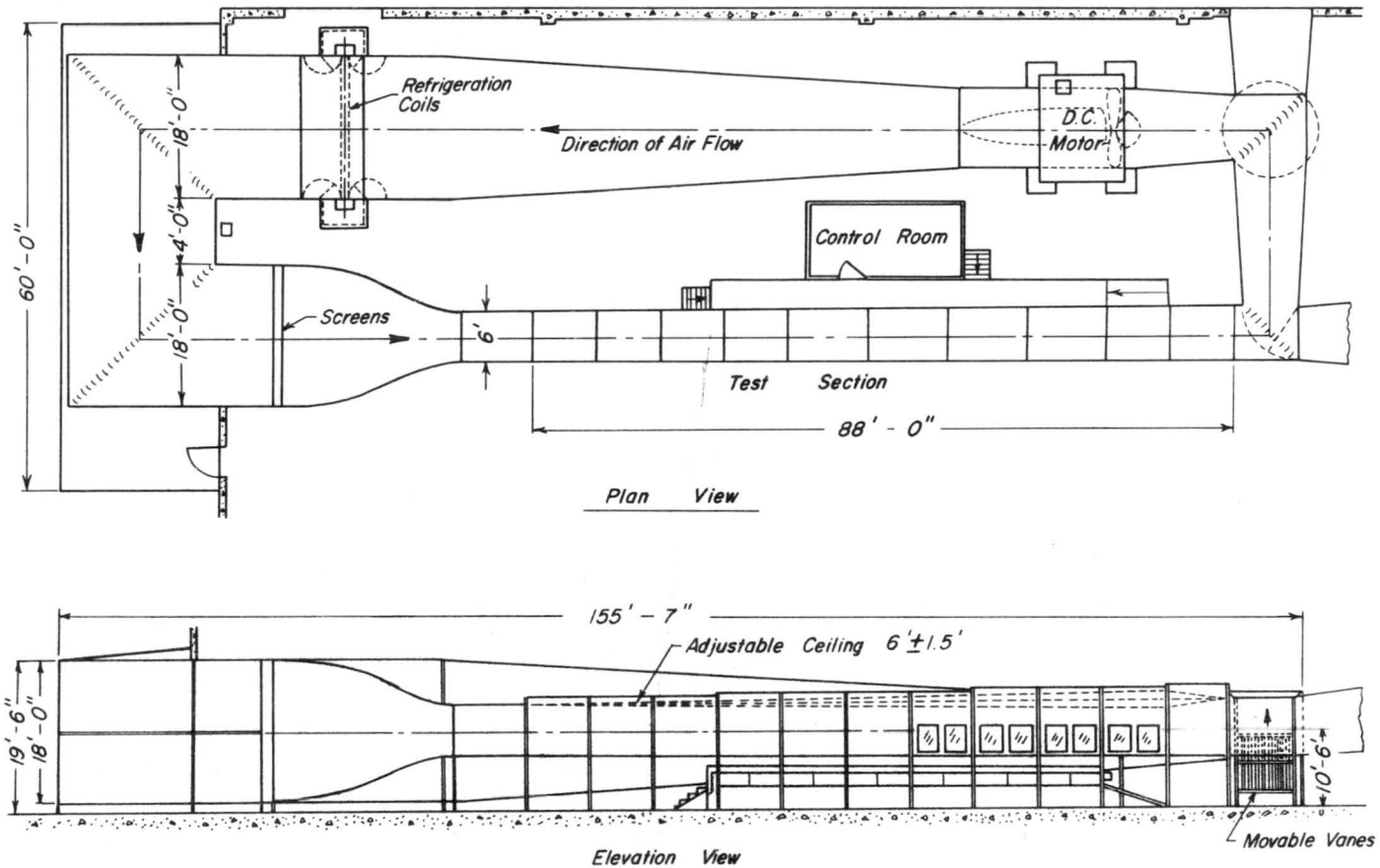

Fig 2 Army Meteorological Wind Tunnel

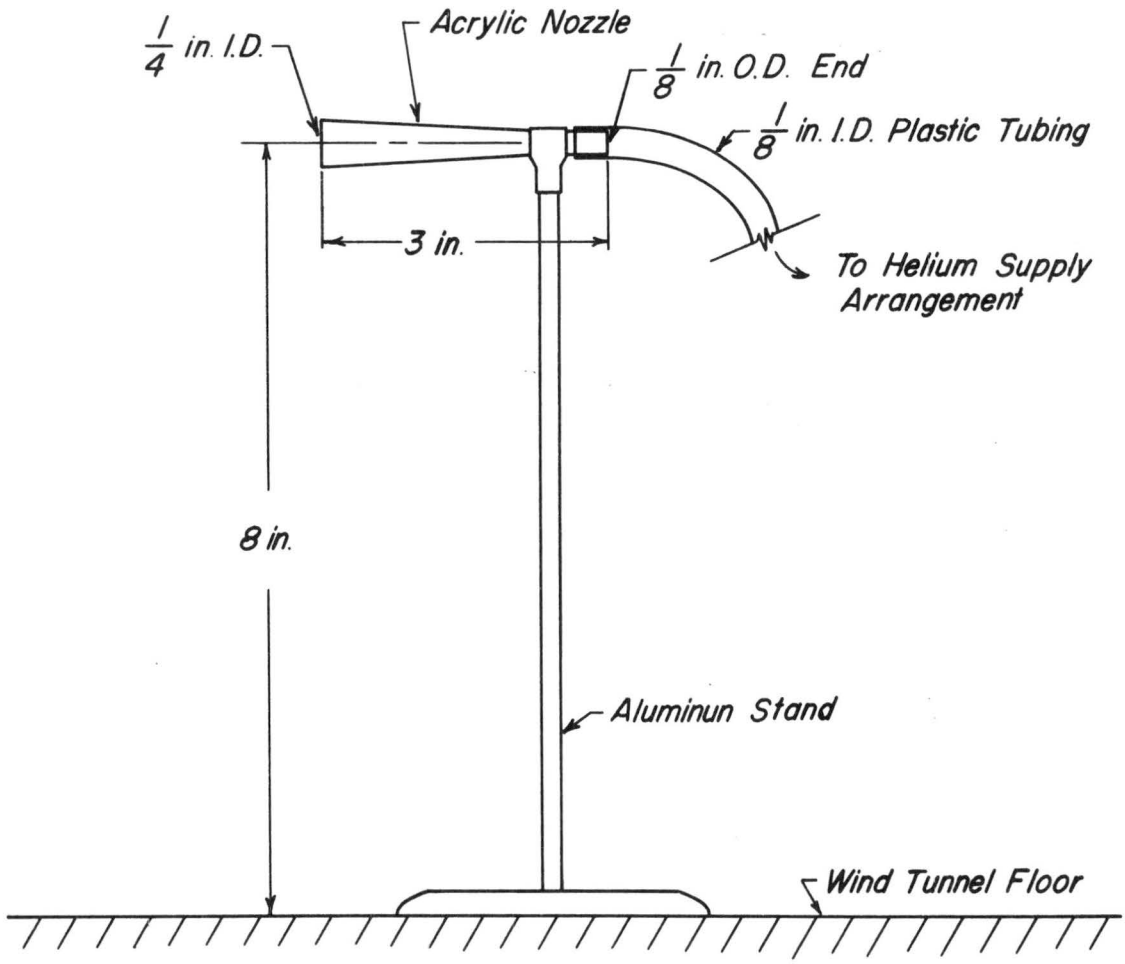

Fig. 3 INJECTION PROBE

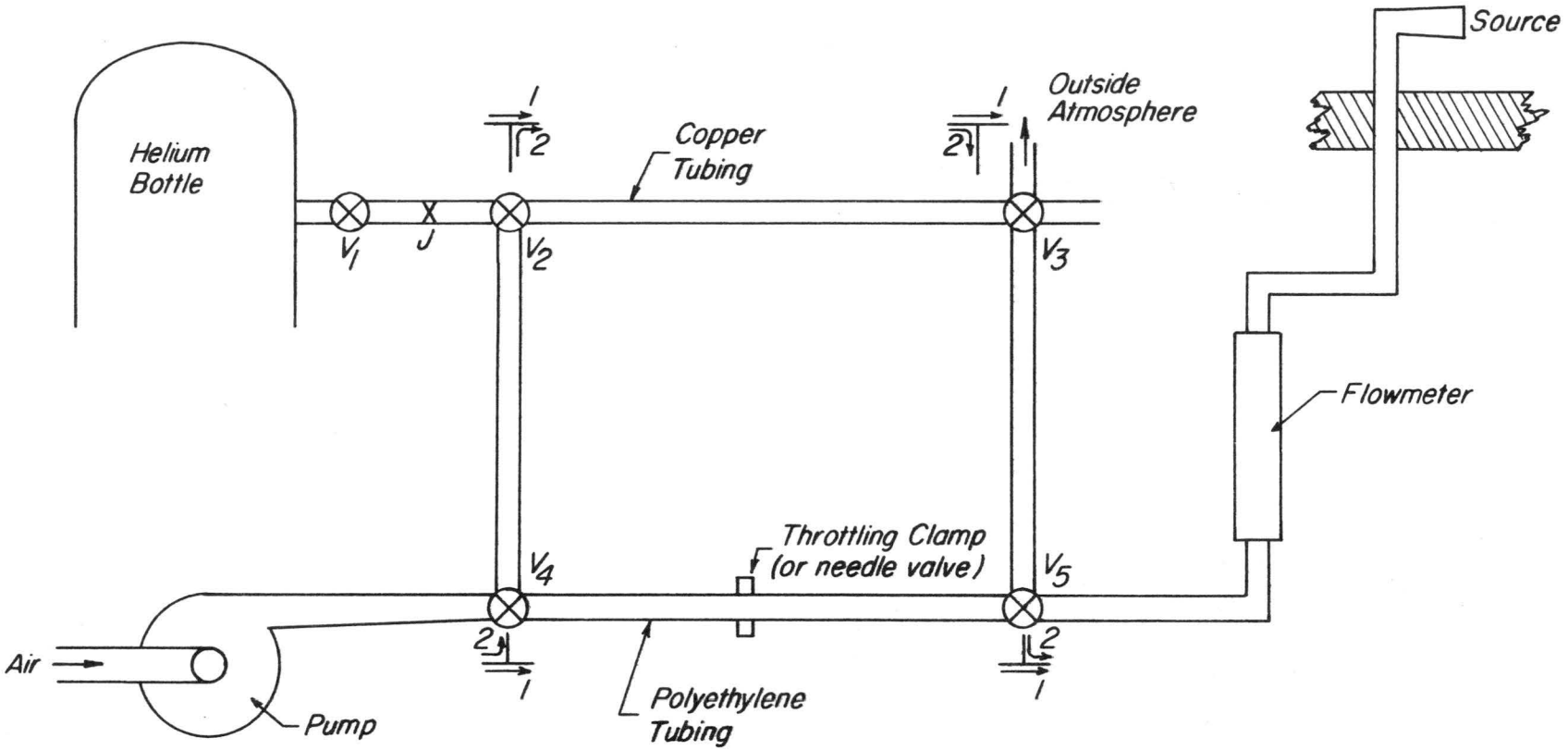

Fig. 4 HELIUM SUPPLY ARRANGEMENT

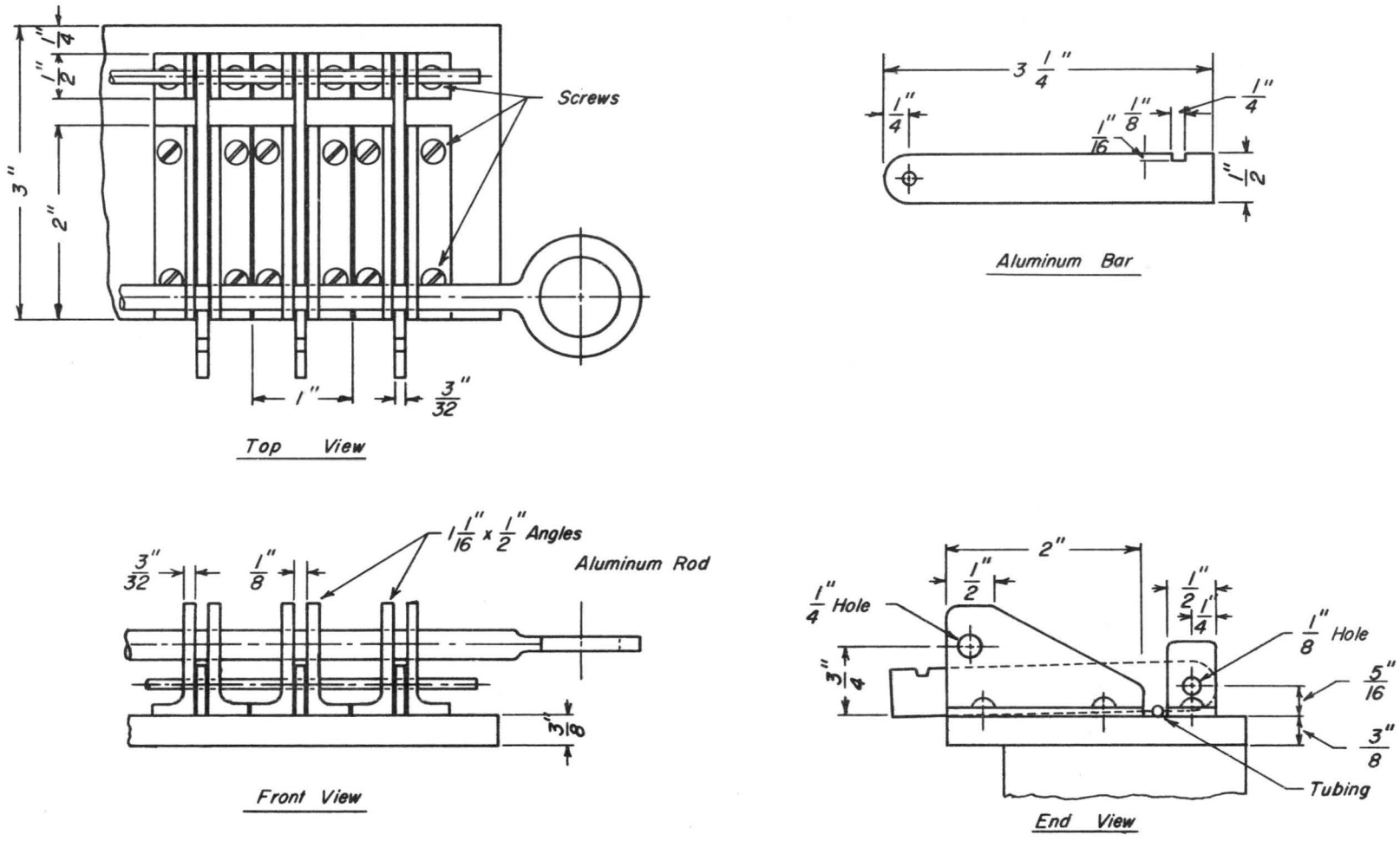

Fig. 5 THE SAMPLING APPARATUS

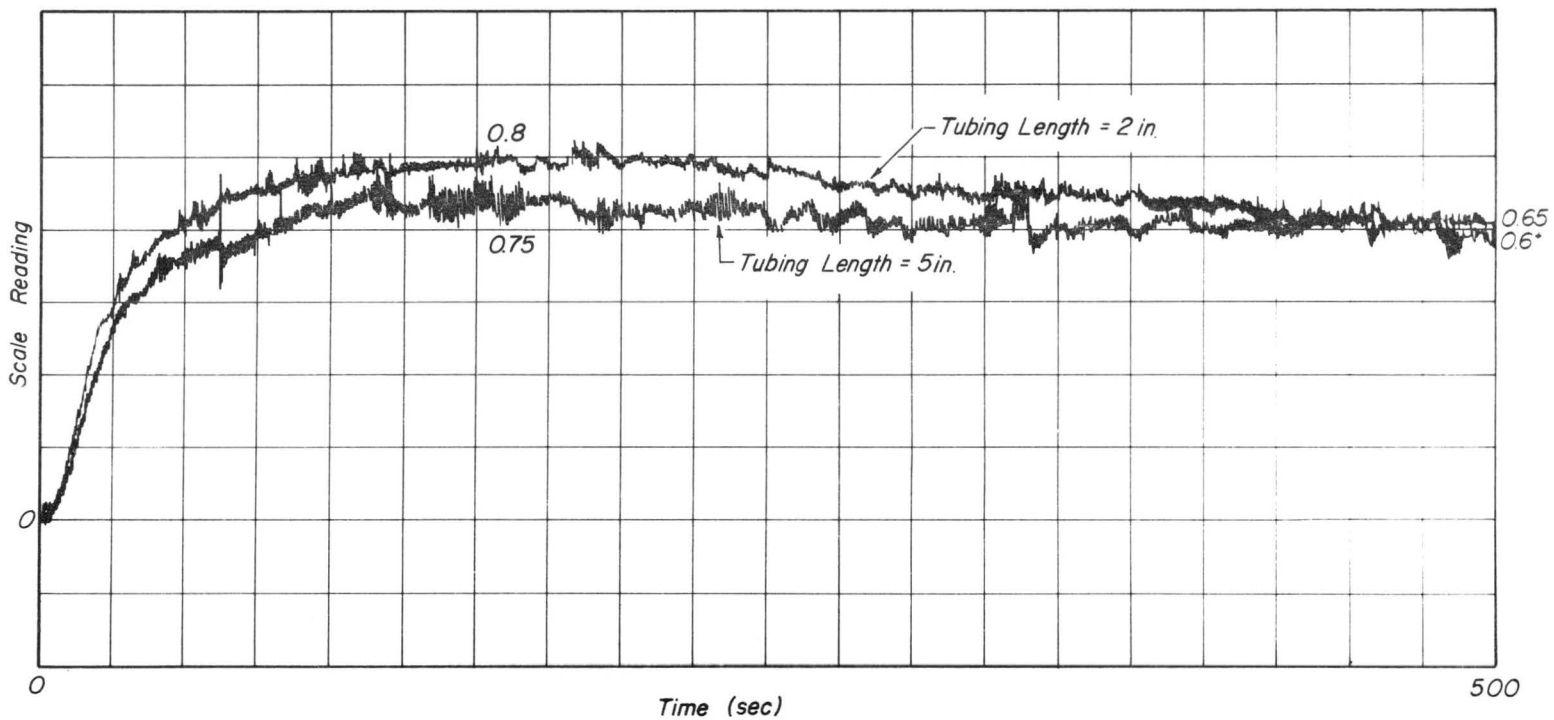

Fig. 6 EFFECT OF TUBING LENGTH

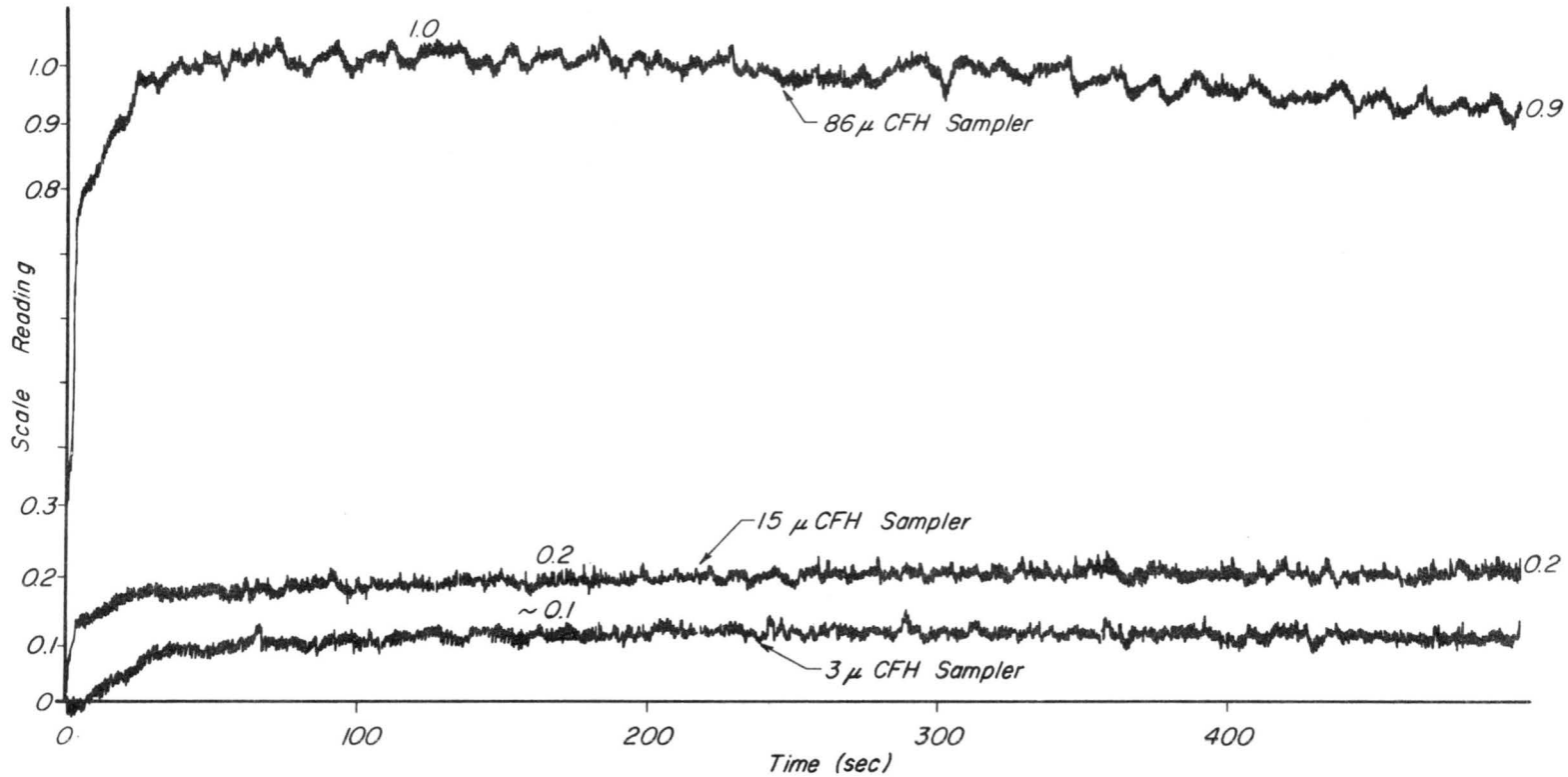

Fig. 7 TYPICAL RECORDINGS OF GAS MIXTURES CONTAINED IN A 5" POLYETHYLENE TUBING OF 1/8" I.D.

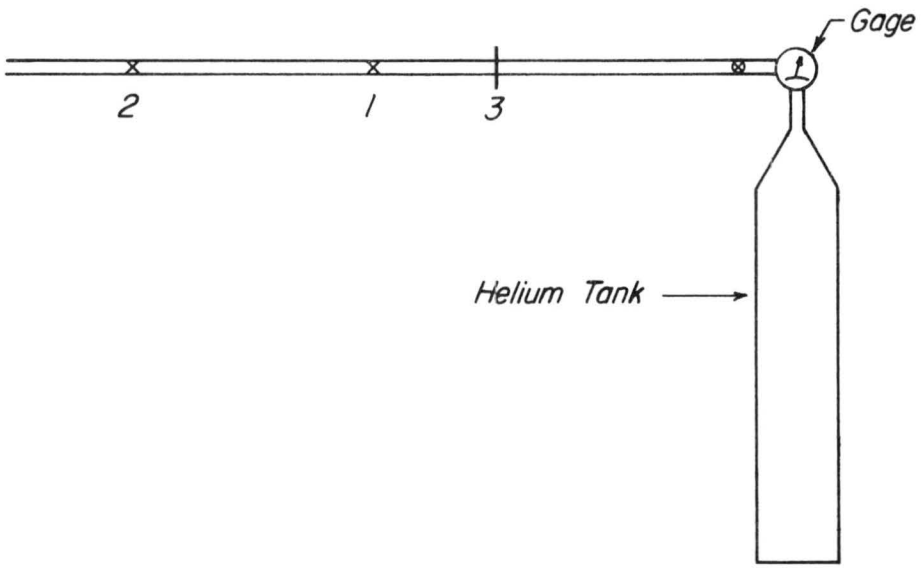

Fig. 8 PREPARATION OF SAMPLES FOR PRELIMINARY EXPERIMENTS.

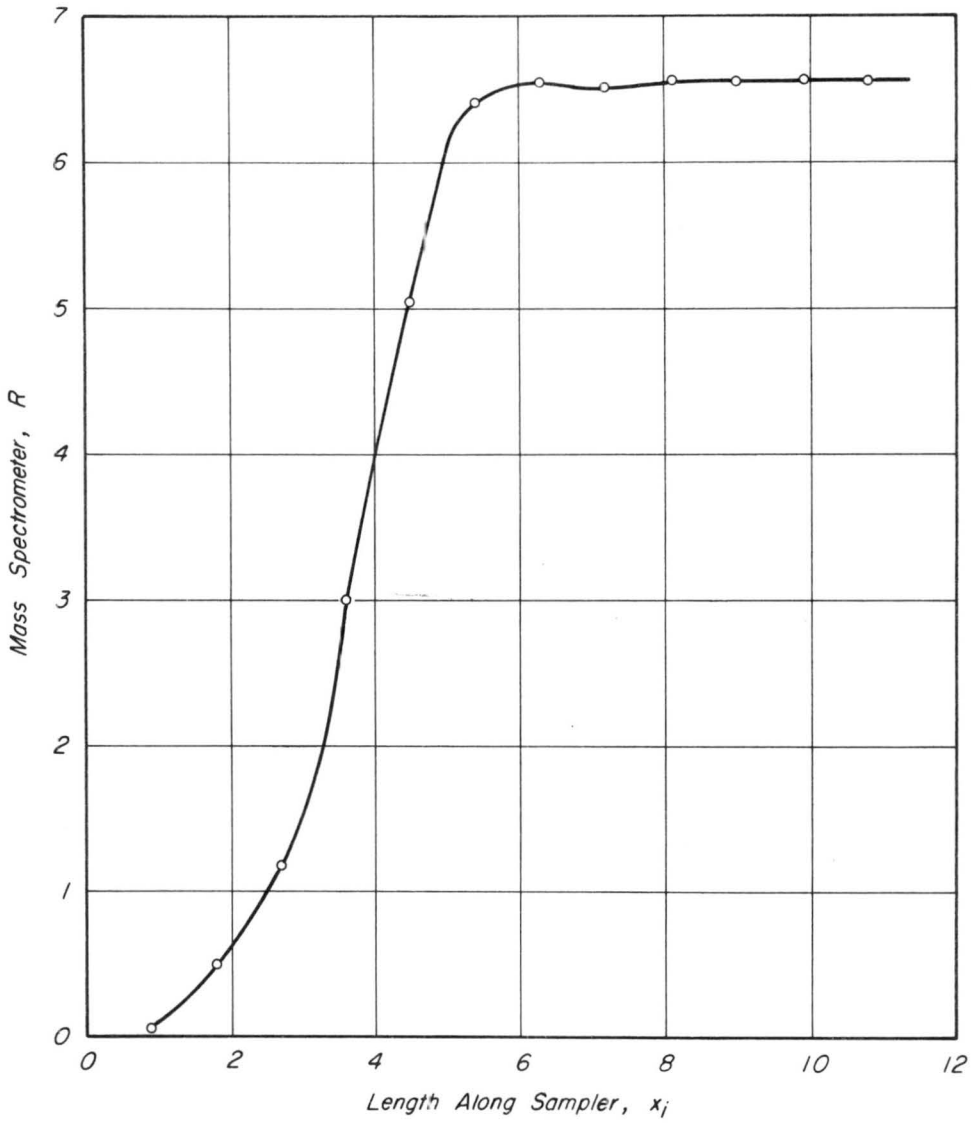

Fig. 9 DISTORTION OF DIFFUSION CLOUD THROUGH THE TUBING.

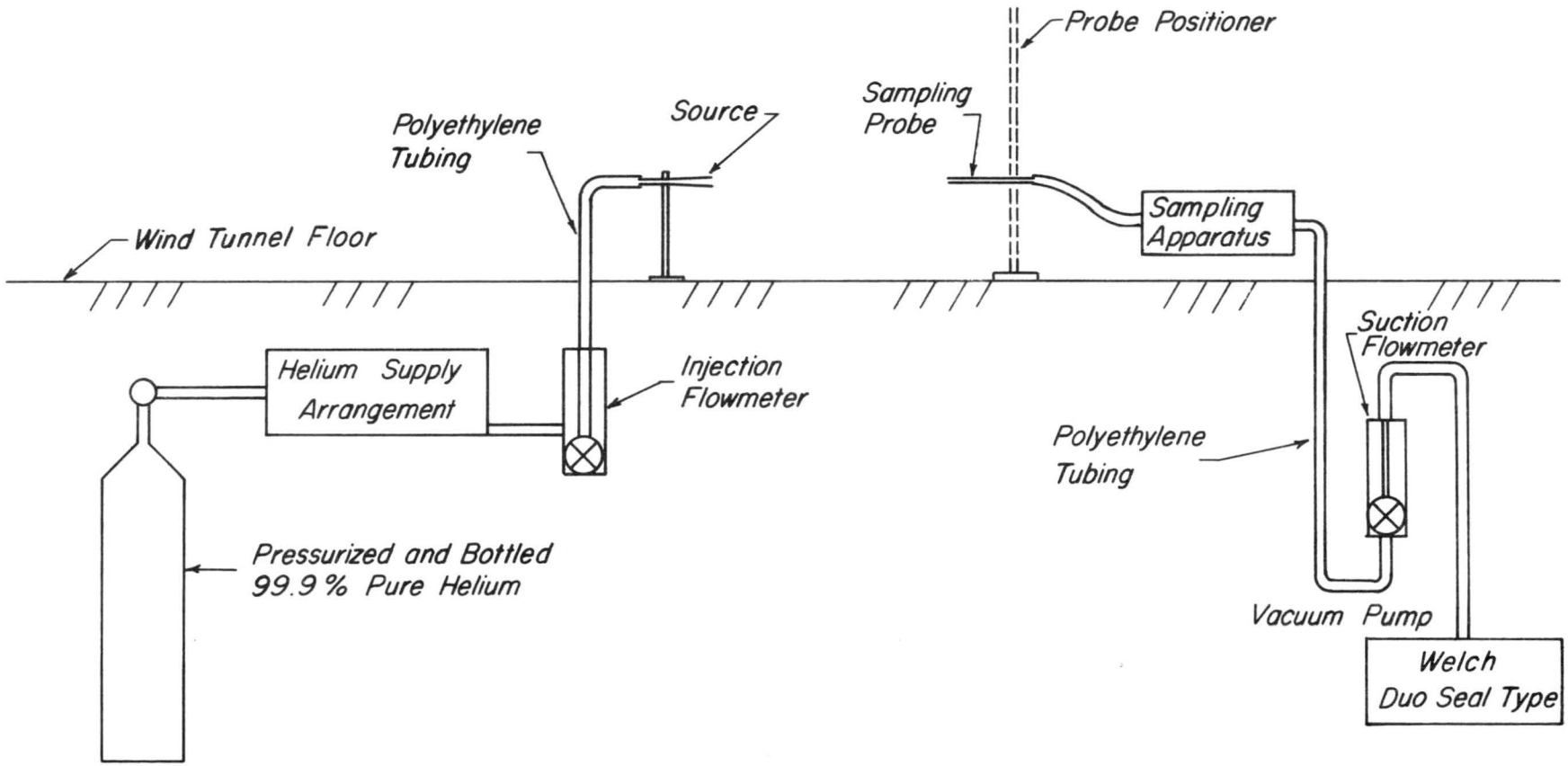

Fig. 10 SCHEMATIC LAYOUT OF THE SAMPLING METHOD

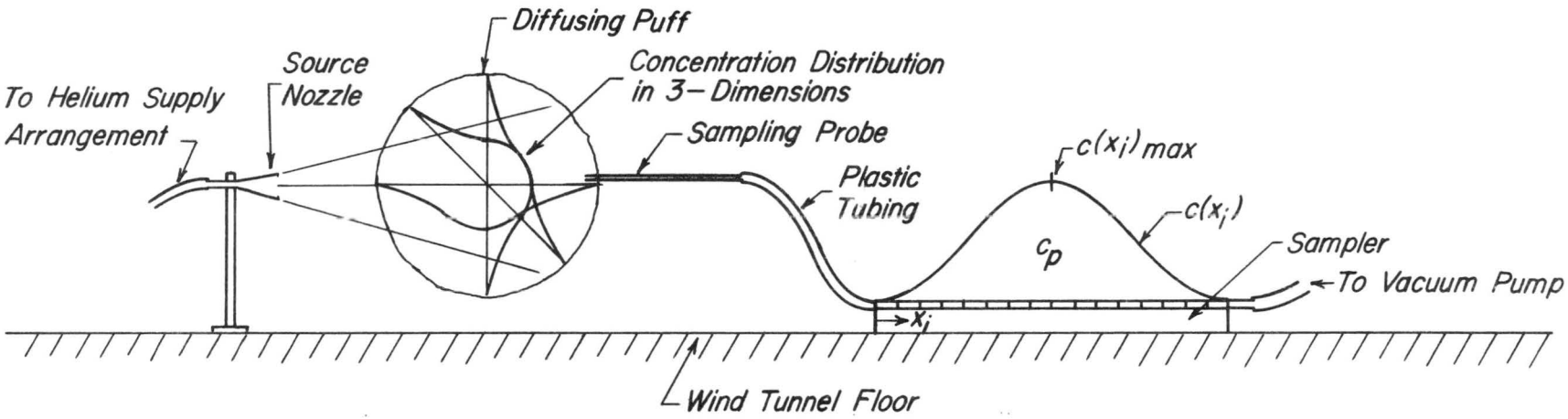

Fig. 11 DEFINITION SKETCH FOR CONCENTRATION PARAMETERS,

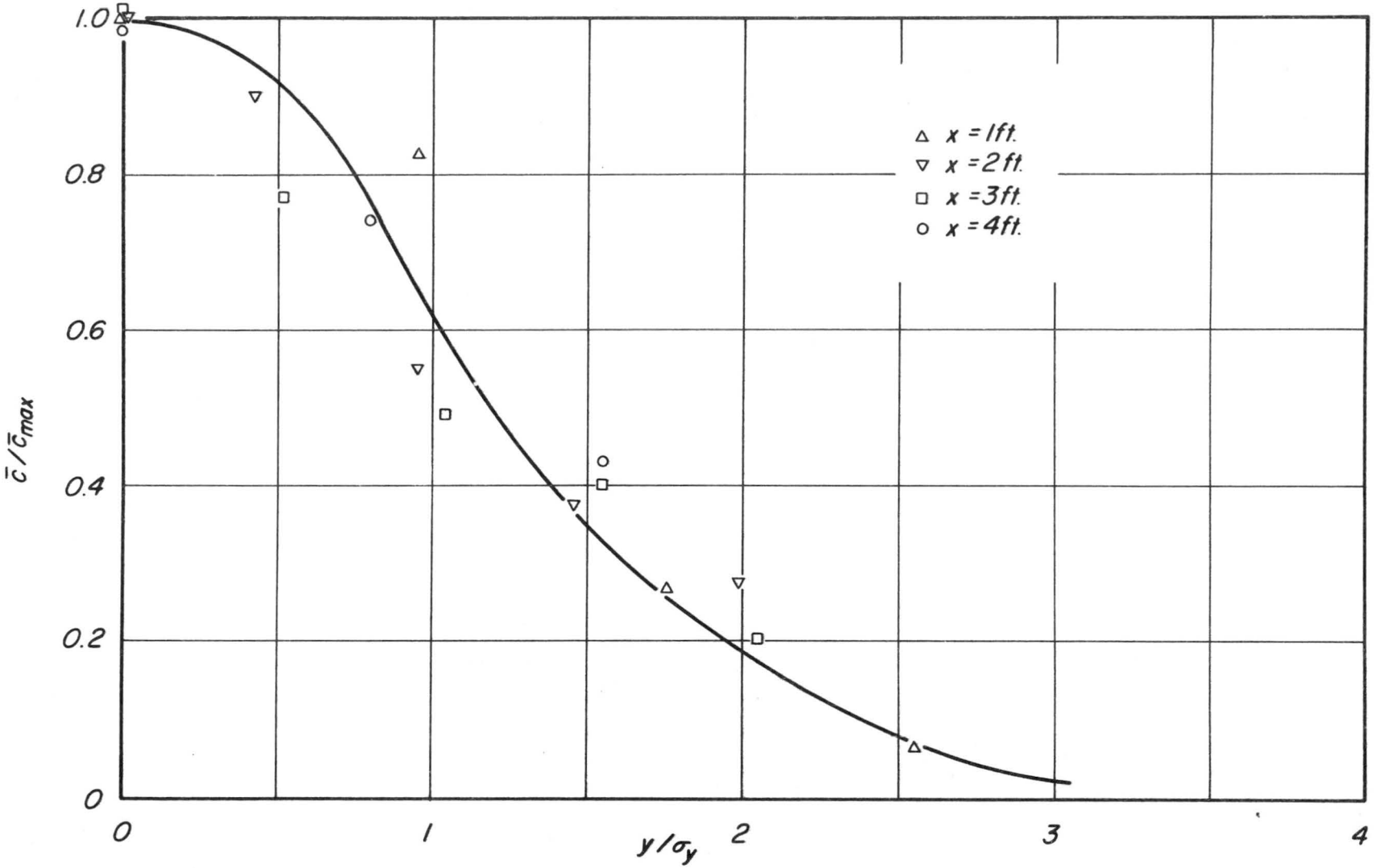

Fig. 12 DIMENSIONLESS CONCENTRATION DISTRIBUTION IN LATERAL DIRECTION.

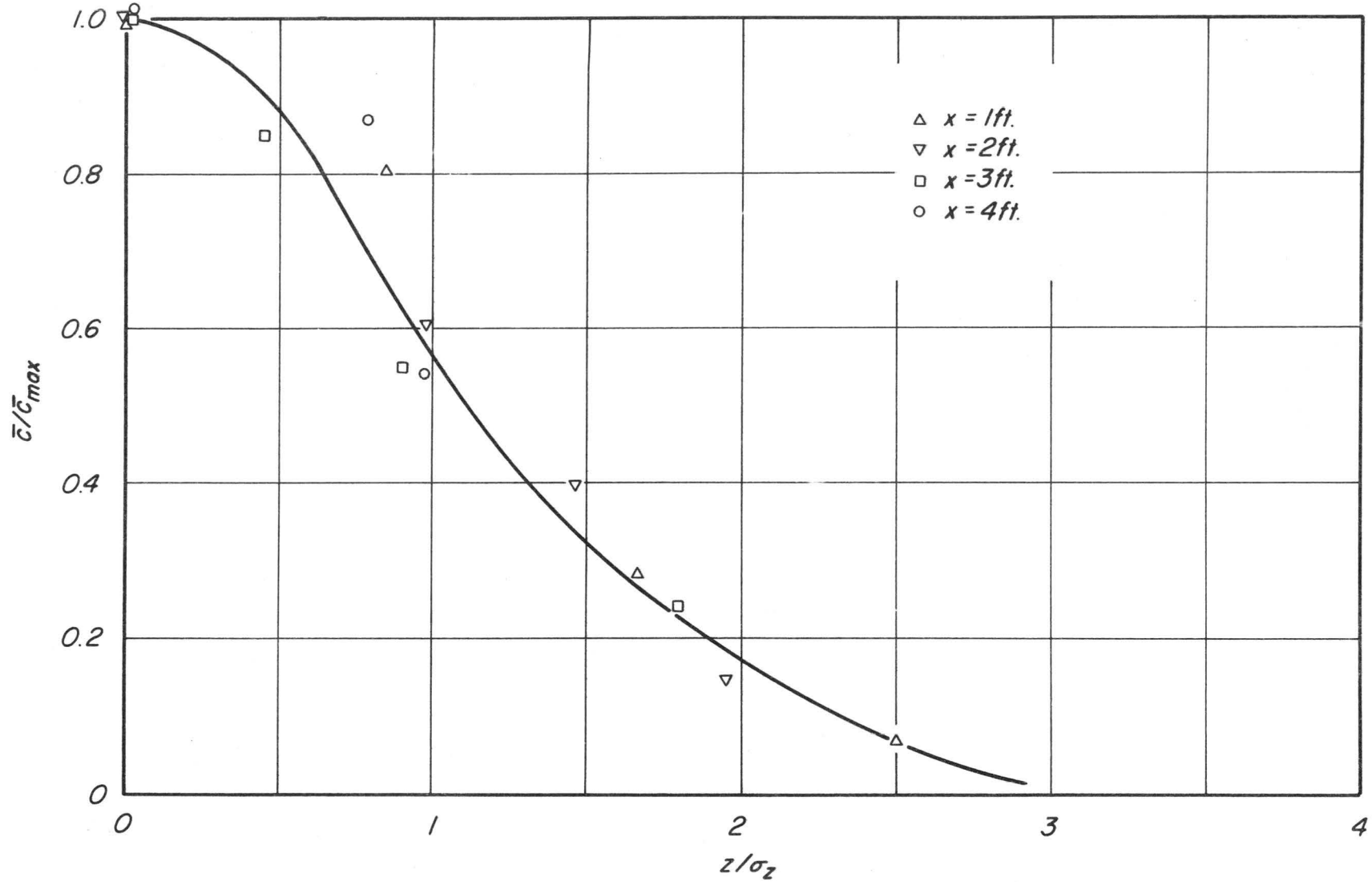

Fig. 13 DIMENSIONLESS CONCENTRATION DISTRIBUTION IN VERTICAL DIRECTION.

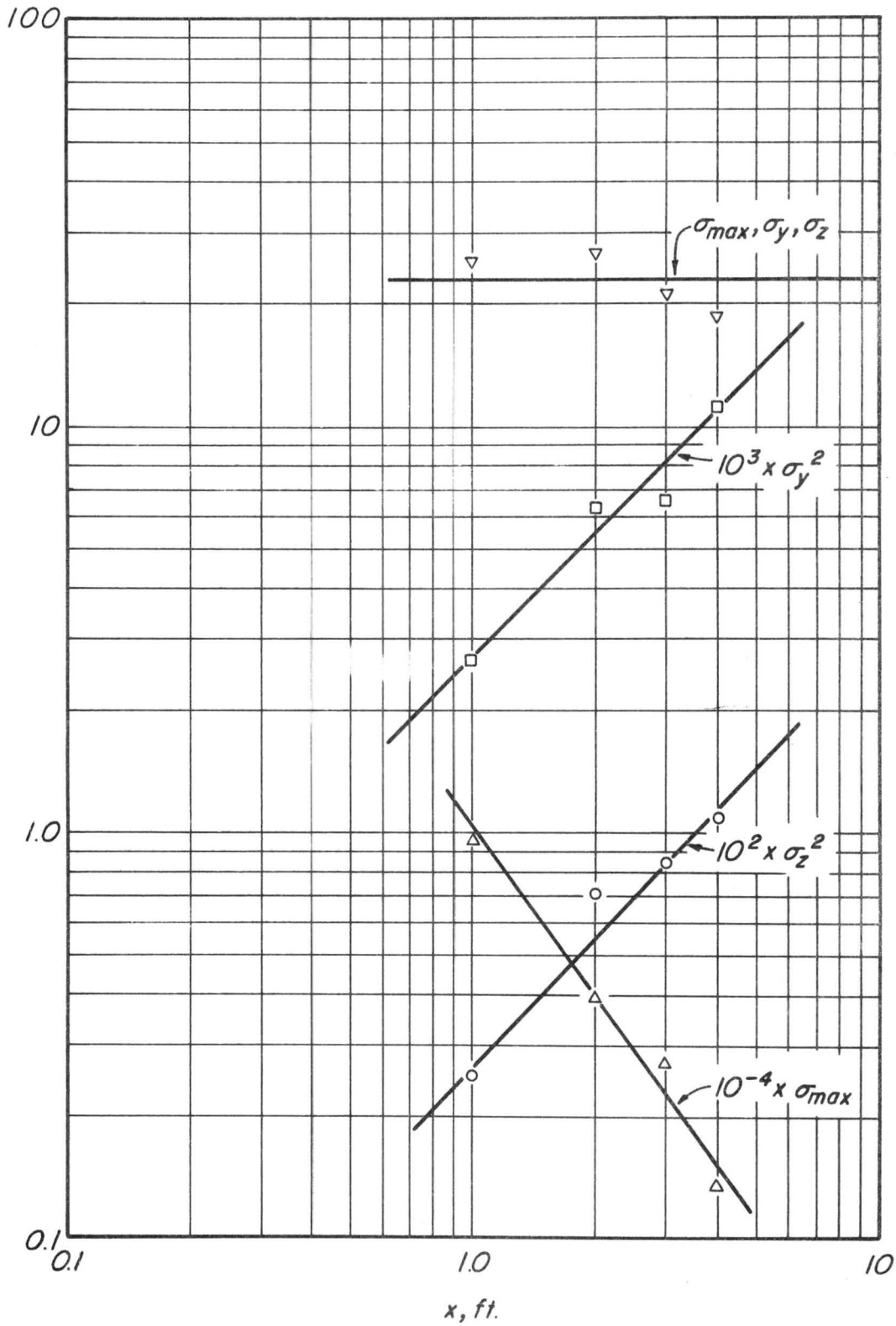

Fig. 14 CONCENTRATION PARAMETERS VERSUS TRAVEL DISTANCE.

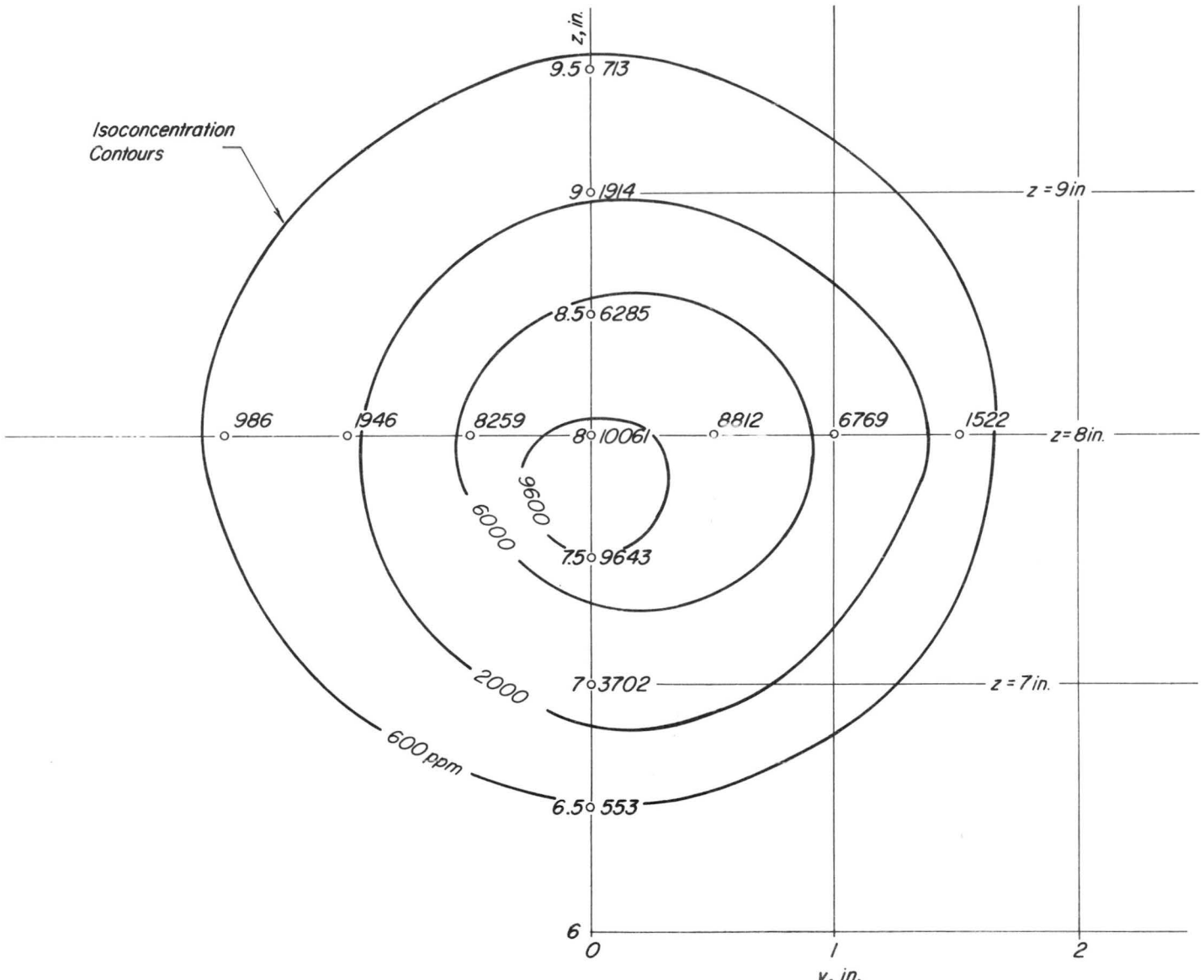

Fig. 15 CLOUD CROSS SECTION AT x = 1ft.

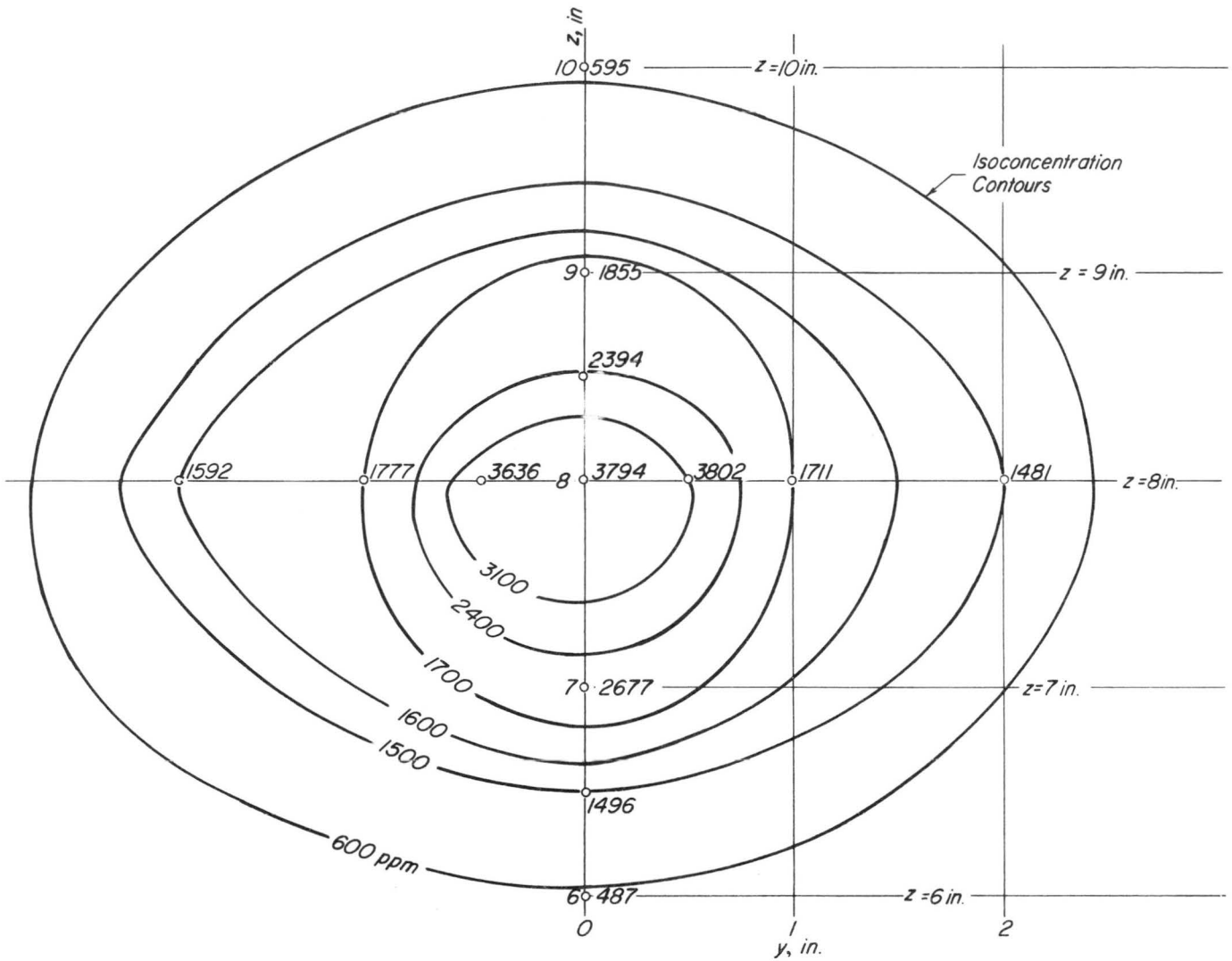

Fig. 16 CLOUD CROSS SECTION AT x = 2 ft.

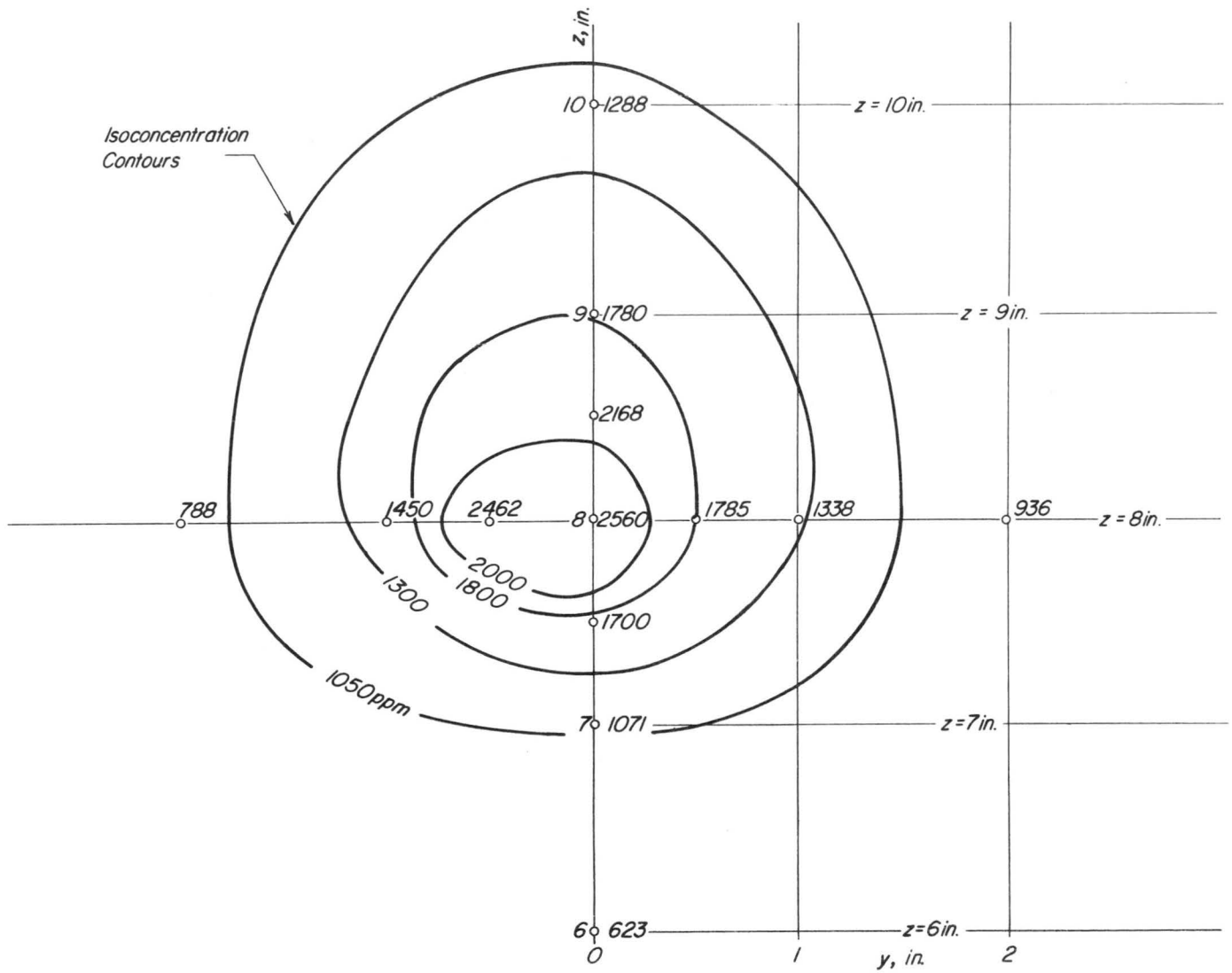

Fig.17 CLOUD CROSS SECTION AT x=3ft.

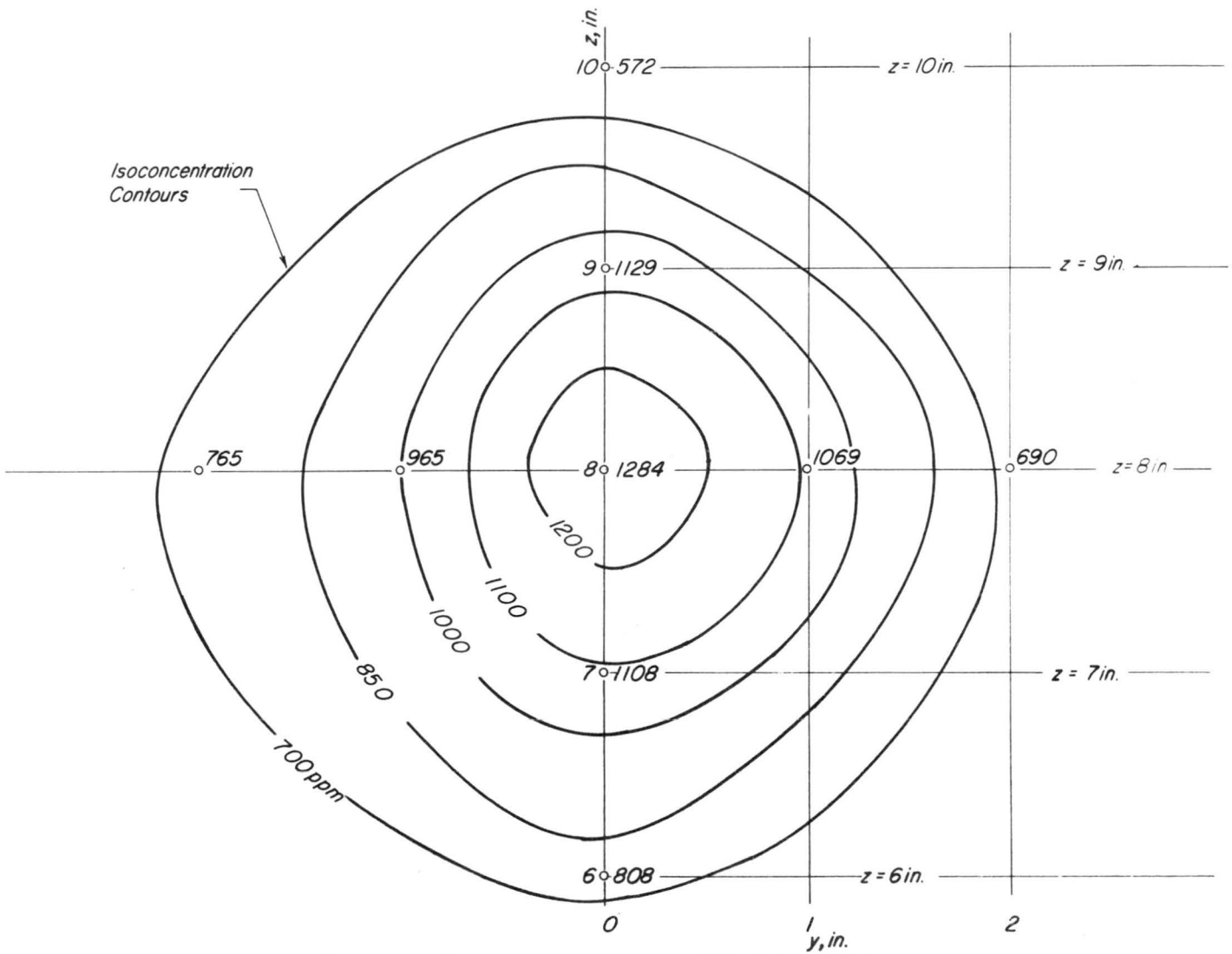

Fig. 18 CLOUD CROSS SECTION AT x = 4 ft.

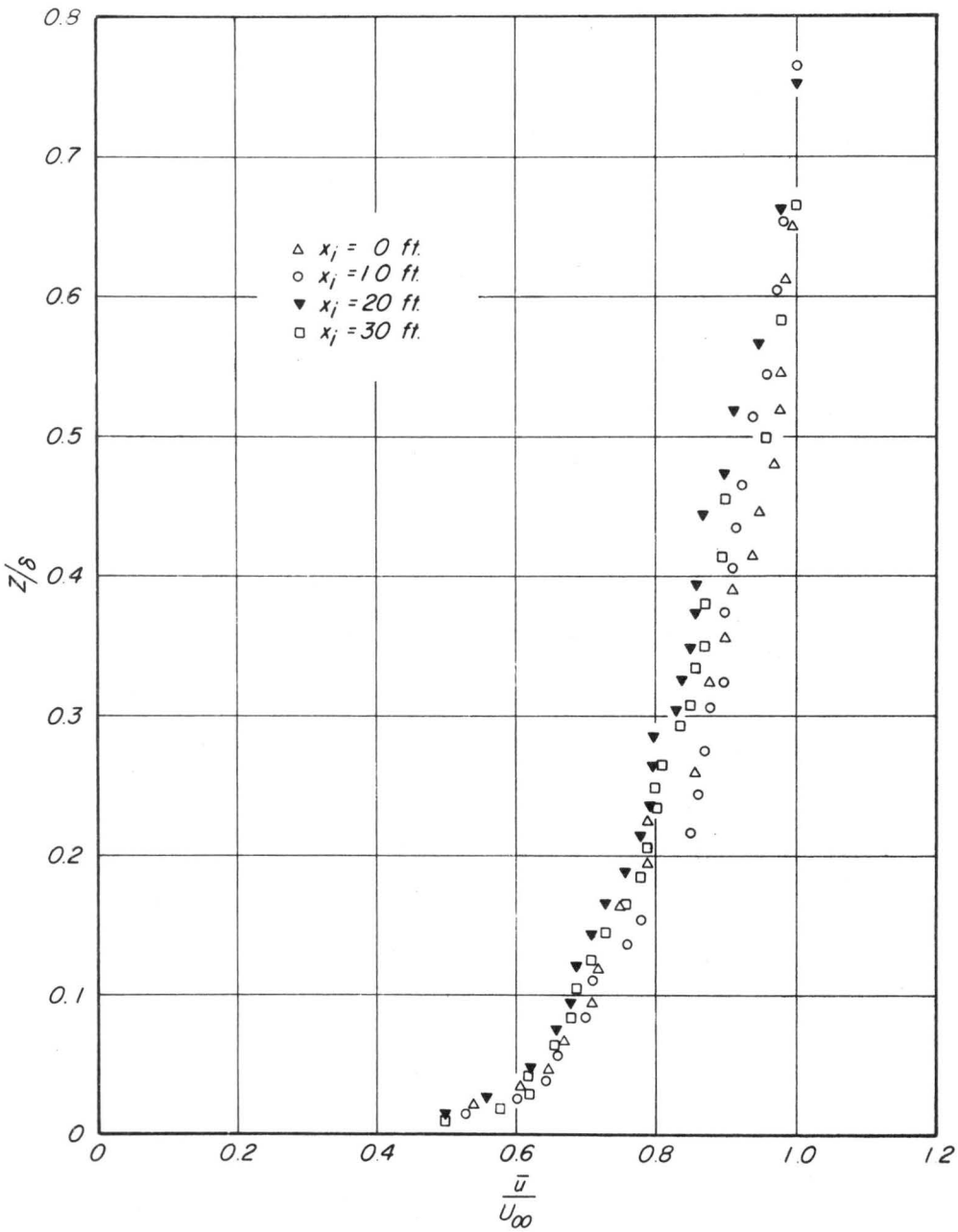

Fig. 19 VELOCITY PROFILES

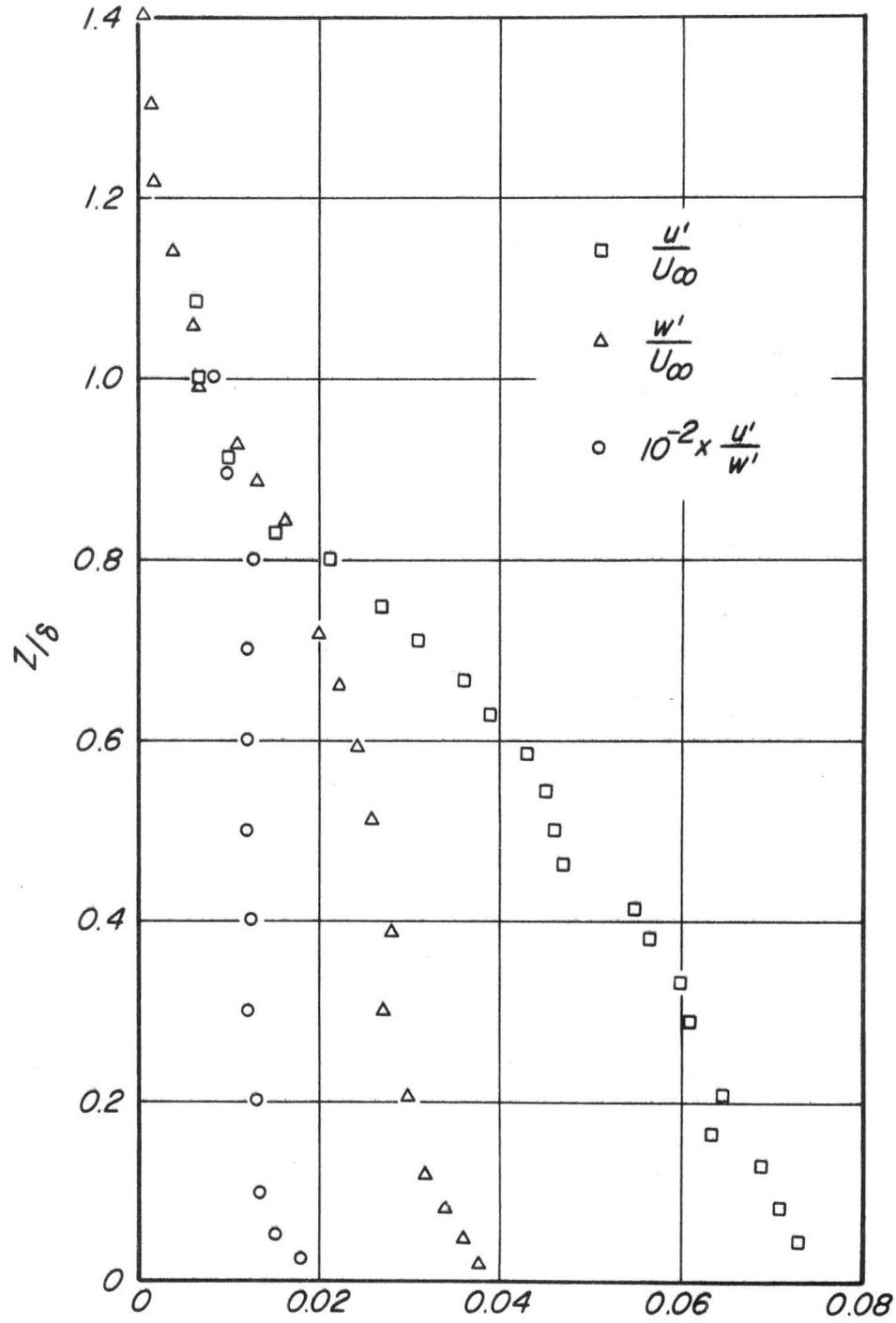

Fig. 20 VARIATION OF TURBURENCE PARAMETERS AS A FUNCTION OF z/δ.

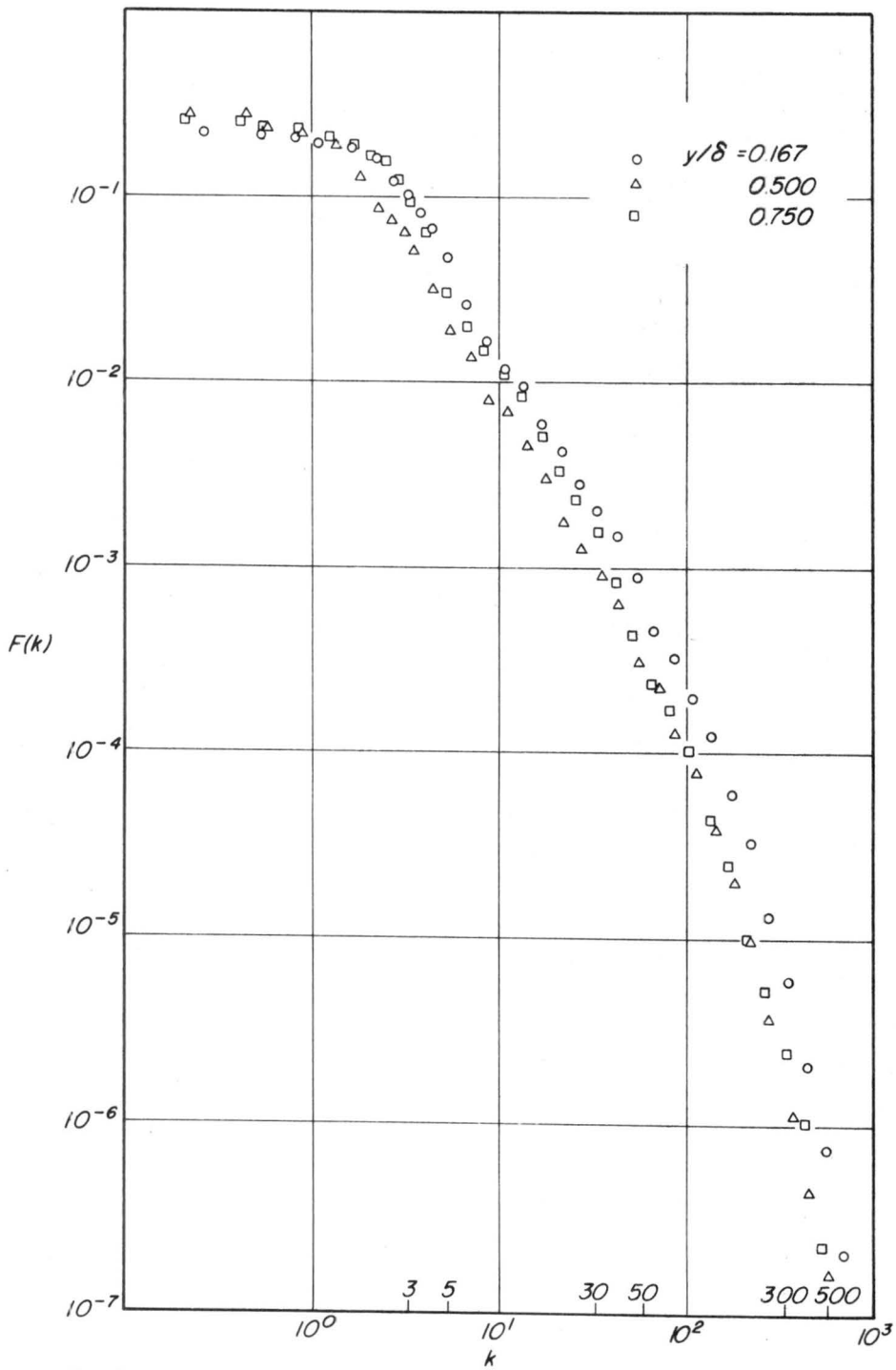

Fig. 21 SPECTRAL ENERGY DISTRIBUTION OF LONGITUDINAL COMPONENT.

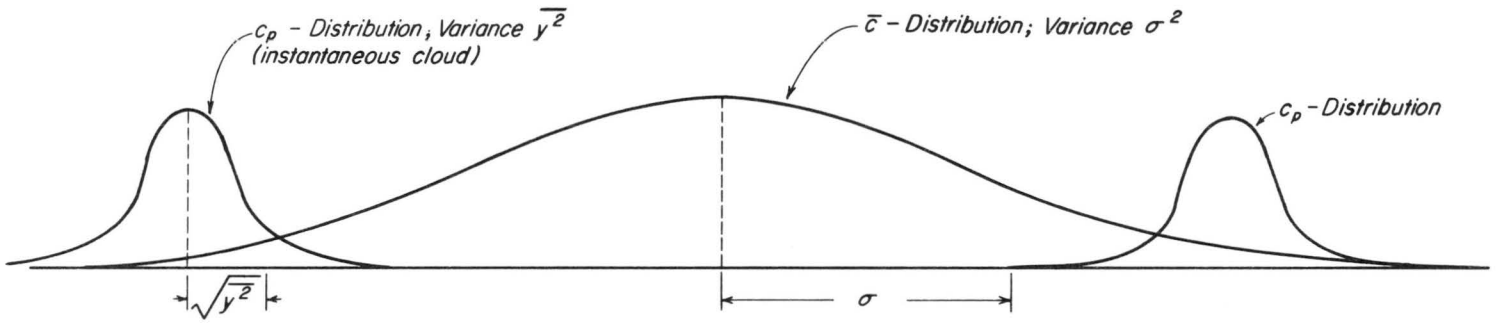

Fig. 22 SIMILARITY CONSIDERATIONS FOR CONCENTRATION DISTRIBUTION IN THE DIFFUSION CLOUD.

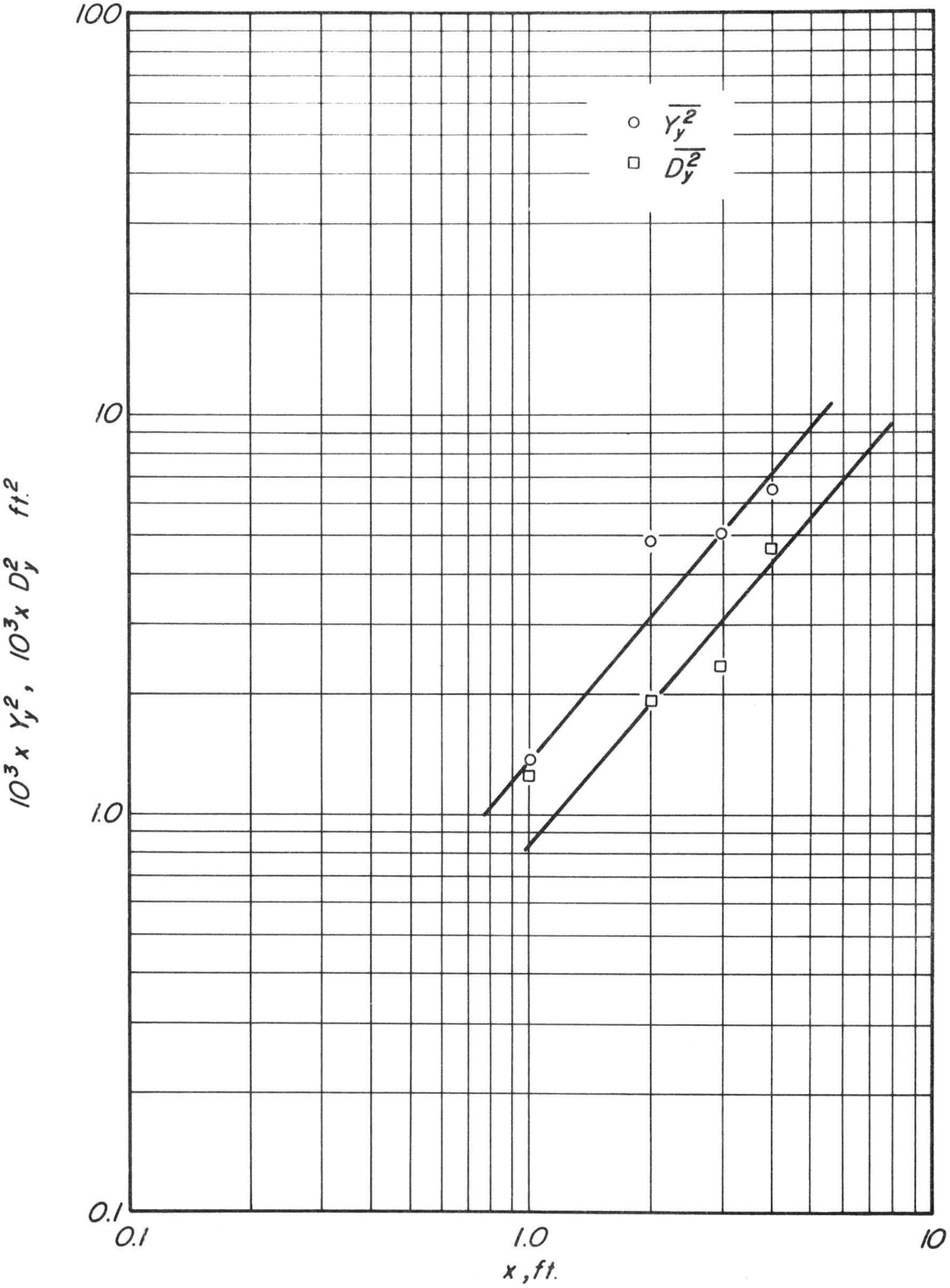

Fig. 23 SPREADING AND MEANDERING VARIANCE VERSUS TRAVEL DISTANCE.

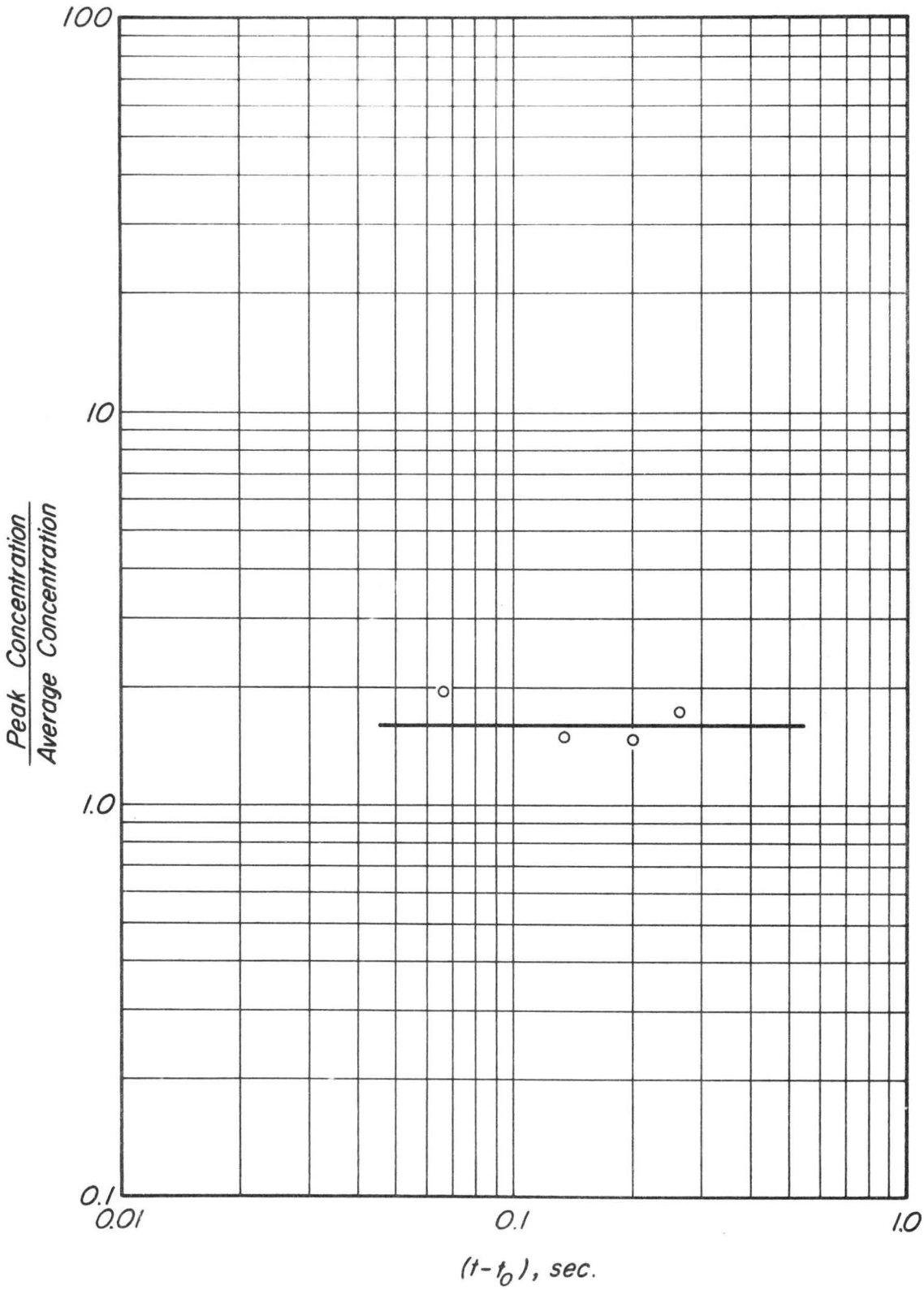

Fig. 24 PEAK-TO-AVERAGE CONCENTRATION RATIOS AS A FUNCTION OF DISPERSION TIME.

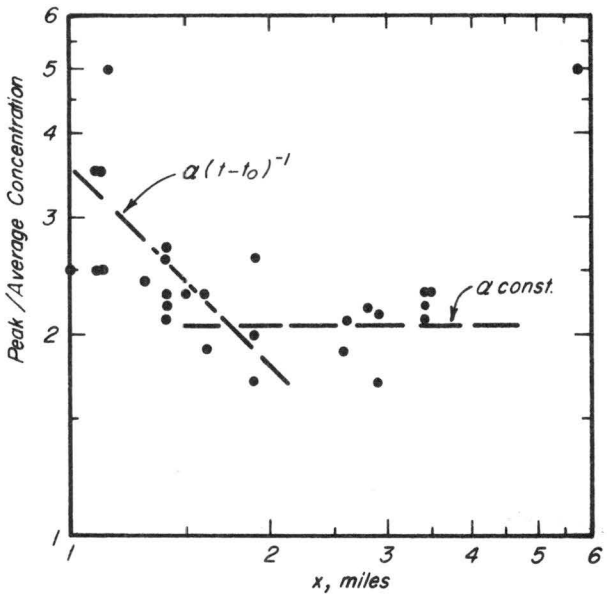

Fig. 25 PEAK TO AVERAGE CONCENTRATION RATIOS AS A FUNCTION OF DISPERSION DISTANCE ; DATA OF WANTA AND GARTRELL.

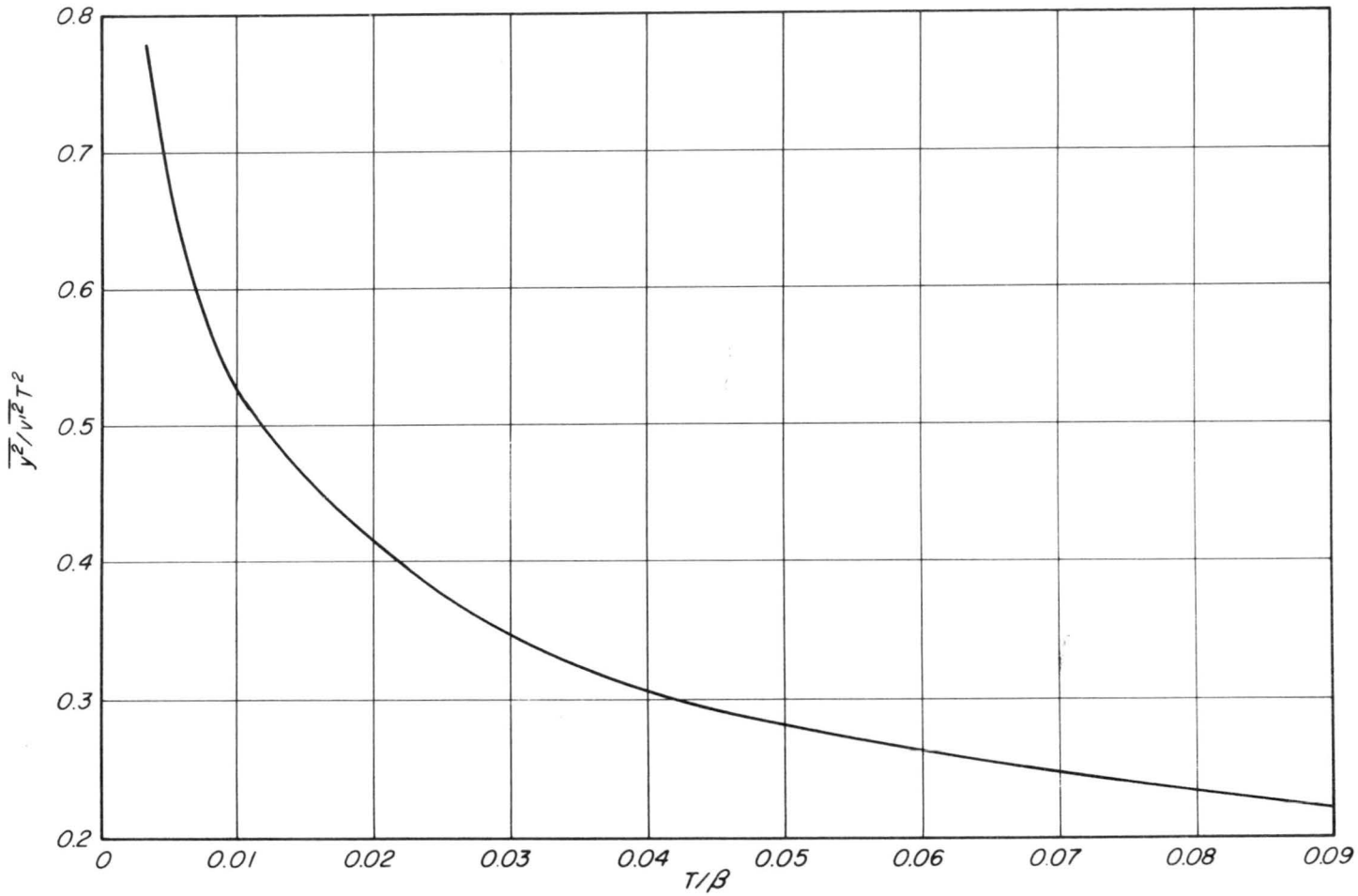

Fig. 26 DETERMINATION OF THE HAY — PASQUILL SCALE PARAMETER.

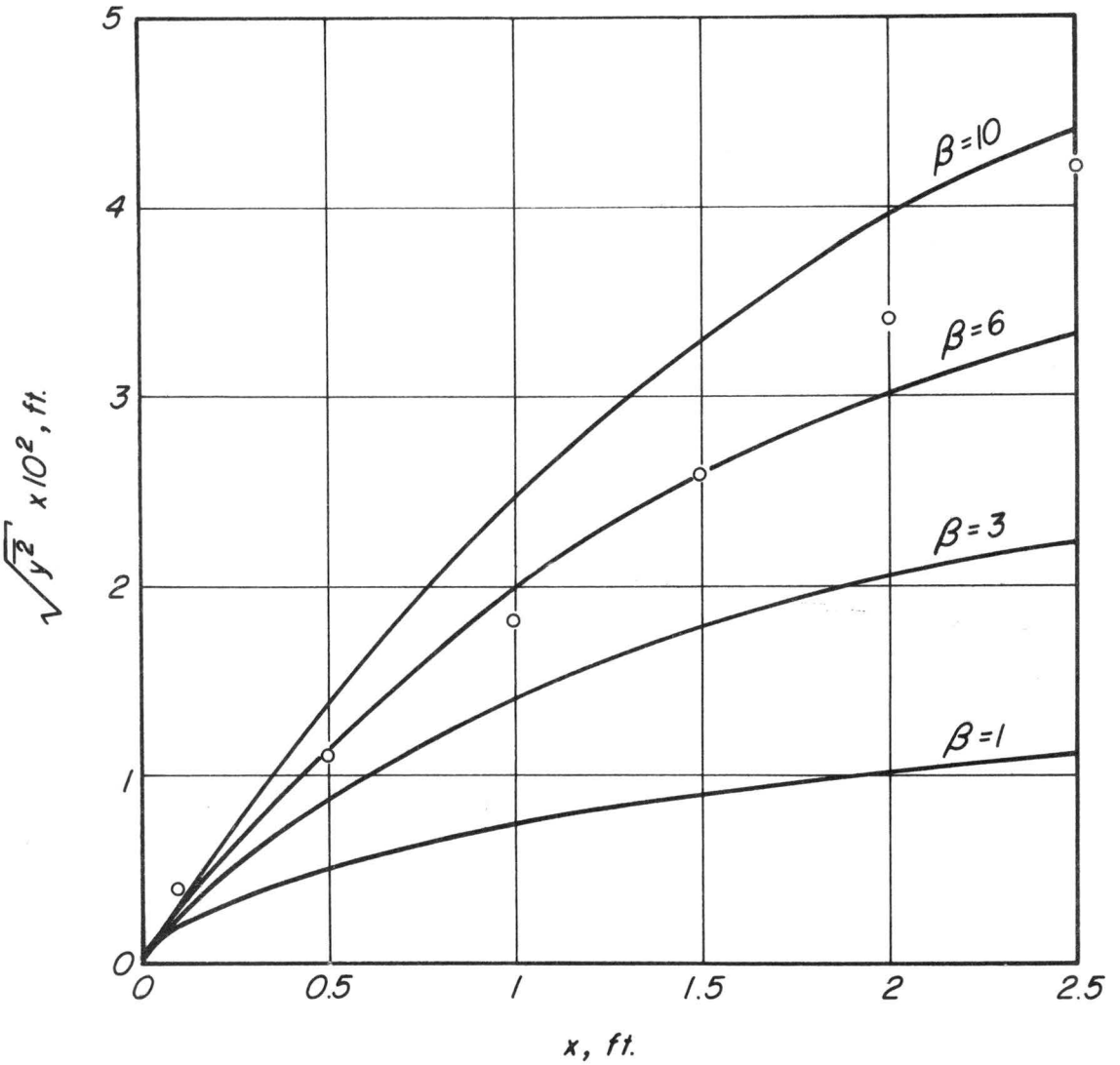

Fig. 27 VALUES OF THE HAY–PASQUILL SCALE PARAMETER FOR MICKELSEN'S DATA.

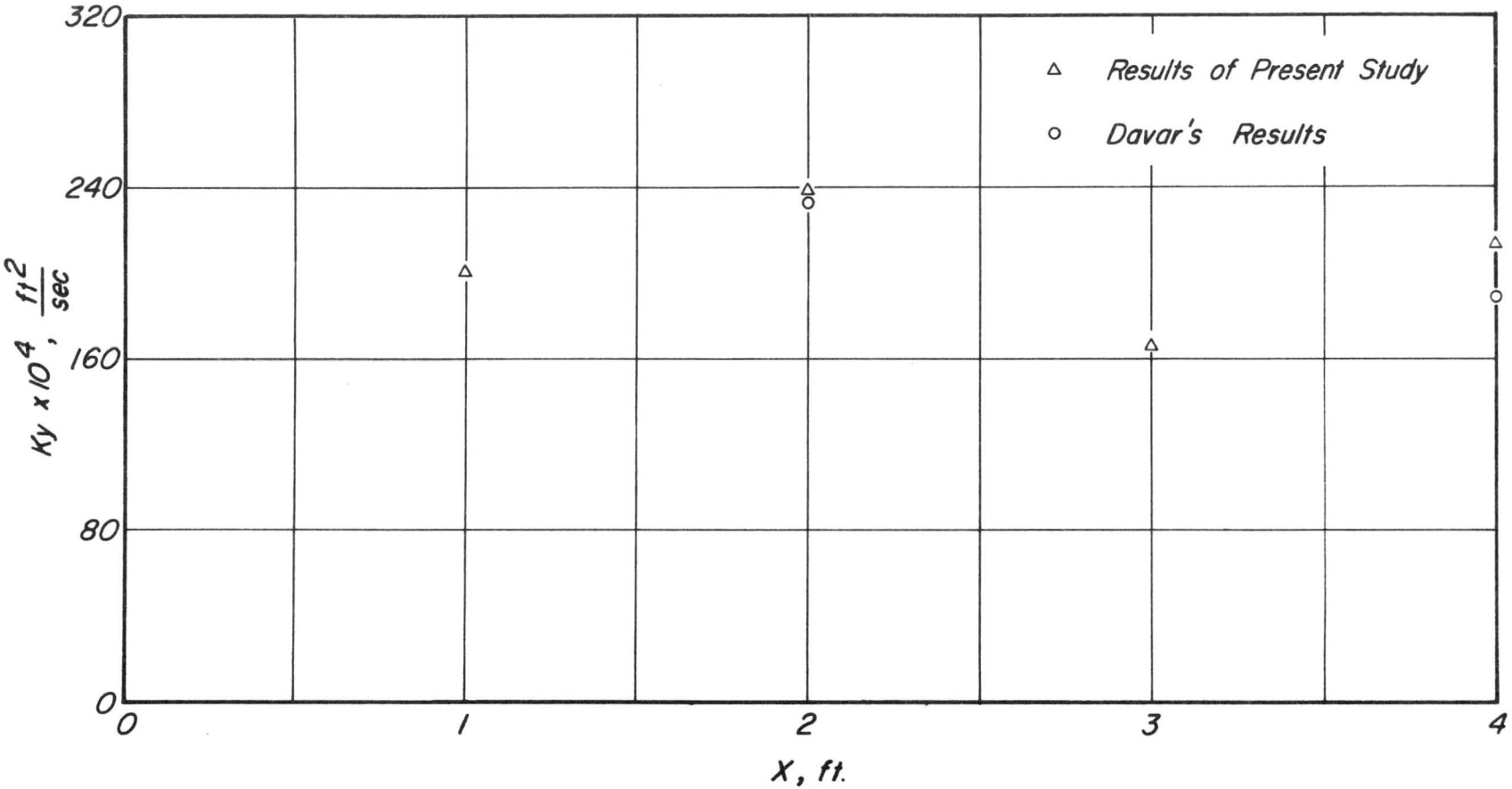

Fig. 28 LATERAL DIFFUSIVITY AT DIFFERENT STATIONS.

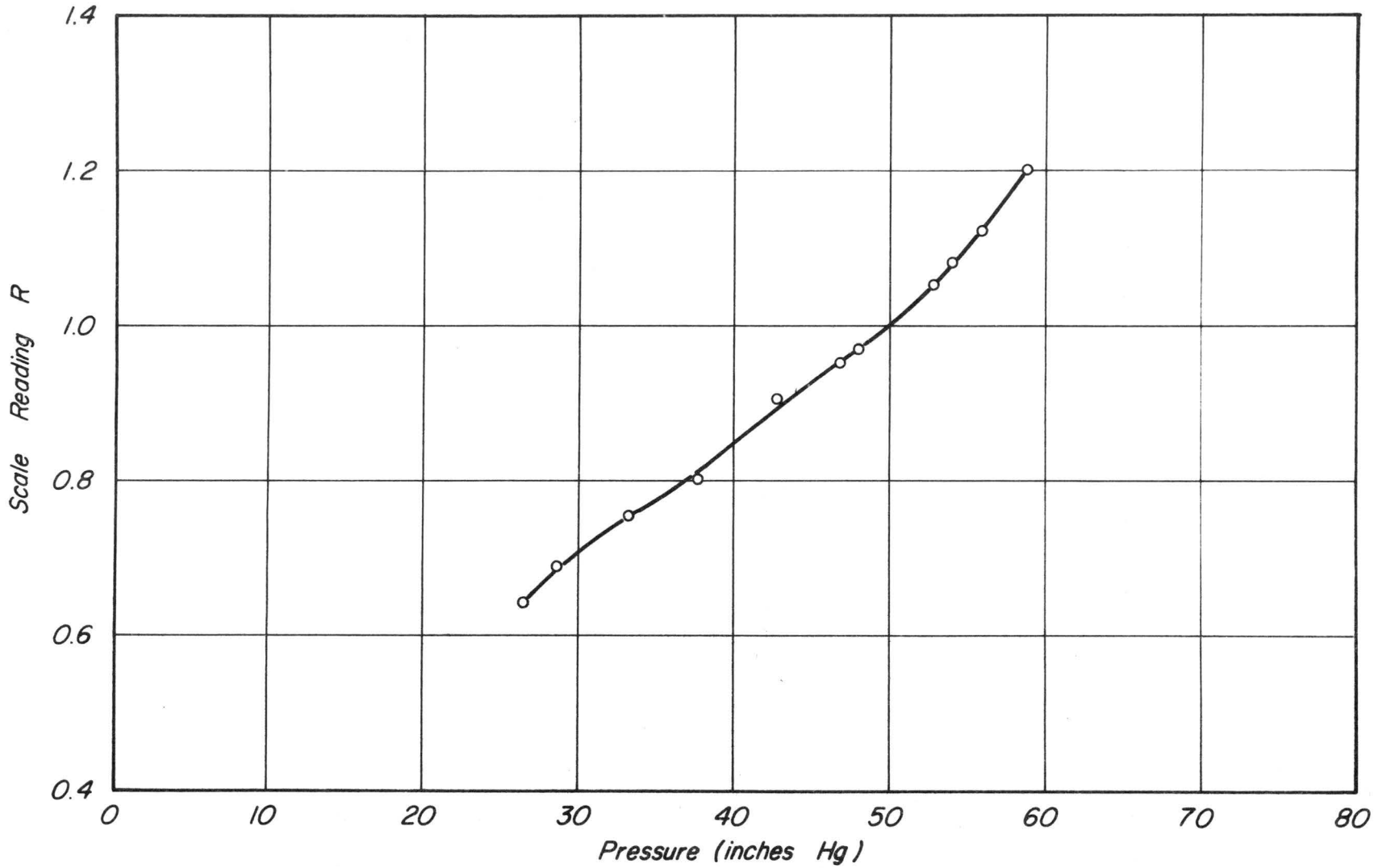

Fig. A-1 SCALE READING AS A FUNCTION OF PRESSURE.

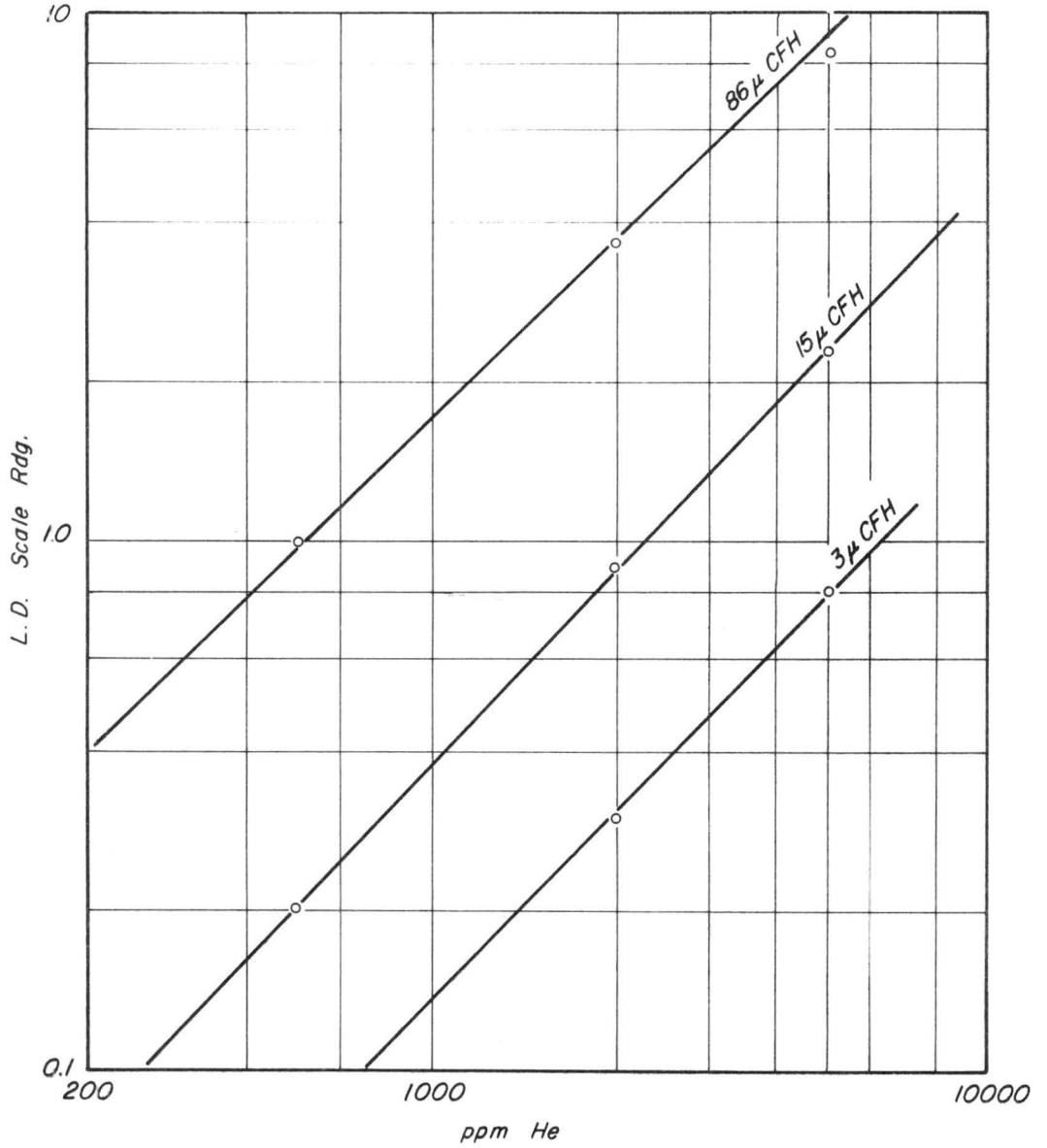

Fig. A-2 SCALE READING AS A FUNCTION OF CONCENTRATION AT ATMOSPHERIC PRESSURE.

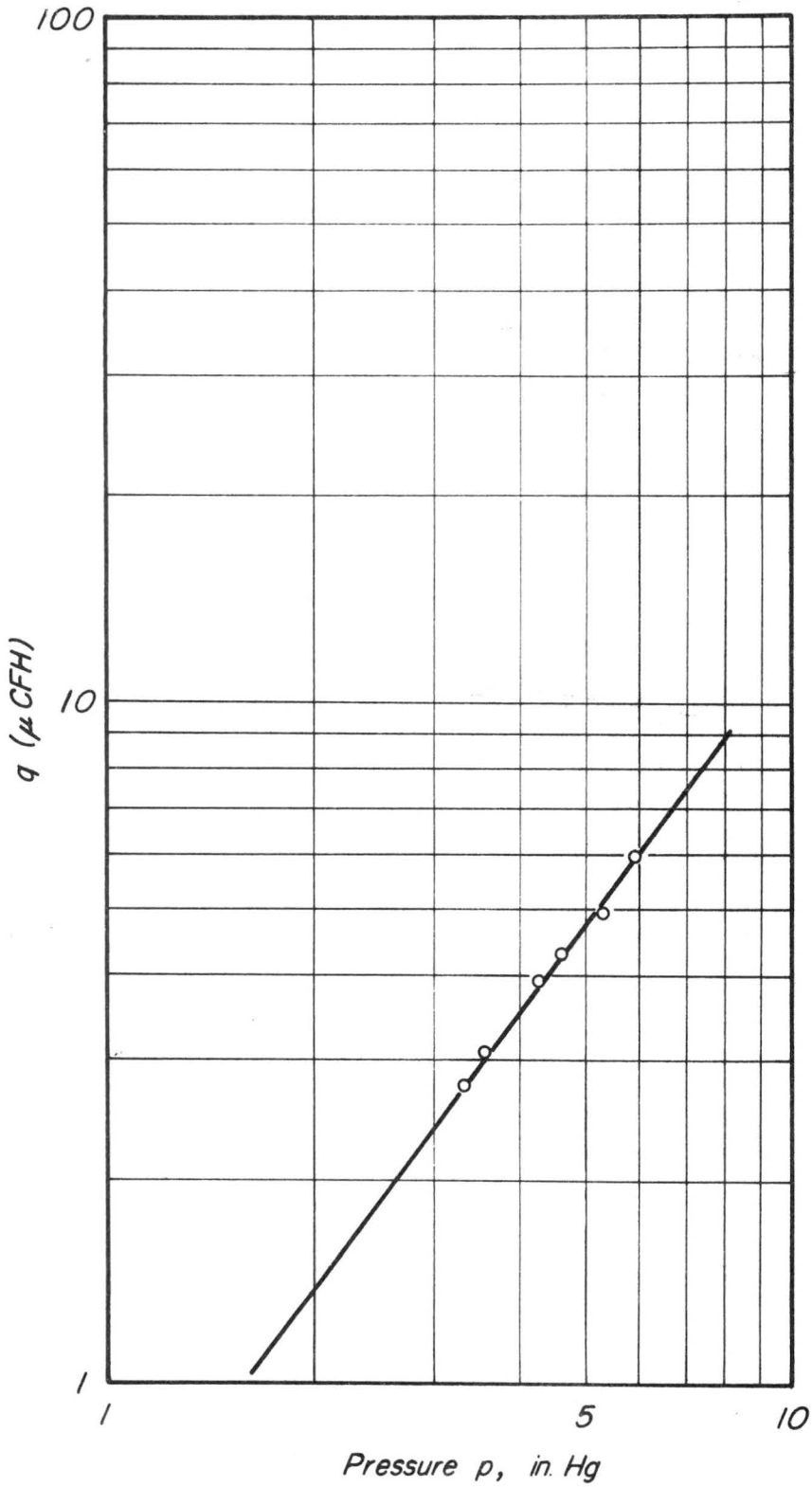

Fig. A-3 LEAK RATE AS A FUNCTION OF PRESSURE

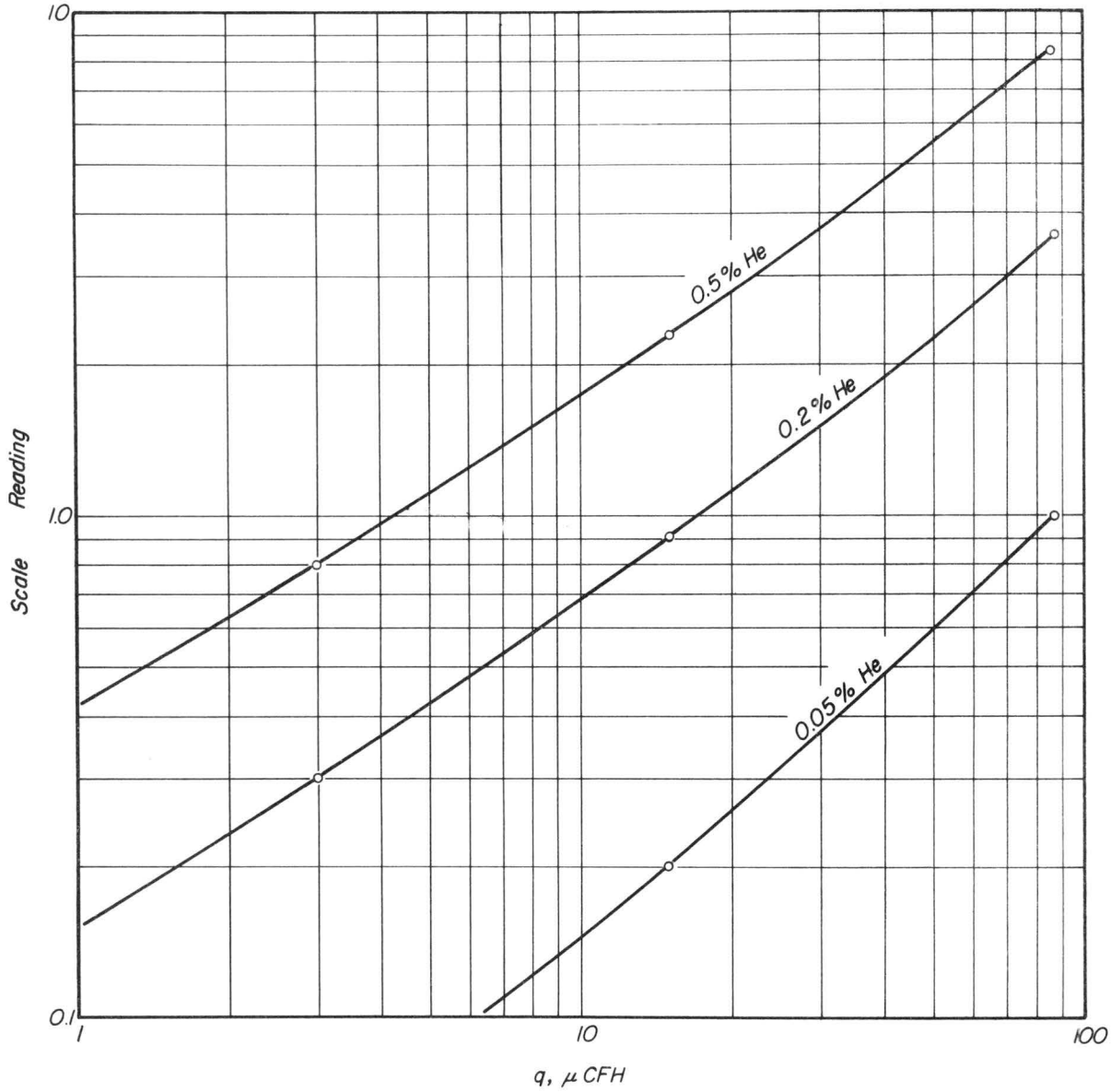

Fig. A-4 SCALE READING AS A FUNCTION OF LEAK RATE.

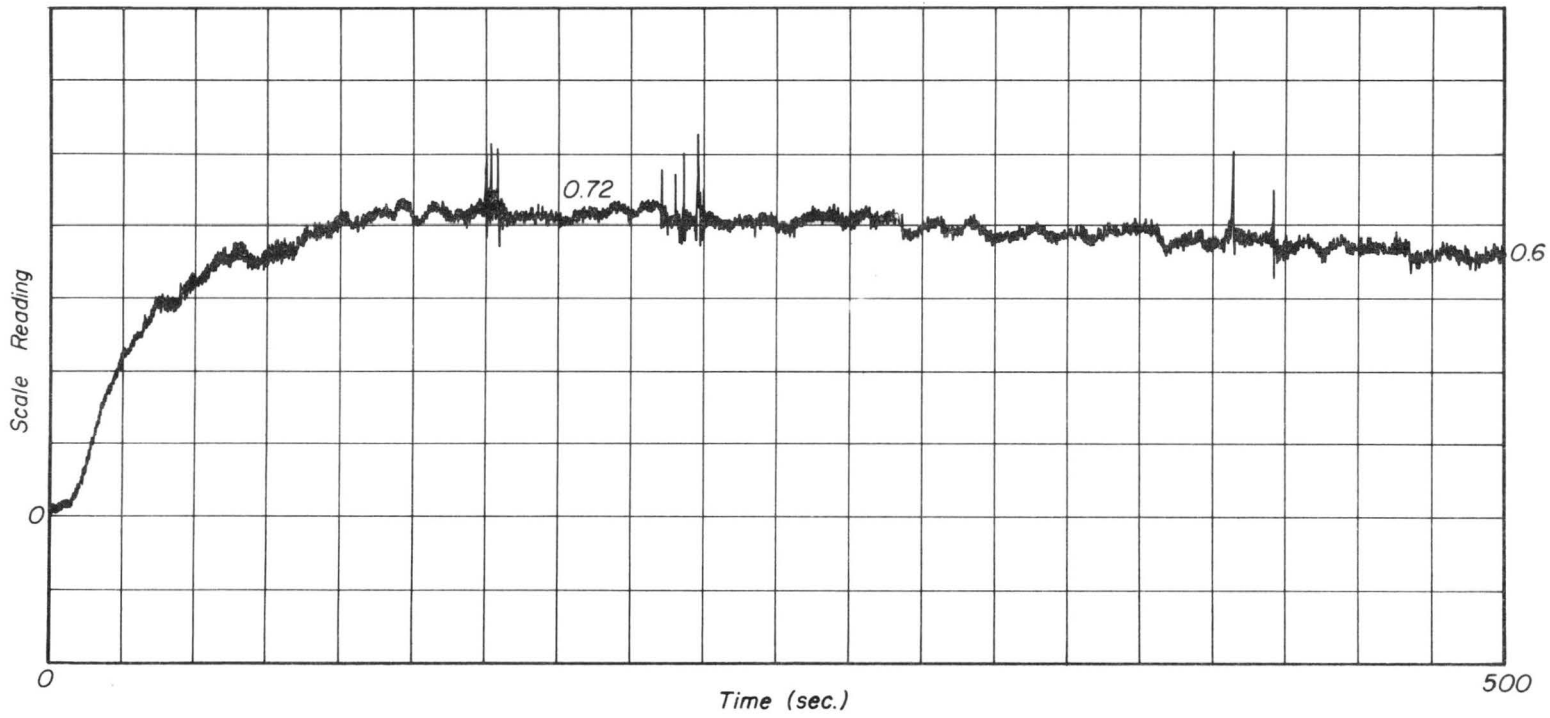

Fig. A-5 CONCENTRATION-TIME RELATIONSHIP FOR 0.5% HELIUM MIXTURE.

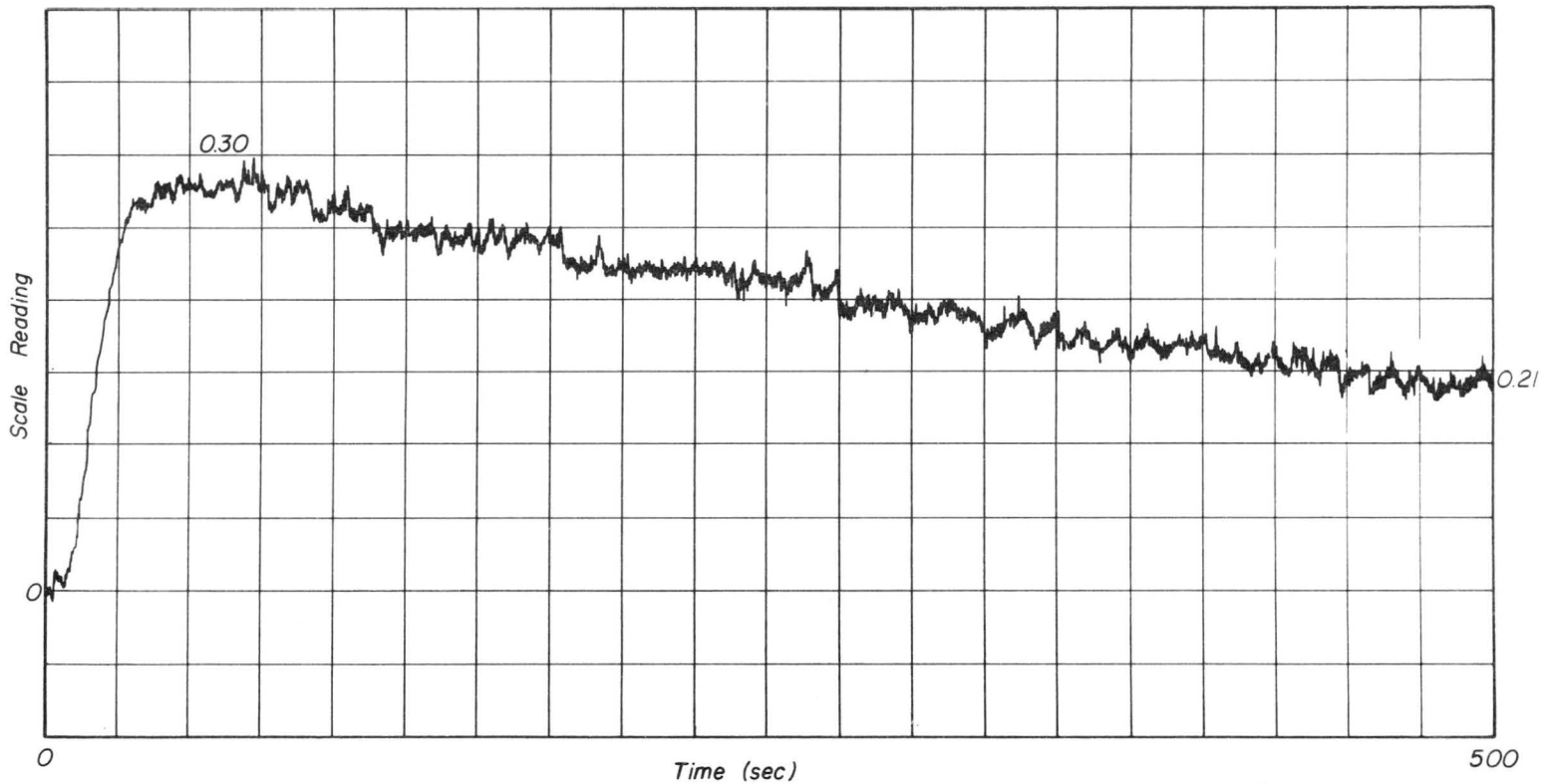

Fig. A-6 CONCENTRATION-TIME RELATIONSHIP FOR 0.2% HELIUM MIXTURE.

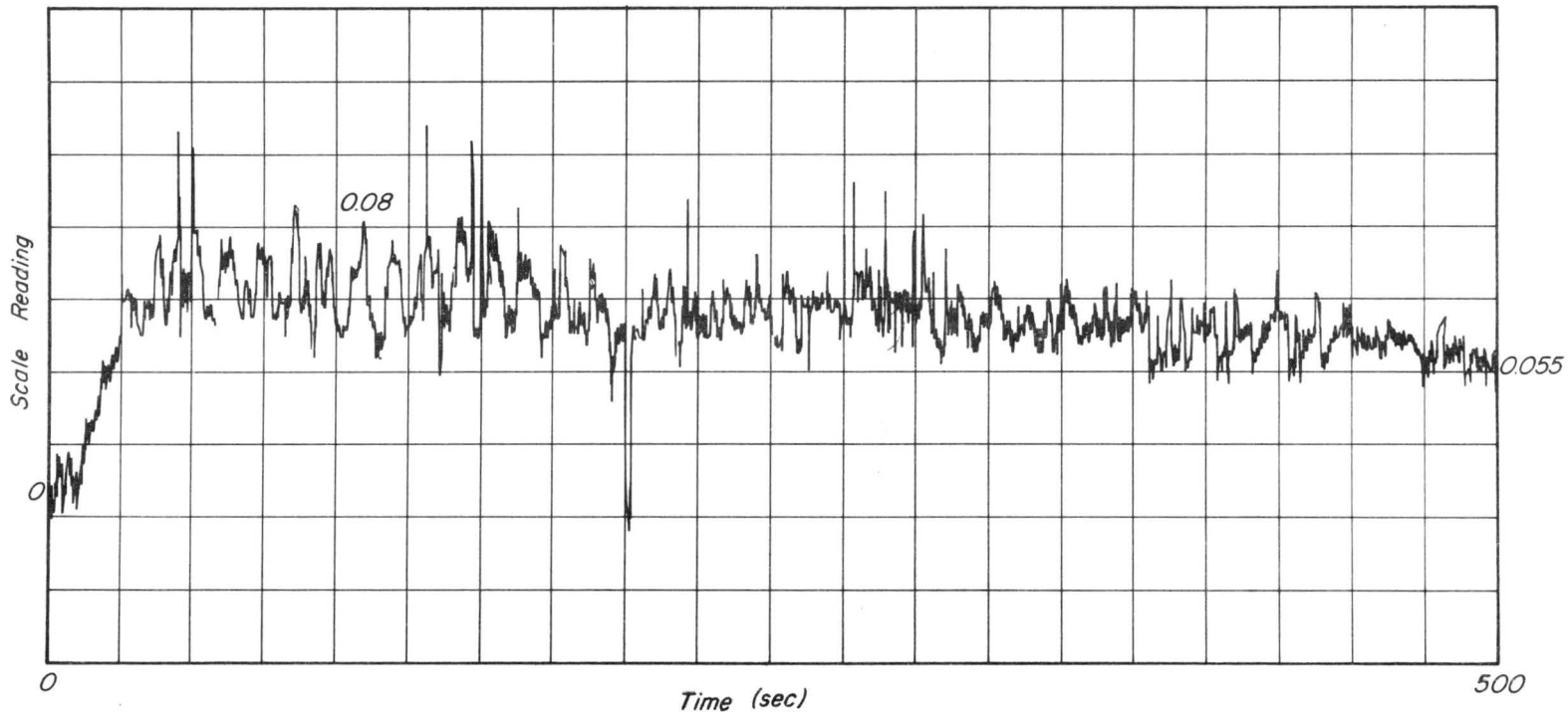

Fig. A-7 CONCENTRATION - TIME RELATIONSHIP FOR 0.05% HELIUM MIXTURE

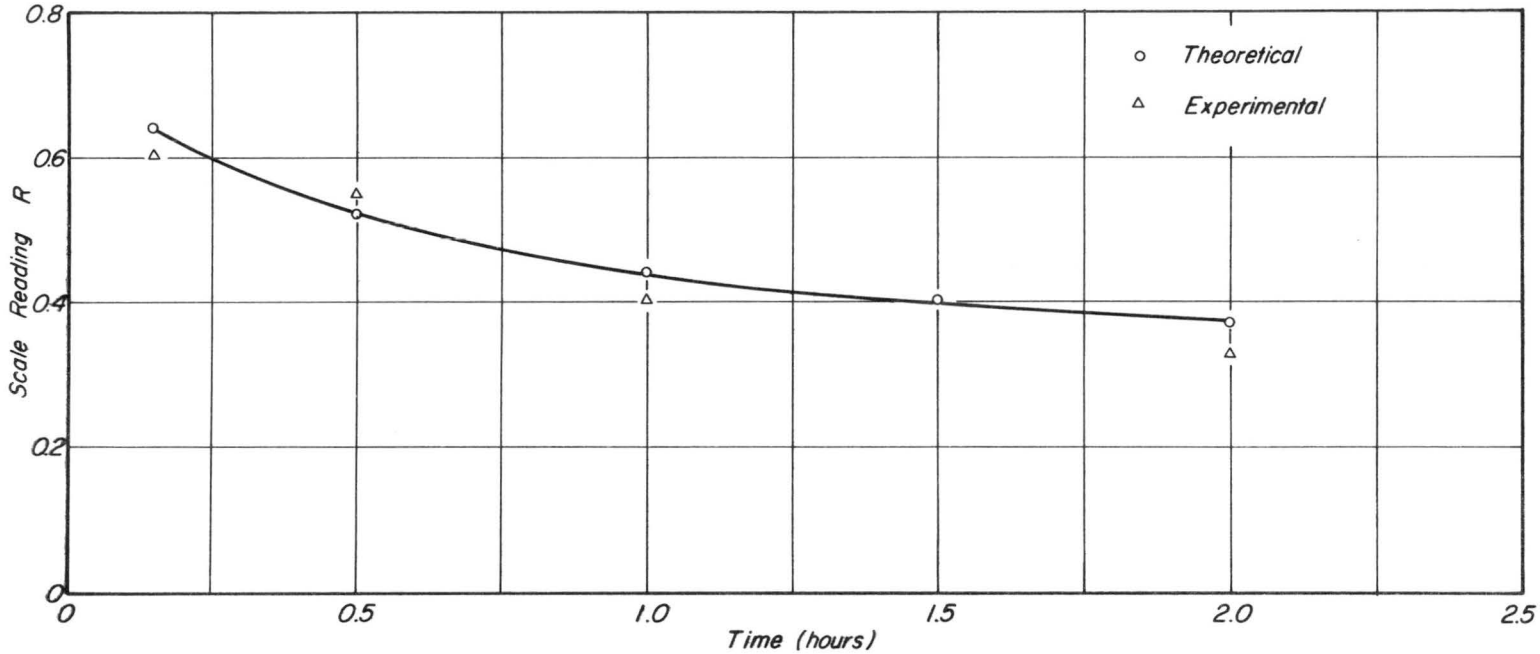

Fig. A-8 COMPARISON OF PREDICTED AND EXPERIMENTAL RESULTS.

Unclassified

Security Classification

DOCUMENT CONTROL DATA - R&D

(Security classification of title, body of abstract and indexing annotation must be entered when the overall report is classified)

1. ORIGINATING ACTIVITY *(Corporate author)*
Fluid Mechanics Program, College of Engineering
Colorado State University
Fort Collins, Colorado

2a. REPORT SECURITY CLASSIFICATION
Unclassified

2b. GROUP
Unclassified

3. REPORT TITLE
DIFFUSION FROM AN INSTANTANEOUS POINT SOURCE INTO A TURBULENT BOUNDARY LAYER

4. DESCRIPTIVE NOTES *(Type of report and inclusive dates)*
Technical Report

5. AUTHOR(S) *(Last name, first name, initial)*
Suresh Chandra

6. REPORT DATE	7a. TOTAL NO. OF PAGES	7b. NO. OF REFS
August 1967	141	22

8a. CONTRACT OR GRANT NO.
DA-AMC-28-043-65-G20

b. PROJECT NO.
2246

c.

d.

9a. ORIGINATOR'S REPORT NUMBER(S)
CER 67-68 SC 7

9b. OTHER REPORT NO(S) *(Any other numbers that may be assigned this report)*

10. AVAILABILITY/LIMITATION NOTICES
Distribution of this report is unlimited

11. SUPPLEMENTARY NOTES

12. SPONSORING MILITARY ACTIVITY
Fort Monmouth Procurement Division
Procurement and Production Directorate
U.S. Army Electronics Command
Fort Monmouth, New Jersey 07703

13. ABSTRACT

Diffusion of helium gas from an instantaneous point source within a neutra boundary layer has been studied. The investigation was made in a wind tunnel of the Fluid Dynamics and Diffusion Laboratory.

Concentrations from a simulated point source, located at a fixed height of eight inches above a smooth surface, were measured for several downstream cross-sections of the diffusing cloud. The free stream velocity for the entire study was 20 ft/sec. Statistical parameters have been used to describe the concentration data in terms of the time-average as well as the maximum instantaneous concentration at a point in the diffusion field.

The lateral and vertical diffusivities are determined from the diffusion data. Comparison of data from the instantaneous point source, in terms of the time-averaged concentration parameters, with the continuous point source data of other investigators shows good agreement. The concentration data are presented in terms of dimensionless parameters.

Separation of the total dispersion into two components, spreading and meandering, is obtained on the basis of Gifford's fluctuating plume model. The results of this analysis have been used to determine the Hay-Pasquill scale parameter which related the Lagrangian and Eulerian scales of turbulence.

DD FORM 1 JAN 64 1473

Unclassified

Security Classification

14. KEY WORDS	LINK A		LINK B		LINK C	
	ROLE	WT	ROLE	WT	ROLE	WT

INSTRUCTIONS

1. ORIGINATING ACTIVITY: Enter the name and address of the contractor, subcontractor, grantee, Department of Defense activity or other organization *(corporate author)* issuing the report.

2*a*. REPORT SECURITY CLASSIFICATION: Enter the overall security classification of the report. Indicate whether "Restricted Data" is included. Marking is to be in accordance with appropriate security regulations.

2*b*. GROUP: Automatic downgrading is specified in DoD Directive 5200.10 and Armed Forces Industrial Manual. Enter the group number. Also, when applicable, show that optional markings have been used for Group 3 and Group 4 as authorized.

3. REPORT TITLE: Enter the complete report title in all capital letters. Titles in all cases should be unclassified. If a meaningful title cannot be selected without classification, show title classification in all capitals in parenthesis immediately following the title.

4. DESCRIPTIVE NOTES: If appropriate, enter the type of report, e.g., interim, progress, summary, annual, or final. Give the inclusive dates when a specific reporting period is covered.

5. AUTHOR(S): Enter the name(s) of author(s) as shown on or in the report. Enter last name, first name, middle initial. If military, show rank and branch of service. The name of the principal author is an absolute minimum requirement.

6. REPORT DATE: Enter the date of the report as day, month, year; or month, year. If more than one date appears on the report, use date of publication.

7*a*. TOTAL NUMBER OF PAGES: The total page count should follow normal pagination procedures, i.e., enter the number of pages containing information.

7*b*. NUMBER OF REFERENCES: Enter the total number of references cited in the report.

8*a*. CONTRACT OR GRANT NUMBER: If appropriate, enter the applicable number of the contract or grant under which the report was written.

8*b*, 8*c*, & 8*d*. PROJECT NUMBER: Enter the appropriate military department identification, such as project number, subproject number, system numbers, task number, etc.

9*a*. ORIGINATOR'S REPORT NUMBER(S): Enter the official report number by which the document will be identified and controlled by the originating activity. This number must be unique to this report.

9*b*. OTHER REPORT NUMBER(S): If the report has been assigned any other report numbers *(either by the originator or by the sponsor)*, also enter this number(s).

10. AVAILABILITY/LIMITATION NOTICES: Enter any limitations on further dissemination of the report, other than those imposed by security classification, using standard statements such as:

(1) "Qualified requesters may obtain copies of this report from DDC."

(2) "Foreign announcement and dissemination of this report by DDC is not authorized."

(3) "U. S. Government agencies may obtain copies of this report directly from DDC. Other qualified DDC users shall request through _____."

(4) "U. S. military agencies may obtain copies of this report directly from DDC. Other qualified users shall request through _____."

(5) "All distribution of this report is controlled. Qualified DDC users shall request through _____."

If the report has been furnished to the Office of Technical Services, Department of Commerce, for sale to the public, indicate this fact and enter the price, if known.

11. SUPPLEMENTARY NOTES: Use for additional explanatory notes.

12. SPONSORING MILITARY ACTIVITY: Enter the name of the departmental project office or laboratory sponsoring *(paying for)* the research and development. Include address.

13. ABSTRACT: Enter an abstract giving a brief and factual summary of the document indicative of the report, even though it may also appear elsewhere in the body of the technical report. If additional space is required, a continuation sheet shall be attached.

It is highly desirable that the abstract of classified reports be unclassified. Each paragraph of the abstract shall end with an indication of the military security classification of the information in the paragraph, represented as *(TS), (S), (C), or (U)*.

There is no limitation on the length of the abstract. However, the suggested length is from 150 to 225 words.

14. KEY WORDS: Key words are technically meaningful terms or short phrases that characterize a report and may be used as index entries for cataloging the report. Key words must be selected so that no security classification is required. Idenfiers, such as equipment model designation, trade name, military project code name, geographic location, may be used as key words but will be followed by an indication of technical context. The assignment of links, rules, and weights is optional.

MINIMUM BASIC DISTRIBUTION LIST FOR USAMC SCIENTIFIC AND TECHNICAL REPORTS IN METEOROLOGY AND ATMOSPHERIC SCIENCES

Commanding General (1)
U. S. Army Materiel Command
Attn: AMCRD-RV-A
Washington, D. C. 20315

Commanding General (1)
U. S. Army Electronics Command
Attn: AMSEL-EW
Fort Monmouth, New Jersey 07703

Commanding General (1)
U. S. Army Test and Evaluation Command
Attn: NBC Directorate
Aberdeen Proving Ground, Maryland 21005

Commanding Officer (1)
U. S. Army Ballistics Research Laboratories
Attn: AMXBR-IA
Aberdeen Proving Ground, Maryland 21005

Chief, Atmospheric Physics Division (2)
Atmospheric Sciences Laboratory
U. S. Army Electronics Command
Fort Monmouth, New Jersey 07703

U. S. Army Munitions Command (1)
Attn: Irving Solomon
Operations Research Group
Edgewood Arsenal, Maryland 21010

Commanding Officer (1)
U. S. Army Dugway Proving Ground
Attn: Meteorology Division
Dugway, Utah 84022

Commanding Officer (1)
U. S. Army CDC, CBR Agency
Attn: Mr. N. W. Bush
Fort McClellan, Alabama 36205

Commanding General (1)
U. S. Army Test and Evaluation Command
Attn: AMSTE-EL
Aberdeen Proving Ground, Maryland 21005

Commandant (1)
U. S. Army Signal School
Attn: Meteorological Department
Fort Monmouth, New Jersey 07703

Assistant Chief of Staff for Force Development (1)
CBR Nuclear Operations Directorate
Department of the Army
Washington, D. C. 20310

Director (1)
Atmospheric Sciences Programs
National Sciences Foundation
Washington, D. C. 20550

Assistant Secretary of Defense (1)
Research and Engineering
Attn: Technical Library
Washington, D. C. 20301

R. A. Taft Sanitary Engineering Center (1)
Public Health Service
4676 Columbia Parkway
Cincinnati, Ohio

Dr. Hans A. Panofsky (1)
Department of Meteorology
The Pennsylvania State University
University Park, Pennsylvania

Commanding General (1)
U. S. Continental Army Command
Attn: Reconnaissance Branch ODCS
for Intelligence
Fort Monroe, Virginia 23351

Commander (1)
Air Force Cambridge Research Laboratories
Attn: CRZW
1065 Main Street
Waltham, Massachusetts

President (1)
U. S. Army Artillery Board
Fort Sill, Oklahoma 73504

National Center for Atmospheric Research (1)
Attn: Library
Boulder, Colorado

Dr. J. E. Cermak, Head (15)
Fluid Mechanics Program
Colorado State University
Fort Collins, Colorado 80521

Author (1)

Chief of Research and Development (1)
Department of the Army
Attn: CRD/M
Washington, D. C. 20310

Commanding General (1)
U. S. Army Missile Command
Attn: AMSMI-RRA
Redstone Arsenal, Alabama 35809

Commanding General (1)
U. S. Army Natick Laboratories
Attn: Earth Sciences Division
Natick, Massachusetts 01762

Director, U. S. Army Engineer (1)
Waterways Experiment Station
Attn: WES-FV
Vicksburg, Mississippi 39181

Chief, Atmospheric Sciences Research Division (5)
Atmospheric Sciences Laboratory
U. S. Army Electronics Command
Fort Huachuca, Arizona 85613

Commanding Officer (1)
U. S. Army Frankford Arsenal
Attn: SMUFA-1140
Philadelphia, Pennsylvania 19137

Commandant (1)
U. S. Army Artillery and Missile School
Attn: Target Acquisition Department
Fort Sill, Oklahoma 73504

Commanding General (1)
U. S. Army Electronics Proving Ground
Attn: Field Test Department
Fort Huachuca, Arizona 85613

Commanding General (1)
U. S. Army Test and Evaluation Command
Attn: AMSTE-BAF
Aberdeen Proving Ground, Maryland 21005

Office of Chief Communications - Electronics (1)
Department of the Army
Attn: Electronics Systems Directorate
Washington, D. C. 20315

Chief of Naval Operations (1)
Department of the Navy
Attn: Code 427
Washington, D. C. 20350

Director (1)
Bureau of Research and Development
Federal Aviation Agency
Washington, D. C. 20553

Director of Meteorological Systems (1)
Office of Applications (FM)
National Aeronautics and Space Administration
Washington, D. C. 20546

Director (1)
Atmospheric Physics and Chemistry Laboratory
Environmental Science Services Administration
Boulder, Colorado

Andrew Morse (1)
Army Aeronautical Activity
Ames Research Center
Moffett Field, California 94035

Commanding Officer (2)
U. S. Army Cold Regions Research and
Engineering Laboratories
Attn: Environmental Research Branch
Hanover, New Hampshire 03755

Mr. Ned L. Kragness (1)
U. S. Army Aviation Materiel Command
SMOSM-E
12th and Spruce Streets
Saint Louis, Missouri 63166

Commanding Officer, U. S. Army (1)
Artillery Combat Development Agency
Fort Sill, Oklahoma 73504

Commander, USAR Air Weather Service (MATS) (1)
Attn: AWSSS/TIPD
Scott Air Force Base, Illinois

Dr. John Bogusky (1)
7310 Cedardale Drive
Alexandria, Virginia 22308

Commanding General (1)
U. S. Army Combat Development Command
Attn: CDCMR-E
Fort Belvoir, Virginia 22060

Commanding General (1)
U. S. Army Munitions Command
Attn: AMSMU-RE-R
Dover, New Jersey 07801

Commanding Officer (1)
U. S. Army Ballistics Research Laboratories
Attn: AMXBR-B
Aberdeen Proving Ground, Maryland 21005

Director (2)
Atmospheric Sciences Laboratory
U. S. Army Electronics Command
Fort Monmouth, New Jersey 07703

Chief, Atmospheric Sciences Office (2)
Atmospheric Sciences Laboratory
U. S. Army Electronics Command
White Sands Missile Range, New Mexico 88002

Commanding Officer (1)
U. S. Army Picatinny Arsenal
Attn: SMUPA-TV-3
Dover, New Jersey 07801

Commanding Officer (1)
U. S. Army Communications - Electronics
Combat Development Agency
Fort Monmouth, New Jersey 07703

Commanding General (1)
Deseret Test Center
Attn: Design and Analysis Division
Fort Douglas, Utah 84113

Commandant (1)
U. S. Army CBR School Micrometeorological
Section
Fort McClellan, Alabama 36205

Assistant Chief of Staff for Intelligence (1)
Department of the Army
Attn: ACSI-DERSI
Washington, D. C. 20310

Officer in Charge (1)
U. S. Naval Weather Research Facility
U. S. Naval Air Station, Building 4-28
Norfolk, Virginia 23500

Chief, Fallout Studies Branch (1)
Division of Biology and Medicine
Atomic Energy Commission
Washington, D. C. 20545

Director (1)
U. S. Weather Bureau
Attn: Librarian
Washington, D. C. 20235

Dr. Albert Miller (1)
Department of Meteorology
San Jose State College
San Jose, California 95114

Mrs. Francis L. Wheedon (1)
Army Research Office
3045 Columbia Pike
Arlington, Virginia 22201

Commander (1)
Air Force Cambridge Research Laboratories
Attn: CRXL
L. G. Hanscom Field
Bedford, Massachusetts

Harry Moses, Asso. Meteorologist (1)
Radiological Physics Division
Argonne National Laboratory
9700 S. Cass Avenue
Argonne, Illinois 60440

Defense Documentation Center (20)
Cameron Station
Alexandria, Virginia 22314

Office of U. S. Naval Weather Service (1)
U. S. Naval Air Station
Washington, D. C. 20390

Dr. Gerald Gill (1)
University of Michigan
Ann Arbor, Michigan 48103